

**About the influence of the breaking arc voltage
on the decay characteristics of
near-to-generator short-circuit current's
DC-component**

Master's thesis
Written by
DI Bettina Hofer, BSc.

Graz University of Technology

Institute of High Voltage Engineering and System Management
Ao.Univ.-Prof. Dipl.-Ing. Dr.techn. Stephan Pack

Graz, November 2013

EIDESSTATTLICHE ERKLÄRUNG

Ich erkläre an Eides statt, dass ich die vorliegende Arbeit selbstständig verfasst, andere als die angegebenen Quellen/Hilfsmittel nicht benutzt und die den benutzten Quellen wörtlich und inhaltlich entnommene Stellen als solche kenntlich gemacht habe.

Graz, am

.....

(Unterschrift)

STATUTORY DECLARATION

I declare that I have authored this thesis independently, that I have not used other than the declared sources / resources, and that I have explicitly marked all material which has been quoted either literally or by content from the used sources.

.....

date

.....

(signature)

Kurzfassung

In der vorliegenden Masterarbeit wird der Einfluss einer Lichtbogenspannung auf das Abklingen der Gleichstromkomponente bei generatornahen Kurzschlüssen untersucht. Unter ungünstigen Rahmenbedingungen ist es möglich, dass im zeitlichen Verlauf des Kurzschlussstromes aufgrund der wirksamen Impedanzen anfänglich Stromnulldurchgänge fehlen. Dies ist beim Ausschalten der Fehlerströme insbesondere dann zu berücksichtigen, wenn das zeitliche Schaltfenster des Leistungsschalters, wie bei SF₆-Schaltern, auf etwa drei bis fünf Halbwellen begrenzt ist. Die Lichtbogenspannung beeinflusst das Abklingverhalten des Gleichstromgliedes zugunsten der Vorverlagerung der Stromnulldurchgänge.

Der Schwerpunkt der vorliegenden Masterarbeit liegt auf der mathematischen Modellierung der Netzstruktur, unter besonderer Berücksichtigung der Lichtbogenspannung und der Analyse ausgewählter Lichtbogenmodelle auf das Abklingen der Gleichstromkomponente im Kurzschlussfall. Mithilfe grundlegender physikalisch-elektrotechnischer Überlegungen wird gezeigt, dass es für eine erste Analyse des Einflusses der Lichtbogenspannung auf den Stromverlauf im Fehlerfall ausreicht, die Lichtbogenspannung als konstanten Wert über die Dauer des Lichtbogenintervalls zu modellieren. Als entscheidender Parameter wurde die Höhe der Lichtbogenspannung identifiziert. Eine weiterführende, tiefergehende Modellbildung der Lichtbogenspannung ist mit einem deutlichen Mehraufwand, nicht zuletzt für das Auffinden geeigneter Parameter, verbunden. Diese hat im Vergleich zum Modell mit konstanter Lichtbogenspannung jedoch nur geringen zusätzlichen Einfluss auf die Vorverlagerung der Stromnulldurchgänge.

Abstract

The on hand Master's thesis is concerned with the impact of the breaking arc voltage on the decay characteristics of the DC-component of near-to-generator short-circuits. At disadvantageous conditions it is possible that there are missing current zero-crossings at the beginning because of the effective impedances. A particular consideration has to be given to that at the circuit breaking operations in case of a fault, not least because of the limitation of the time slot for breaking, which is about three to five half-waves by using SF₆ circuit breakers. The arc voltage makes an influence on the DC-component's decay characteristic for the benefit of the circuit breaker. As a result, earlier current zero-crossings are possible.

The focus of the on hand Master's thesis is on the mathematical modeling of the network configuration with respect to the arc voltage and analyzes of selected models with respect to their influence on the decay characteristic of the DC-component in case of a short-circuit. By using basic physical-electrical considerations it is shown that modeling the arc voltage as a constant value for the duration of the arc is alright for first investigations. The value of the arc voltage is detected as critical parameter. For further studies a more comprehensive modeling of the arc voltage is profitable but ongoing with a significant amount of investment concerning the identification of suitable model parameters. Compared to the model with constant d.c. arc voltage the additional influence of the arc voltage on the current's signal shift is still small.

Vorwort

Nur durch die Herausforderungen, denen man sich im Laufe der Zeit stellt und stellen muss, wird unser Leben erst interessant und aufregend. Diese zeigen Chancen und Möglichkeiten auf um sich selbst weiterzuentwickeln und Erfahrungen zu sammeln. Doch auch die besten Chancen sind nur ein einfacher Stein am Lebensweg, wenn es keine Unterstützung gibt, daraus etwas Schönes zu bauen.

Allen Personen, die mich während meiner Studienzeit an der TU Graz und meiner Masterarbeit unterstützt haben, gilt mein Dank, insbesondere dem Team von „Frauen in die Technik“ und den Mitarbeitern des Instituts für Elektrische Anlagen, ohne die ich vermutlich nie ein technisches Studium inskribiert hätte.

Außerdem möchte ich mich bei meinen Betreuern und Mentoren herzlichst bedanken: bei Herrn Ao.Univ.-Prof. Dipl.-Ing. Dr. techn. Stephan Pack für die Übernahme der Betreuung und die konsequente Sicherstellung organisatorischer Rahmenbedingungen; bei Dr. Hansjörg Hauer für zahlreiche Inputs und die fachliche Unterstützung während meiner wissenschaftlichen Arbeit; bei Dipl.-Ing. Jürgen Plesch für die seinen persönlichen Einsatz und die laufende Unterstützung. Allen künftigen Absolventen der Technischen Universität Graz kann ich eine Betreuung der Abschlussarbeit durch das Institut für Hochspannungstechnik und Systemmanagement und dessen Mitarbeiterinnen und Mitarbeitern nur ans Herz legen: unbürokratisch, unkompliziert und unermüdlich. Diese stete Unterstützung und die wertvollen Ratschläge haben wesentlich zum Gelingen der vorliegenden Arbeit beigetragen.

Vielen lieben Dank auch an Sonja, Astrid, Andreas, Elisabeth, Christa, Christian, Birgit und Uwe für ermunternde Gespräche, motivierende Worte und die unzähligen Versuche meine zielgerichteten Gedanken für einige Momente auf scheinbar Unwesentliches zu lenken.

Mama und Papa, ich bin euch sehr dankbar dafür, dass ich ohne eure Einwände meine eigenen Wege gehen durfte und ich jederzeit auf eure Unterstützung und euer Vertrauen zählen kann.

Danke Thomas, für ein offenes Ohr und ein motivierendes Gespräch zu jeder Zeit, und dafür, dass du an mich glaubst und hinter mir stehst. Das Ende eines Vorworts steht immer auch für den Beginn eines neuen Kapitels.

*„Man kann einen Menschen nichts lehren, man kann ihm nur helfen,
es in sich selbst zu entdecken.“
(Galileo Galilei)*

Contents

1	Introduction.....	1
2	Technical-physical background	4
2.1	Structure	4
2.2	Selected synchronous generators in case of short-circuit	5
2.2.1	Initial conditions.....	5
2.2.2	Characteristics in case of near-to-generator short-circuit faults	7
2.3	High voltage circuit breakers	11
2.3.1	Circuit breakers	12
2.3.2	Physics of the electric arc.....	16
3	Modeling.....	24
3.1	Modeling of structure.....	25
3.2	Modeling of electric arc	29
4	Results and discussion.....	32
4.1	Worst-case point on wave with respect to the DC-component.....	32
4.2	Selection of operating points	34
4.3	Comparison of arc models, single-phase.....	36
4.4	Evaluation of results, single-phase	41
4.5	Implementation of relevant arc models, three-phase	48
4.5.1	Model with constant d.c. arc voltage.....	48
4.5.2	Mayr's equation.....	55
4.5.3	Comparison of model with constant d.c. arc voltage and model with Mayr's equation	59
4.6	Impact of arc voltage on zero-crossing of current considering the wye connection of the transformer.....	60
4.7	Impact of arc voltage on zero-crossing of current considering the ground connection of the fault.....	62
5	Conclusion.....	65
	Bibliography	67
	Figures	70
	Tables.....	73
	Abbreviations	74
	Appendix.....	78

1 Introduction

A near-to-generator short-circuit fault causes a current characteristic which differs from the characteristic in undisturbed operation. Under certain circumstances, like special initial condition of the generator and the resulting active short-circuit reactances current zero-crossings can be missing. That occurs because the alternating current is superposed by a DC-component which decays slower than the AC-component. As a result missing current zero-crossings may appear in one or two phases of the short-circuited electrical network. An exemplary structure of a circuit with an occurring near-to-generator short-circuit fault as a basis for missing current zero-crossings is shown in Figure 1.¹²

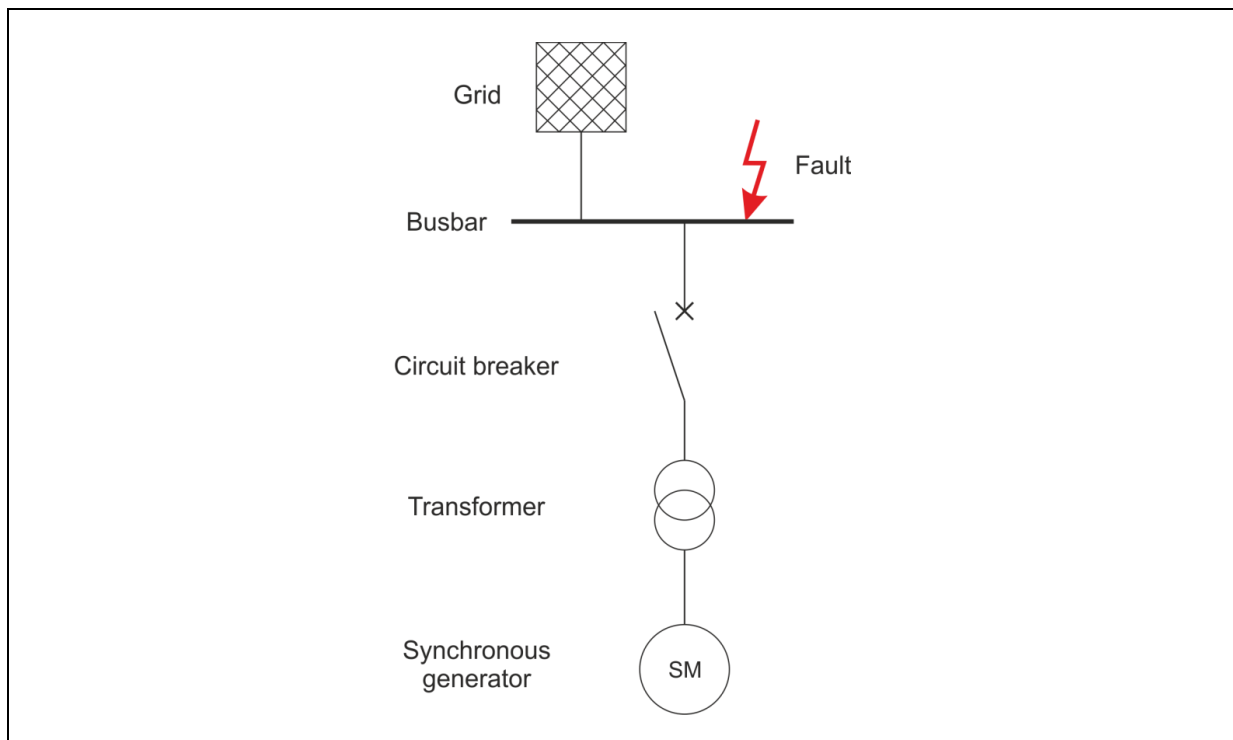


Figure 1: Overview of the described structure

The interrupting operation can only take place at the instant of current's zero. That implies that such fault currents with missing zero-crossings can't be interrupted immediately after occurring in most cases. It has to be waited until the DC-component decays in its natural way. But if the circuit breaker's contacts separate after a fault, an electric arc occurs and the current continues flowing through the arc. As a result of the occurring electric arc the DC-component decays faster and the current first zero-crossing takes place earlier compared to the current characteristic without an electric arc.³⁴

The aim of the on hand Master's thesis is to analyze that instanced impact of the breaking arc voltage on the decay characteristic of the current's DC-component. Both simple and

¹ cf. FENSKE, S. (2011), p. 1

² cf. ABB AB (2013), p. 16

³ cf. BRINKHOFF, R.; KULICKE, B.; SCHRAMM, H.-H. (1978), p. 385

⁴ cf. FENSKE, S. (2011), p. 1

complex types of arc models should be compared concerning the arc voltage's influence on the decay characteristic of the DC-component. The impact of the arc voltage on the zero-crossing of the current with respect to the ground connection of the fault should also be shown.

The study area is focused on an electrical circuit with the defined elements grid (380 kV level), transformer and synchronous generator, whereby the generator is a chosen salient-pole machine. A schematic figure of the overall structure can be seen in the figure above. As fault a three-phase short-circuit without ground connection is defined.

The process with its main focuses is clarified in Figure 2.

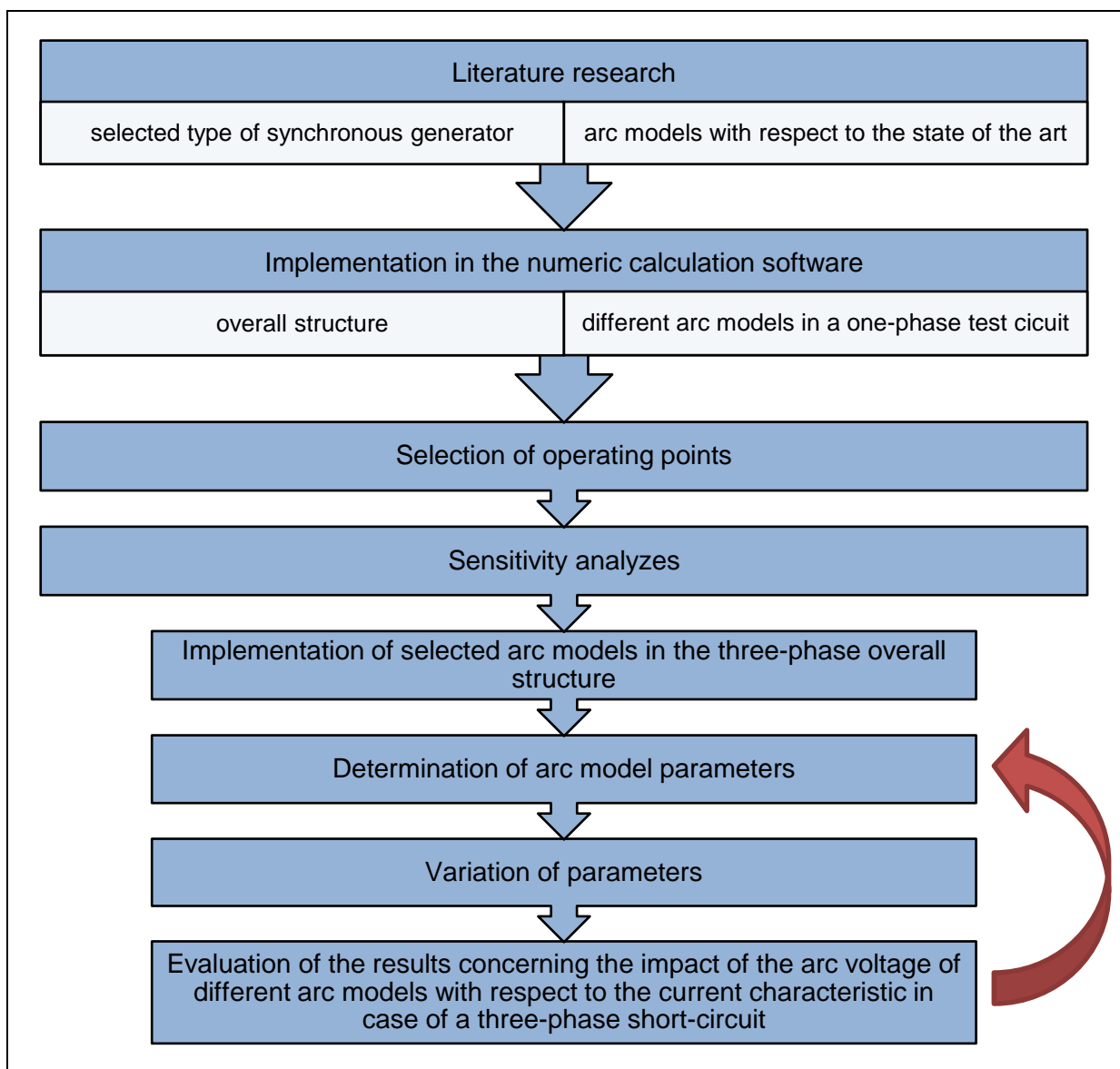


Figure 2: Schematic figure of the procedure

After a literature research concerning salient-pole machines and their characteristics in case of short-circuits, different arc models will be researched with respect to the state of the art.

The implementation in the numeric simulation software will consist in two steps: implementation of the overall structure and implementation of the different electric arc models. The initial conditions of the synchronous generator will be set before starting with further analyzes. For initial studies the models will be implemented in a one-phase test circuit to do basic analyzes and sensitivity analyzes concerning their parameter sensitivities. Suitable arc models will be implemented in the three-phase overall structure afterwards. The last procedure will consist in three different steps, which will run in a loop, like shown in Figure 2: arc model parameter determination, parameter variation and evaluation of the results concerning the impact of the arc voltage on the current characteristic in case of a three-phase short-circuit.

2 Technical-physical background

In this chapter the technical-physical background of the on hand Master's thesis are concerned, including

- the structure of the model,
- the technical-physical background of selected synchronous generators,
- the technical-physical background of high voltage circuit breakers and
- the physics of the electric arc including different arc models.

On the one hand this chapter provides an overview of the characteristics of selected salient-pole machines in case of short-circuits, especially concerning the combination of the different time constants of the generator. On the other hand it also gives an overview of the physics of the electric arc and in particular an overview of the common used arc models

2.1 Structure

The following figure shows the equivalent network of the circuit to be analyzed.

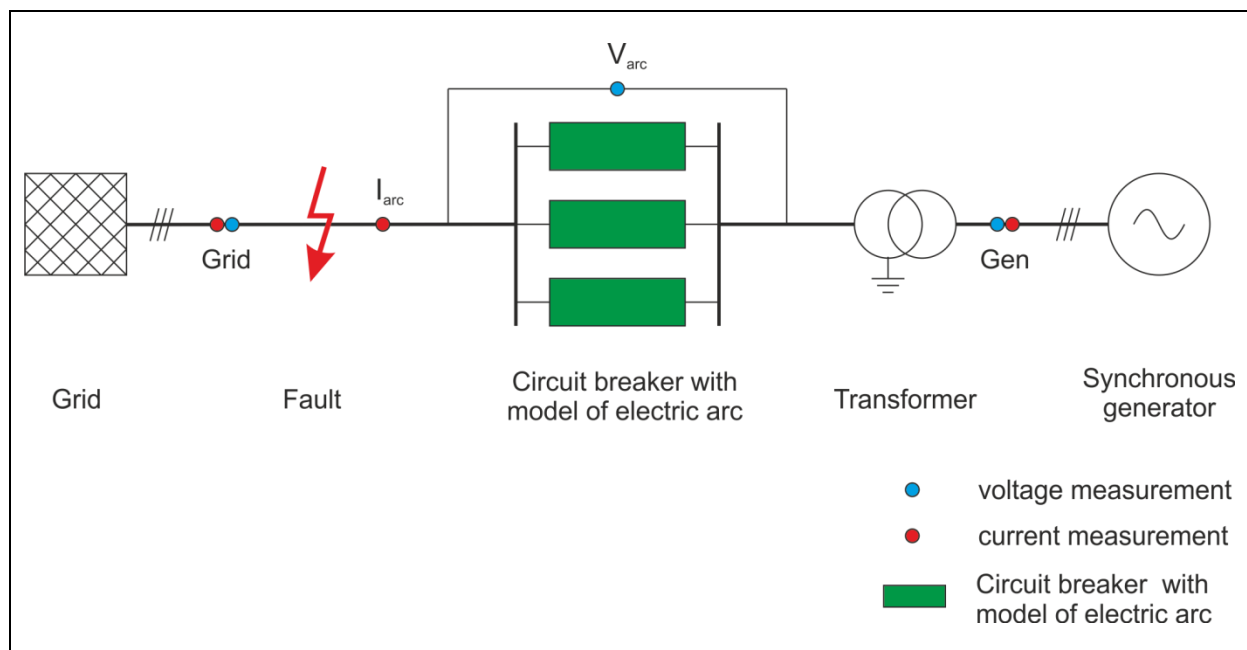


Figure 3: Equivalent network

As shown in Figure 3 the circuit to be analyzed includes different elements, but with the addition that the grid is only for voltage stabilization and has no nameable influence on the characteristic of the current profile in case of a short-circuit fault.

Therefore it's necessary to analyze the impact of the elements "synchronous generator" and "circuit breaker with model of electric arc" on the characteristic of the analyzing fault's current profile in the measurement point I_{arc} (cf. Figure 3).

2.2 Selected synchronous generators in case of short-circuit

This paragraph provides an overview of salient-pole machines concerning their initial conditions (operating points) focused on the interaction of the different time-constants in case of short-circuits. In this matter on hand salient-pole machines with a field winding and a damper winding on d-axis and damper winding on q-axis are considered. The saturation is untended and the armature winding connection is wye (floating).

2.2.1 Initial conditions

A synchronous machine can work even as a motor and as a generator. In generator mode the machine delivers real power to the grid. It is also possible to set the conditions concerning the reactive power. The machine works like a capacitor when delivering reactive power to and like an inductance when taking up reactive power from the grid.⁵

Capability curves according to synchronous generators are used to outline the stability limits of the selected machine. The axis of abscissas the reactive power in per-unit values is applied. The axis of ordinate shows the real power in per-unit values. They are also used to define several operating points of the selected machine. Operating points define the initial condition of the selected generator, which have an impact on the voltage and current signal sequences, especially on their position relative to each other and on the current magnitude. Different operating points cause different characteristics of current and voltage signal sequences.

In general there are four different operating conditions belonging to synchronous machines.

	Over-excited mode	Under-excited mode
Motor operation	<ul style="list-style-type: none"> • consumes capacitive reactive power • delivers inductive reactive power • Phase angle φ: $-\pi/2 < \varphi < 0$ • Load angle $\vartheta > 0$ 	<ul style="list-style-type: none"> • consumes inductive reactive power • delivers capacitive reactive power • Phase angle φ: $0 < \varphi < \pi/2$ • Load angle $\vartheta > 0$
Generator operation	<ul style="list-style-type: none"> • consumes capacitive reactive power • delivers inductive reactive power • Phase angle φ: $-\pi < \varphi < -\pi/2$ • Load angle $\vartheta < 0$ 	<ul style="list-style-type: none"> • consumes inductive reactive power • delivers capacitive reactive power • Phase angle φ: $\pi/2 < \varphi < \pi$ • Load angle $\vartheta < 0$

Table 1: Operating conditions of synchronous generators

⁵ cf. SPRING, E. (1998, 2006, 2009) p. 354

For these considerations both motor operations, over-excited and under-excited mode, represented in the above Table 1, can be intended.

The following figure shows the capability diagram of a selected salient-pole synchronous generator with nominal power 223 MVA. In addition to that Table 2 lists the data belonging to the marked points in capability diagram. Short explanations belonging to the different operating points and their specific attributes, referring to the information in Table 1, follow afterwards.

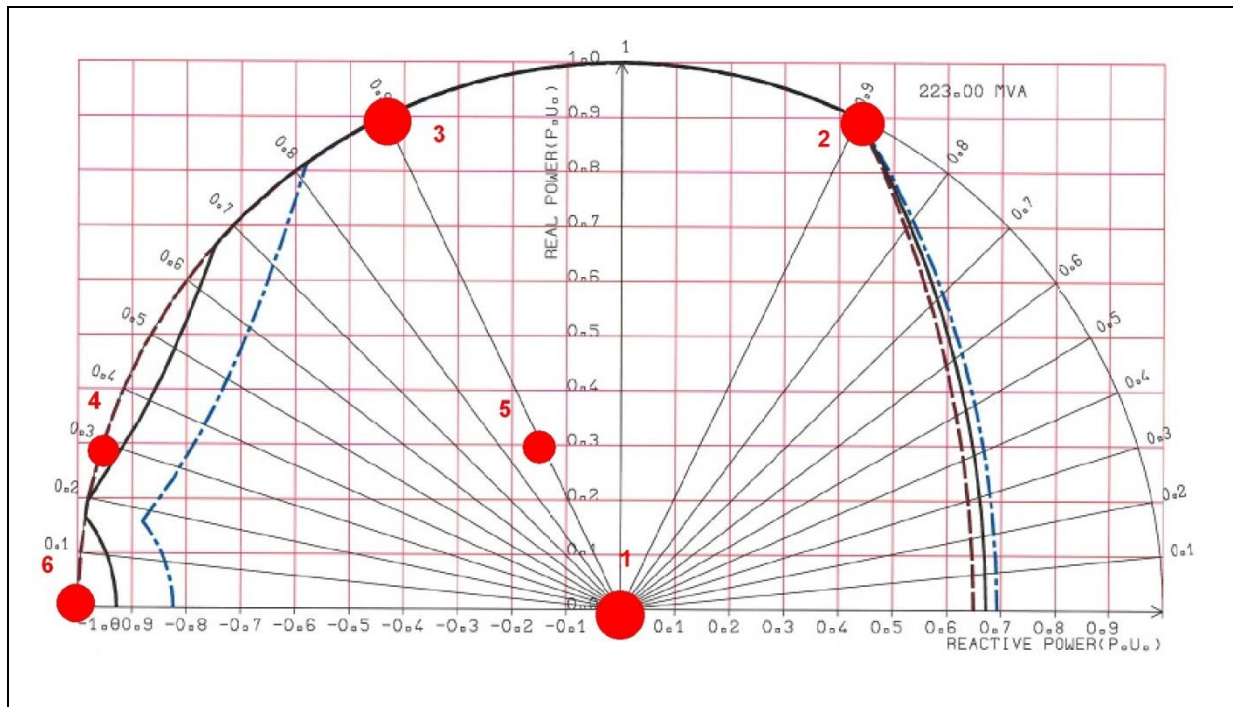


Figure 4: Capability diagram and operating points of the chosen synchronous generator

No.	Description	p in p.u.	q in p.u.
OP 1	Open-circuit point	0,000	0,00
OP 2	Nominal rating point	0,900	0,44
OP 3	Under-excited rated power factor, nominal power	0,900	-0,44
OP 4	Maximum under-excited reactive power, minimal turbine output	0,300	-0,90
OP 5	Under-excited rated power factor, minimal turbine output	0,300	-0,25
OP 6	Under-excited phase-shifting point	-0,001	-1,00

Table 2: Operating points of synchronous generator (belonging to Figure 4)

OP 1: Open-circuit point

Characterizing for the open-circuit point is, that the generator is unloaded. It means that there is no delivered power or power consumption.

OP 2: Nominal rating point

At nominal rating point the synchronous generator delivers or consumes the rated power. In that case, the generator delivers inductive power to the grid. The phase angle φ (between voltage and current) is between $-\pi$ and $-\pi/2$. The load angle ϑ (angle between rotor and phase voltage) is negative. That implies that the generator is in over-excited mode.

OP 3: Point of under-excited rated power factor at nominal power

Operating point 3 is characterized by delivering the nominal power at under-excited mode. The synchronous generator acts like a capacitor. Both, the phase angle φ and the load angle ϑ are negative (cf. Table 1).

OP 4: Point of maximum under-excited reactive power at minimal turbine output

At operating point 4 the synchronous generator acts like a capacitor, the phase angle φ and the load angle ϑ are negative, like at OP 3 (cf. Table 1). The active power, which is delivered by the turbine, is at minimum (0.3 p.u.).

OP 5: Point of under-excited rated power factor at minimal turbine output

At operating point 5 the active power delivered by the turbine is at minimum, like at OP 4. Although the generator doesn't deliver the rated power, it acts like a capacitor. Both, the phase angle φ and the load angle ϑ are negative (cf. Table 1).

Note: The point in the capability diagram belonging to No. 5 (Figure 4) is wrong; the data in Table 2 concerning p and q are valid.

OP 6: Under-excited phase-shifting point

Last but not least, operating point 6 is the point of phase shifting. The synchronous generator is in pure capacitive mode. The delivered active power is only to cover the active power losses. The synchronous generator delivers maximum reactive power to the grid.

According to CANAY, D.; KLEIN, H. (1974) the current DC-component becomes high, if the components v_{q0} (voltage in quadrature axis) and i_{d0} (current in direct axis) are relatively small. That case appears if the synchronous generator works in under-excited mode near the stability limits. In the on hand task that situation occurs for instance at the operating points 4 and 6.⁶

2.2.2 Characteristics in case of near-to-generator short-circuit faults

In general there are two different types of short-circuits due to their signal sequences:

- far-from-generator short-circuit faults
- near-to-generator short-circuit faults

A short-circuit fault is a near-to generator fault if in case of fault at least one synchronous machine delivers an expectable initial short-circuit current which is more than the double of

⁶ cf. CANAY, D.; KLEIN, H. (1974), p. 200f.

the machine's rated current. This type of short-circuit fault is considered in the on hand Master's thesis.⁷

The extreme case of a near-to-generator short-circuit fault is a three-pole terminal short-circuit. The characteristic of the current profile is essentially depending on the time-variant synchronous reactance on direct axis $X_d(t)$. In addition to the shifting caused by the DC-component there are also higher values of the current's initial AC component because of the transformer-type coupling between stator windings and rotor circuits. These higher values are based on two additional balancing processes on the form of the transient reactance X_d' and the sub-transient reactance X_d'' .⁸

Figure 5 shows the current characteristic in case of a near-to-generator short-circuit fault using a salient-pole synchronous generator with damper winding.

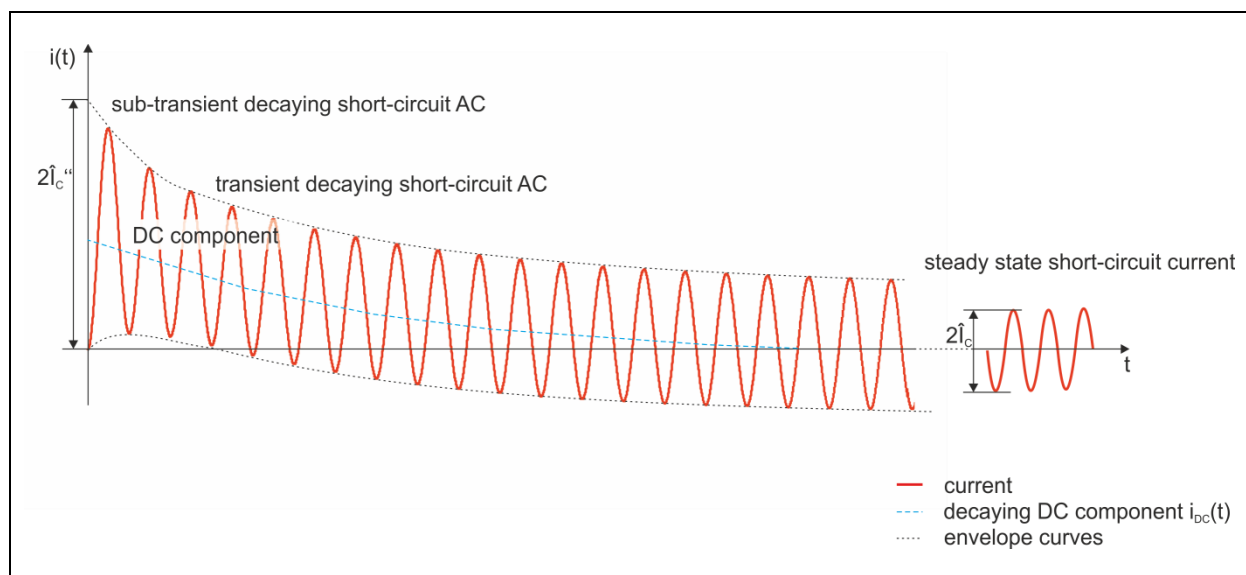


Figure 5: Schematic figure of current characteristic in case of short-circuit⁹¹⁰¹¹

The sub-transient decay short-circuit alternating current I_c'' is obtained by drawing the envelope curves of the signal and interpolating these curves until the short-circuit's starting point. The distance between the two envelopes is equivalent to the double peak value of sub-transient decay short-circuit alternating current $2\hat{I}_c''$, as shown in Figure 5. With the passing of time this mentioned distance decreases until it is equivalent to the double peak value of steady state short-circuit current $2\hat{I}_c$. Depending on the timing of the short-circuit there is a DC-component beside the alternating current in each phase which is characterized by an exponential decay with a DC time constant. The highest DC-component occurs if the short-circuit enters in time of voltage zero-crossing in one phase. In time of maximum voltage there is almost no DC-component.¹²

⁷ cf. BALZER, G.; NELLES, D.; TUTTAS, C. (2009), p. 225f.

⁸ cf. SCHWAB, A. (2012), p. 330ff.)

⁹ cf. SCHWAB, A. (2012), p. 332)

¹⁰ cf. SPRING, E. (1998, 2006, 2009), p. 394

¹¹ cf. KLAMT, J. (1962), p. 106f.

¹² cf. SPRING, E. (1998, 2006, 2009), p. 395

In conformity with KLAMT, J. (1962) in general there is a difference between the reactances in direct-axis (d-axis) and those in quadrature-axis (q-axis). Although for the determination of the total short-circuit current it's enough to consider the reactances in d-axis. In general the reactances also depend on the state of saturation, which is neglected in this case.¹³

In following the characteristic parameters of synchronous generators are explained based on KLAMT, A. (1962), SCHWAB, A. (2012) and SPRING, E. (1998, 2006, 2009).

Synchronous reactances X_d and X_q

The synchronous reactance in d-axis is the sum of main reactance and leakage reactance. It is the quotient of rated voltage and steady-state short-circuit current. The synchronous reactance is assigned to the longitudinal field caused by the longitudinal armature flux and the excitation flux. In general the synchronous reactance in q-axis X_q is smaller than X_d . The synchronous reactances and the rotor voltage are mainly defining the behavior of the machine in steady-state symmetric operation, but also at very slow changes on the load.^{14,15}

According to SCHWAB, A. (2012) the synchronous reactance in quadrature axis X_q is about 0.5 ... 0.7 X_d .¹⁶

Negative sequence reactance X_2 and negative sequence resistance R_2

These two parameters are parameters of a separate model to describe it in case of unbalanced operating conditions. Usually if the armature currents form an asymmetric three-phase-system they will be excluded in a positive sequence which turns with the rotor and a negative sequence which turns contrary to the rotor. The negative sequence field induces currents in the rotor's damper winding, which reduce the armature field. These negative sequence currents cause an effective negative sequence armature voltage which results from the product of the negative sequence current's rms-value and the negative impedance Z_2 , whereby it applies $Z_2 = \sqrt{R_2^2 + X_2^2}$.¹⁷

According to KLAMT, J. (1962) the negative sequence reactance X_2 is the quotient of voltage and current if there is only one active negative sequence system.¹⁸

Zero sequence reactance X_0 and zero sequence resistance R_0

If the sum of the three armature currents is not zero, the method of symmetric components also provides a zero sequence system in addition to the positive and the negative sequence system. In the zero sequence system all AC-components, which are in phase in the three-phase armature circuit, appear. The zero sequences of the armature currents don't make any contributions to the flux' fundamental oscillation. The voltages and currents of the zero sequence are related to each other by the zero sequence impedance Z_0 , whereby it applies $Z_0 = \sqrt{R_0^2 + X_0^2}$. The magnetic flux, which is associated to the zero sequence reactance, forms itself on the armature leakage. The zero sequence soaks the damper winding and the

¹³ cf. KLAMT, J. (1962), p. 105

¹⁴ cf. KLAMT, J. (1962), p. 105

¹⁵ cf. KOMITEE 311 (2004), p. 76

¹⁶ cf. SCHWAB, A. (2012), p. 302f.

¹⁷ cf. KOMITEE 311 (2004), p. 77f.

¹⁸ cf. KLAMT, J. (1962), p. 105

poles up to a particular share. That's the reason why the zero sequence resistance R_0 includes the DC resistances of the armature and an additional value which considers the losses caused by the zero sequence in the damper winding and in parts of the rotor.¹⁹

Direct axis synchronous transient reactance X_d'

In dynamic processes the field building and the field reduction in direct axis depends on the change of direct axis armature AC, on the field current, on the current in direct axis of substitute damper winding and on eddy currents in solid (pole) parts. At nearly constant field current the field's rate of change in direct axis correlates to the q-axis component of armature voltage. A sudden short-circuit causes a clear rate of change concerning the q-axis component of voltage, and a minimum rate of change concerning the d-axis component of voltage. The synchronous transient reactance X_d' is a result of the alternating current at the beginning of the transient period.²⁰

According to KLAMT, J. (1962) the leakage between armature and field winding controls the synchronous transient reactance X_d' .²¹

SCHWAB, A. (2012) describes the synchronous transient reactance X_d' as a reason for the higher short-circuit AC-amplitude at the beginning. The changing of the stator current and the resulting change of the magnetic field at the moment, when a short-circuit occurs, induces a circulation voltage in the field winding which is short-circuited over the field voltage source. This circulation voltage drives a current through the field-winding, which is linked to a magnetic field. This field tries to compensate the flux alteration of the stator field (Lenz's law) and tries to keep the air-gap flux on the constant value from the point of time before the short-circuit occurred. In general current and flux are directly proportional by the quotient of inductivity and by current passed windings. For this reason the inductivity must decrease if the current increases by a constant flux; a minor inductivity L_d' means a minor reactance X_d' .²²

Direct axis synchronous sub-transient reactance X_d''

At synchronous generators with damper winding the effect, which causes the transient reactance X_d (as described above) also appears a second time, but in damper winding. This causes the sub-transient reactance X_d'' , which is smaller than the transient reactance X_d' . Therefore the initial amplitude of the alternating current increases a further time.²³

According to KLAMT, J. (1962) the sub-transient synchronous reactance X_d'' depends on the leakage of armature, field and damper winding and other dampening metal parts, such as massive stator poles.²⁴

Quadrature axis synchronous sub-transient reactance X_q''

The creation and reduction of the magnetic field in quadrature axis depends on the ratio on the armature current's quadrature component, on the current in quadrature axis of substitute

¹⁹ cf. KOMITEE 311 (2004), p. 78

²⁰ cf. KOMITEE 311 (2004), p. 77

²¹ cf. KLAMT, J. (1962), p. 106

²² cf. SCHWAB, A. (2012), p. 331f.

²³ cf. SCHWAB, A. (2012), p. 332

²⁴ cf. KLAMT, J. (1962), p. 106

damper winding and on eddy currents in solid (pole) parts. The field's rate of change in quadrature axis correlates to the d-axis component of armature voltage. In general the quadrature axis synchronous transient reactance X_q' is not attended in the technical standards.²⁵

Time-constants

Armature short-circuit time constant

The armature short-circuit time constant is also known as DC time constant. The level depends on the phase angle of short-circuit's timing (as mentioned above).²⁶

In SCHWAB, A. (2012) the DC time constant is calculated by the inductance and the resistance of the relevant circuit.²⁷

Transient and sub-transient open-circuit time constant

After a step change of the voltage in the field winding there could be currents in the d-axis damper winding from time to time. The characteristic of the armature voltage and of the field current separates into two periods. The first period is characterized by the sub-transient open-circuit time constant, the second mentioned time period by the transient open-circuit time constant. The transient open-circuit time constant has always a clearly higher value than the sub-transient open-circuit time constant. In general the standard shows an interest on the transient open-circuit time constant.²⁸

Transient and sub-transient short-circuit time constant

The sub-transient short-circuit time constant characterizes the initial fast disappearing of the short-circuit current (sub-transient period). The transient short-circuit time constant is mainly responsible for the later slowly decay of the short-circuit current (transient period). In case of short-circuit the armature and the field winding magnetize contrarily. The main inductivity has a minor part in this process. Therefore the short-circuit time constants have lower values than the open-circuit time constants. The courses of time of armature currents can be divided into a sub-transient initial part with the sub-transient short-circuit time constant, and into a following part characterized by the transient short-circuit time constant which is significant higher than the sub-transient one.^{29,30}

2.3 High voltage circuit breakers

Breaking short-circuit currents in high voltage grids places high requirements on switch gears. In the shortest possible time the circuit breaker should switch between being an ideal conductor to an ideal insulator and vice versa. The occurring of electric arcs at contact

²⁵ cf. KOMITEE 311 (2004), p. 77

²⁶ cf. KOMITEE 311 (2004), p. 79f.

²⁷ cf. SCHWAB, A. (2012) p. 325

²⁸ cf. KOMITEE 311 (2004), p. 79

²⁹ cf. KLAMT, J. (1962), p. 108

³⁰ cf. KOMITEE 311 (2004), p. 79

separation cannot be avoided. If the arc extinct after a short-circuit the voltage may recover. For this reason it is necessary to investigate the electric arc itself and the influence of the electric arc on the current characteristic.³¹

2.3.1 Circuit breakers

For a long time the minimum oil circuit breaker and the air blast circuit breaker have been the successful circuit breakers before the development of the SF₆-circuit breakers started. These SF₆-circuit breakers score with better characteristics for the extinguishing of electric arcs, a better insulating performance and low noise compared to the above mentioned circuit breakers. In general a distinction is made between circuit breakers with arc extinguishing medium and vacuum circuit breakers.³²

Circuit breakers with arc extinguishing medium

According to RAGALLER, K. (1978) the basic concept for all circuit breakers in use today is the same, in spite of design and type, whether minimum oil, air or SF₆. The electric arc burns in a gas under high pressure, with a strong pressure gradient along the arc axis. In the basic design, there are two nozzles (double-nozzle design). High pressure exists in the gas chamber surrounding the nozzle inlet, near the nozzle exits there is an area of low pressure. As a result of this pressure difference there is a flow induced symmetrically into the nozzles on both sides. This configuration exists in air-blast and SF₆-circuit breakers. Usually minimum oil circuit breakers have a different geometry because the arc itself must generate the mentioned high pressure gas by vaporizing the oil. But there is also a burning arc in a strong gradient along the arc axis.³³

Figure 6 shows the main components of a self-blast interrupter.

³¹ cf. CRASTAN, V. (1999, 2006, 2012), p. 533

³² cf. CRASTAN, V. (1999, 2006, 2012), p. 548ff.

³³ cf. RAGALLER, K. (1978), p. 10f.

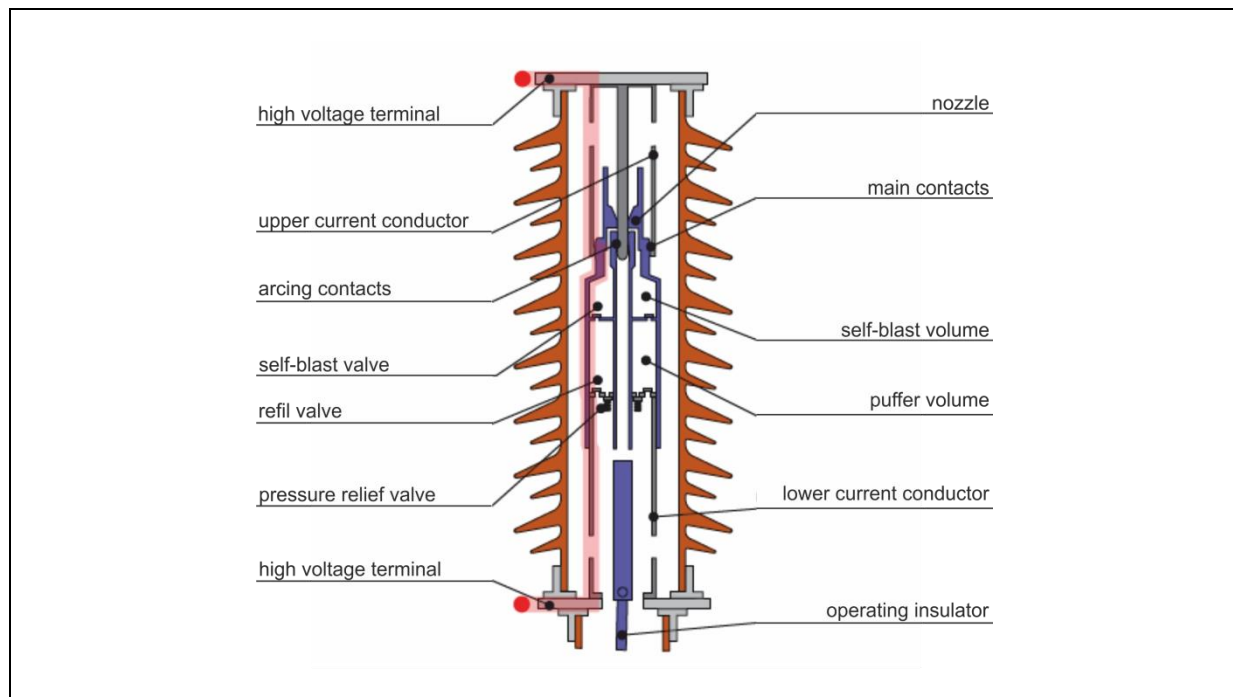


Figure 6: Main components of a self-blast circuit breaker³⁴

After contact separation an electric arc is created, rapidly transported along the axis by the gas flow and the arc roots and driven downstream into the nozzles. As a result there exists a well-defined and reproducible initial condition for the subsequent extinction process. In an optimum situation this process is largely independent of the phase of contact-separation. Only the metal vapor production during contact separation may have an influence on the process.³⁵

Air blast circuit breakers

The compressed air (15 to 30 bar) which is stored in vessels is released in case of switching operation. In general over a voltage of about 60 to 110 kV the chamber is always under pressure. As a result the switching time is shortened and compression waves are avoided. An open air circuit exists. At contact separation the air is emitting to the environment. Compressors are responsible to refill the vessels afterwards. The air is also used as a driving mean for the contact movement, which happens mechanical or hydraulic.³⁶

SF₆-circuit breakers

SF₆-circuit breakers have been in use for more than 30 years. The SF₆ gas is particularly suitable as insulating and quenching medium because of its high dielectric strength and thermal conductivity.³⁷

The process of current interruption in high-voltage circuit breakers is a complex matter due to simultaneous interaction of several phenomena. After the circuit breaker contacts separated, an electric arc establishes and the current flow continues through the arc, which consists of a

³⁴ ABB AB (2013), p. 22

³⁵ cf. RAGALLER, K. (1978), p. 11ff.

³⁶ cf. CRASTAN, V. (1999, 2006, 2012), p. 550

³⁷ cf. ABB AB (2013), p. 16

core of extremely hot gas with a high temperature (up to 20000 K). That column of gas is fully ionized. If the current decreases to zero, the diameter of the arc also decreases, with a cross-section proportional to the current. In the area of current's zero-crossing the gas cools down to a temperature of about 2000 K and is no longer ionized plasma and therefore no longer electrical conducting.³⁸

The earliest circuit breakers using SF₆ gas had one extinguishing chamber, which was separated into two parts with different pressures (double-pressure circuit breaker). But they worked on the same principle as air-blast circuit breakers. In SF₆ puffer circuit breakers the gas pressure for the cooling is created during the opening stroke in a compression cylinder. The starting time of the gas compression is the same as the contacts start their motion. The compressed gas is blown out of a nozzle, in which the electric arc burns.³⁹

In a normal puffer circuit breaker the major part of the pressure is created by the energy of the operating mechanism. But it would be more ideal if the arc itself produces the blast pressure and the operating mechanism only needs to deliver enough energy to enable the contact movement. That self-blast principle will make problems at interrupting lower currents but it represents a large step forward on the way of reducing the operating energy. For higher currents the energy, which produces the blast pressure is taken from the arc, which heats the gas. Figure 6 shows the system of a self-blast circuit breaker and its components. The red color represents the current's path through the closed interrupter. It also can be seen that the extinguishing chamber is divided into two sections: the self-blast volume and the puffer volume which are separated by the self-blast valve (cf. Figure 6). If high fault currents are interrupted, the pressure in the self-blast volume, which is generated by the electric arc, is as high, that the valve will close. This should prevent the gas from an escape into the puffer volume. Instead of escaping the pressurized gas flows through the nozzles and extinguishes the arc. The following figure shows a process of high current interruption by a self-blast SF₆ interrupter with pre-compression. The process of current interruption will be explained by that figure.⁴⁰

³⁸ cf. ABB AB (2013), p. 16

³⁹ cf. ABB AB (2013), p. 19

⁴⁰ cf. ABB AB (2013), p. 22ff.

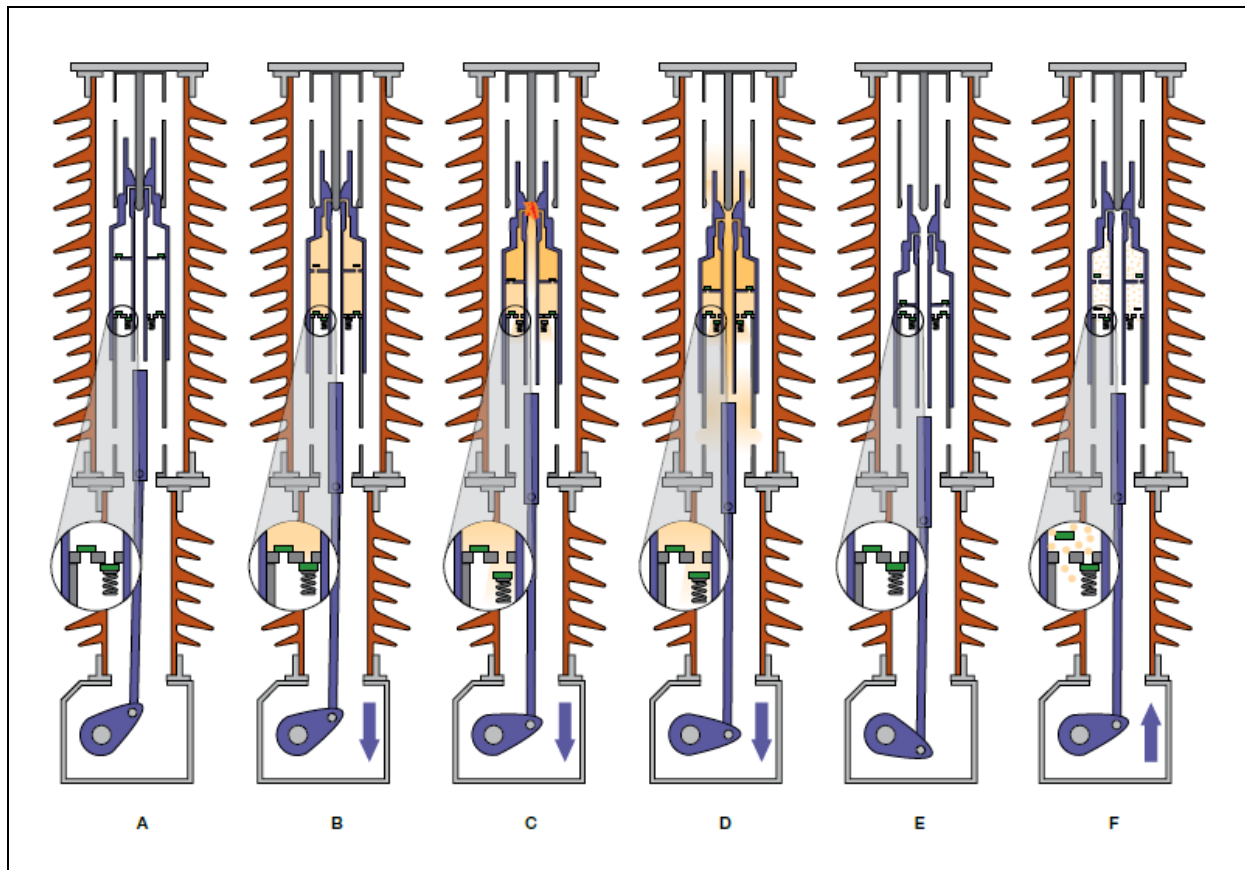


Figure 7: Process of high current interruption by a self-blast SF₆ interrupter with pre-compression⁴¹

Part A in Figure 7 shows the interrupter at closed position. The current conduction is through the main contacts. Afterwards in part B the contact separation starts. The moving contacts have started to change their positions and the main contacts have parted. The pressure starts to build up in both, the puffer and the self-blast volume. The current commutated to the arcing contacts. When the arcing contacts separated, an electric arc establishes between them (part C). The arc's heat generates pressure in the self-blast volume. If the pressure is higher than the pressure in the puffer volume, the valves will close. Part D in the figure above shows the arc extinction. The current approaches zero and the gas in the self-blast volume blasts up through the nozzles. It cools the arc and induces the arc extinction. The pressure in the puffer volume, which is not needed, is released through the pressure relief valve. Afterwards the contacts are open (part E). The contact motion is damped and stopped by the operating mechanism. While the contacts are closing in part F, the puffer volume is being refilled with cold gas and made ready for the next opening operation.⁴²

Today in high voltage nets SF₆ circuit breakers with combined arcing chambers (thermic and blast pistons) are used. These SF₆-circuit breakers are used up to 63 and 80 kA. Their limitation is given by the possibility of motion and the heat dissipation.⁴³

⁴¹ ABB AB (2013), p. 23

⁴² cf. ABB AB (2013), p. 23

⁴³ cf. CRASTAN, V. (1999, 2006, 2012), p. 550f.

Vacuum circuit breakers

Vacuum circuit breakers are the state of the art in medium voltage distributions. The large dielectric strength, the life cycle and the low need of maintenance honor this type of circuit breaker. Generally in vacuum there are no ionizable atoms, so an electric arc can only occur if contact-material vaporizes. Electrons and metal ions diffuse into the vacuum, build conducting plasma and recombine on the metal surfaces of the circuit breaker. At the current zero-crossing the development of the charge carriers stops and it is possible to deionize the switching path fast. Because of the different extinguishing principle, these types of circuit breakers are independent of their mechanical motion.⁴⁴

The main disadvantage of a vacuum circuit breaker is its usability up to about 30 kV, which is the maximum. Furthermore vacuum circuit breakers are not connected in series, in contrast to the usability of circuit breakers with an arc extinguishing medium.

2.3.2 Physics of the electric arc

The efforts to describe the electric arc mathematically started many years ago. Classified by the field of application and the type of arc the mathematic modeling has several differences. As a result different approaches to describe the attributes of the electric arc were developed. A common used way to describe the electric arc is the so called two-terminal-model. This model is characterized by the relation of voltage and current on the terminals of an element. The behavior of the element by using its terminals can be described by a differential equation. This form of mathematical description is based on an integral relation, which describes the electrical behavior of the electric arc. The physical processes inside the electric arc are often neglected.⁴⁵

At the beginning of the researches concerning electric arcs, stationary and quasi-stationary models of electric arc were developed. Current, voltage and arc's length do not vary during an experiment or process. But the physics of the electric arc can't be described in such an easy way. The upgrade of the arc's physic to a dynamic description was essential concerning the systematic development and the improvement of electrical switch gears.⁴⁶

The physical basic of the modeling is the consideration of the arc column concerning its power balance. In stationary case the arc conductance depends on the radial temperature profile and therefore on the thermal capacity Q . In this case the dissipated power $P_{\text{diss}} = V \cdot I$ is only as high as needed to compensate the stationary thermic losses P_{out} . The thermal capacity Q of the arc column is constant. A change of the input power implicates a temperature change in the inner of the column and of the temperature profile as well as a change on the thermal capacity. That influences on the conductivity and reacts on the power requirements of the arc. The following applies:⁴⁷

$$\frac{dQ}{dt} = p - p_{\text{diss}} \quad (2.1)$$

⁴⁴ cf. CRASTAN, V. (1999, 2006, 2012), p. 551f.

⁴⁵ cf. BERGER, S. (2007), p. 10f.

⁴⁶ cf. BERGER, S. (2007), p. 12f.

⁴⁷ cf. BERGER, S. (2007), p. 13

If the conductivity g is a function of the thermal capacity Q , the time derivative is, by using the chain rule of differential calculus,

$$\frac{dg}{dt} = \frac{dg}{dQ} (p - p_{\text{diss}}) . \quad (2.2)$$

Some characteristics of the plasma column are premised by the above mentioned equation.⁴⁸

- The arc column is cylindrically symmetric.
- The conductivity g is a differentiable function of the thermal capacity Q .
- The power p_{diss} , which is dissipated of the arc column, is known.

According to RIEDER, W. (1967) mentioned in BERGER, S. (2007) the exact determination of $g(Q)$ and p_{out} is possible, but associated with high efforts at well-known limiting conditions and plasma properties. Anyway useful simplifications and well-defined conditions led to respectable results in former times⁴⁹.

Mayr's model of the electric arc

MAYR, O. (1943) mentioned in BERGER, S. (2007), investigates wall-stabilized arcs in a tube with known limiting conditions at given wall temperature. Additionally he makes the following assumptions.⁵⁰

- cross-section of the arc: $A = \text{const.}$
- thermal capacity: $Q = \text{const.}$
- specific conductivity: $\sigma = \text{const.} \cdot e^{\text{const} \cdot T}$ with T ... temperature of column

On these assumptions, $g(Q)$ can be described as

$$g(Q) = \text{const} \cdot e^{\frac{Q}{Q_0}} , \quad (2.3)$$

where Q_0 is the heat quantity, which is needed to increase the conductivity of the arc column by the factor e . At constant cross-section of the tube and unchanging column temperature the power loss caused by thermal conduction is also constant. Furthermore, if the thermal conduction is the dominant mechanism to dissipate the heat, the dissipated power p_{diss} is constant in first approximation and $p_{\text{diss}} = P_M = \text{const.}$ Out of equation (2.3) the following results:⁵¹

$$\frac{1}{g} \frac{dg}{dt} = \frac{1}{\tau} \cdot \left(\frac{v_{\text{arc}} \cdot i}{P_M} - 1 \right) , \quad (2.4)$$

where the thermic time constant T of the conductivity is

$$\tau = \frac{Q_0}{P_M} = \text{const.} . \quad (2.5)$$

⁴⁸ cf. BERGER, S. (2007), p. 14

⁴⁹ cf. BERGER, S. (2007), p. 14

⁵⁰ cf. BERGER, S. (2007), p. 14

⁵¹ cf. BERGER, S. (2007), p. 14f.

Mayr's equation is a channel model which represents the typical decaying characteristic of low-current arcs in a first approximation. The characteristic of Mayr's arc voltage is shown in the following figure.⁵²

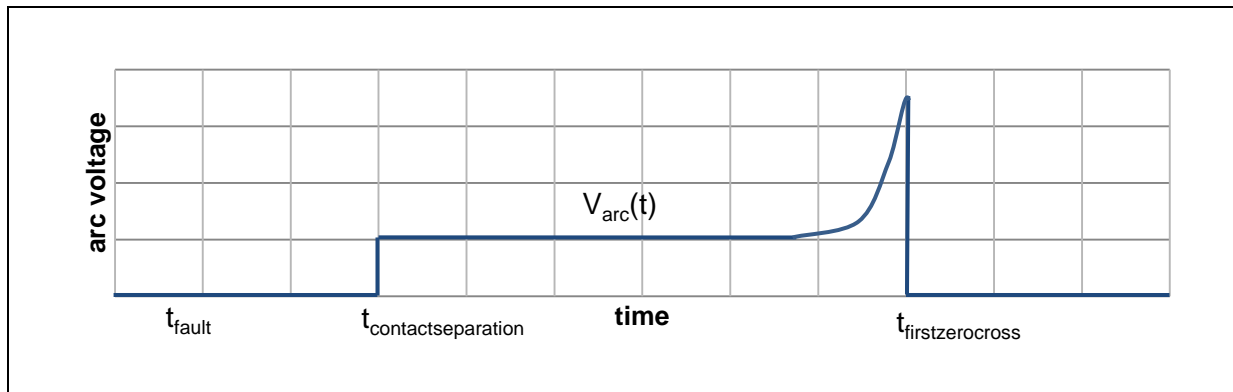


Figure 8: Characteristic of Mayr's arc voltage

After experimental specifications the measures have been shown that the arc parameters T and P_M are not constant. The only independent value is the conductance g . In a first step the power losses P_M can be increased by a current-dependent term $v_M \cdot i$ and Mayr's equation becomes to⁵³

$$\frac{1}{g} \frac{dg}{dt} = \frac{1}{\tau} \cdot \left(\frac{v_{\text{arc}} \cdot i}{P_M + v_M \cdot i} - 1 \right). \quad (2.6)$$

If the parameters P_M and T depend on the conductance g , the modified Mayr's equation can be written down as⁵⁴

$$\frac{1}{g} \frac{dg}{dt} = \frac{1}{\tau(g)} \cdot \left(\frac{v_{\text{arc}} \cdot i}{P(g)} - 1 \right). \quad (2.7)$$

However, the determination of the conductance-dependent parameters is an enormous experimental effort and in general the parameters are adapted to each single application by experimental results of comparable switching-off currents.⁵⁵

According to BERGER, S. (2007) Mayr's equation is not valid in regions of higher currents, because high-current arcs of constant length need a nearly current-independent voltage. This behavior is investigated by Cassie for axial flowed dynamic high-current arcs in cylindrical nozzles and substantiated theoretically by him.⁵⁶

⁵² cf. BERGER, S. (2007), p. 15

⁵³ cf. NEUMANN, C., p. 66

⁵⁴ cf. NEUMANN, C., p. 66

⁵⁵ cf. NEUMANN, C., p. 66

⁵⁶ cf. BERGER, S. (2007), p. 15.

Cassie's model of electric arc

Cassie suspects that the column's cross-section decreases by the axial convection current. Furthermore he simplifies that the arc temperature T and the resulting specific electric conductivity σ were constant and the current density was independent of current:⁵⁷

- current density: $I = \text{const.} \cdot A$ with A ... arc's cross-section
- specific conductivity $\sigma = \text{const.}$

Consequently, the conductance g proportional depends on the arc's cross-section A . At constant temperature the thermal capacity Q is also proportional to the cross-section of the electric arc. From⁵⁸

- conductance: $g = \text{const.} \cdot A$
- thermal capacity: $Q = \text{const.} \cdot A$

follows that

- conductance: $g(Q) = \text{const.} \cdot Q$.

The typical stationary behavior of a high-current arc is that the column's gradient E_c is nearly independent of the current. In stationary case the input power $p = u^2 \cdot g$ is as high as needed to compensate the power $p_{\text{diss}} = v_c^2 \cdot g$, which is dissipated by the convection. By using the chain rule of differential calculus the following equation results:⁵⁹

$$\frac{dg}{dt} = \text{const.} \cdot (v^2 \cdot g - v_c^2 \cdot g) \quad (2.8)$$

The thermal decay constant of the conductance as a result of the interruption of the energy supply is according to BERGER, S. (2007)

$$\tau = \frac{1}{\text{const.} \cdot v_c^2} = \frac{Q}{v_c^2 \cdot g}. \quad (2.9)$$

By using this time constant equation (2.8) leads to

$$\frac{1}{g} \frac{dg}{dt} = \frac{1}{\tau} \left(\frac{v^2}{v_c^2} - 1 \right). \quad (2.10)$$

The following figure shows the characteristic of Cassie's arc voltage.

⁵⁷ cf. BERGER, S. (2007), p. 15

⁵⁸ cf. BERGER, S. (2007), p. 15

⁵⁹ cf. BERGER, S. (2007), p. 15

⁶⁰ cf. BERGER, S. (2007), p. 15

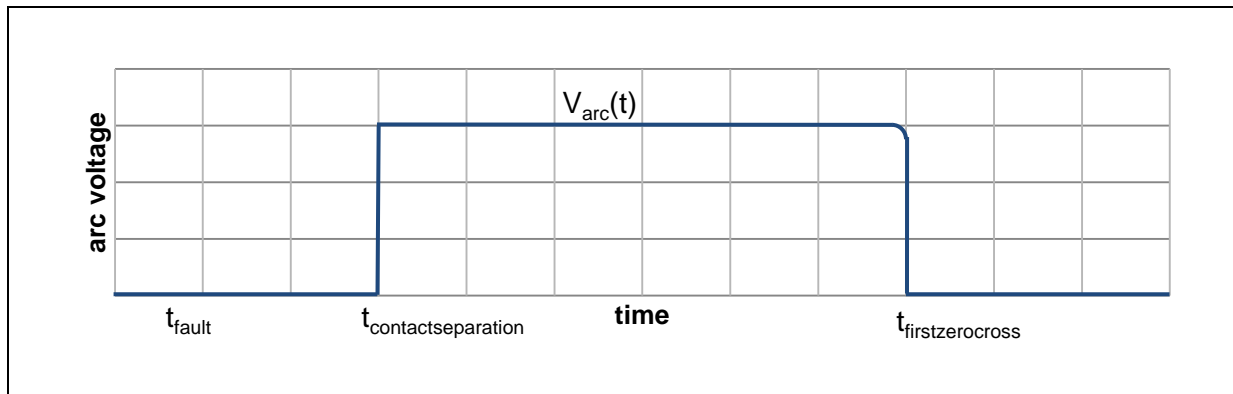


Figure 9: Characteristic of Cassie's arc voltage

According to BERGER, S. (2007) Cassie's model of electric arc is a channel model for high-current arcs, which are determined by the convection, have constant temperature, and their conductance change is caused by the change of the arc's cross-section, which is caused by a convection current. In contrast, however, Mayr's model of electric arc is also a channel model (as described above) but with the difference that the conductivity is not constant over the radius (temperature profile over the radius). In Mayr's model of electric arc the conductivity depends exponentially by the temperature. The characteristics of the high-current arcs are theoretical and experimental founded by LOWKE, J.; KOVITYA, P, AHMED, S. et al (1984) and mentioned in BERGER, S. (2007), even under the influence of both, natural and constrained convection and by using limiting conditions at the electrodes. The theoretical considerations of LOWKE, J.; KOVITYA, P, AHMED, S. et al (1984) mentioned in BERGER, S. (2007) also show that both, Cassie's model of electric arc and Mayr's model of electric arc require specific arc properties. Therefore the range of validity is limited. For this reason there have been and there are many efforts to combine both, Cassie's and Mayr's equation to only one equation.⁶¹⁶²

The combined Cassie-Mayr model of electric arc

As described in BERGER, S. (2007), among others HABEDANK, U.; Siemens AG (1993) combines the above mentioned equations to one. He defines the total conductance g as a series connection of both conductances. One is specified by Mayr's equation and one by Cassie's equation. From this it follows equation (2.11) to⁶³

$$\frac{1}{g} = \frac{1}{g_C} + \frac{1}{g_M}. \quad (2.11)$$

But this approach is not founded physically. In fact Habedank's opinion is, that models on his area of active research of electric current extinguishing would lose all physical relevance in the region of current's zero-crossing. They would only be mathematical tools to calculate the time courses of current and voltage based on experiments. Although this combination of the two mentioned arc models is popular, it's in question if this combined equation is worthy such

⁶¹ cf. BERGER, S. (2007), p. 15f.

⁶² cf. RIEDER, W. (1967), p. 121

⁶³ cf. BERGER, S. (2007), p. 16

an outstanding position, especially in consideration of the amount on mathematical possibilities.^{64,65}

In KOSHIZUKA, T.; SHINKAI, T.; UDAGAWA, K. (2009) the parameters for using the combined Cassie-Mayr model (by using SF₆ gas model circuit breakers at 300 kV, 63 kA, 50 Hz) are described as following, whereby two different sets of parameters are instanced:⁶⁶

$$\begin{array}{ll} T_C = 2.5 \mu\text{s} & T_C = 2.5 \mu\text{s} \\ V_C = 1500 \text{ V} & V_C = 1500 \text{ V} \\ T_M = 1.6 \mu\text{s} & T_M = 0.16 \mu\text{s} \\ P_M = 680 \text{ kW} & P_M = 13.6 \text{ kW} \end{array}$$

BIZJAK, G.; ZUNKO, P.; POVH, D. (2004) defined parameters for the combined circuit breaker model on the basis of measurements tests of real circuit breakers for typical 110 kV SF₆ circuit breakers at a maximum current of 54 kA. The parameters are⁶⁷

$$\begin{array}{l} T_C = 0.8 \mu\text{s} \\ V_C = 2350 \text{ V} \\ T_M = 0.22 \mu\text{s} \\ P_M = 8800 \text{ W} \end{array}$$

Further models of electric arc

Beside the combined Cassie-Mayr model there are many other modifications to describe the electric arc. For better adaption of the varying conditions during the process of arc extinguishing different parameters, also not constant ones are implemented.⁶⁸

It should be considered that many of them are modified for specific experiments and measurements. The universal validity of the different models has not been proved so far.

The model of **Schwarz and Avdonin** is described in FILIPOVIC-GRCIC, B.; UGLESIC, I.; FILIPOVIC-GRCIC, D. (2011) and is

$$\frac{1}{g} \frac{dg}{dt} = \frac{1}{T_0 \cdot g^\alpha} \left[\frac{v \cdot i}{P_0 \cdot g^\beta} - 1 \right].^{69} \quad (2.12)$$

As can be seen, it is a further development of Mayr's model of electric arc, described above (cf. equations (2.4) and (2.7)).

The calculation of the arc conductance requires data on the cooling power P and on the thermal time constant T. These two parameters, P(g) and T(g), are conductance dependent. They also depend on the temperature and the circuit breaker type and design. The cooling power P and the thermal time constant T can be defined as functions of conductance (as shown below), where α and β are constants.⁷⁰

⁶⁴ cf. BERGER, S. (2007), p. 16

⁶⁵ cf. HABEDANK, U.; SIEMENS AG (1993)

⁶⁶ cf. KOSHIZUKA, T.; SHINKAI, T.; UDAGAWA, K. (2009), p. 2

⁶⁷ cf. BIZJAK, G.; ZUNKO, P.; POVH, D. (2004), p. 176f.

⁶⁸ cf. BERGER, S. (2007), p. 17

⁶⁹ cf. FILIPOVIC-GRCIC, B.; UGLESIC, I.; FILIPOVIC-GRCIC, D. (2011), p. 2653

⁷⁰ cf. FILIPOVIC-GRCIC, B.; UGLESIC, I.; FILIPOVIC-GRCIC, D. (2011), p. 2653

$$T(g) = T_0 \cdot g^\alpha \quad (2.13)$$

$$P(g) = P_0 \cdot g^\beta \quad (2.14)$$

The parameter α is described as parameter that influences the conductance dependency of T_0 ; the parameter β influences the conductance dependency of P_0 . Both α and β are experimental constant parameters. For a rated voltage of 245 kV in ORAMA-EXCLUSA, L.; RODRÍGUEZ-MEDINA, B. (2003) following parameter values were determined, with the note that the parameters change according to the device and the circuit conditions:⁷¹

$$P_0 = 2.0 \text{ MW}$$

$$T_0 = 11.2 \text{ } \mu\text{s}$$

$$\alpha = 0.523$$

$$\beta = 0.59$$

The Model ZAGREB in HUTTER, S.; UGLESIC, I. (2007) also describes that type of combined Cassie-Mayr model. The following parameters for the equations (2.13) and (2.14) are used:⁷²

$$P_0 = 4.0 \text{ MW}$$

$$T_0 = 1.5 \text{ } \mu\text{s}$$

$$\alpha = 0.17$$

$$\beta = 0.68$$

The test circuit (60 Hz) consists of a source voltage of 57.7 kV_{peak} and can also be seen in HUTTER, S.; UGLESIC, I. (2007).

In MARTINEZ, J.; MAHSEREDJIAN, J.; KHODABAKHCHIAN, B. (2005) parameters for SF₆ circuit breakers are given as:⁷³

$$P_0 = 1 \text{ MW}$$

$$T_0 = 1.3 \text{ } \mu\text{s}$$

$$\alpha = -0.15$$

$$\beta = -0.28$$

The arc models of Cassie and Mayr were developed in the 1930s and 1940s. Since then many other models were proposed and although they became more complex with time, none of them was truly able to represent the extreme complexity in case of electric arcs and the region of current zero-crossing. A new look on the physics of the electric arc, its interruption process and its extinguishing is made by **Rieder and Urbanek**. Both expressed some doubts regarding the assumption of thermal equilibrium used in most models up to that time. It was finally realized that the combined Cassie-Mayr equation and various modifications of it inadequately describe the physical processes occurring in gas-blast circuit breakers. The

⁷¹ cf. ORAMA-EXCLUSA, L.; RODRÍGUEZ-MEDINA, B. (2003), p. 2

⁷² cf. HUTTER, S.; UGLESIC, I. (2007), p. 2

⁷³ cf. MARTINEZ, J.; MAHSEREDJIAN, J.; KHODABAKHCHIAN, B. (2005), p. 2082

nowadays design engineers are not able to answer several important questions by using the popular Cassie-Mayr models.⁷⁴

The KEMA High Power Laboratory Group introduced one of the innovations in arc models. It is another combination of Cassie's and Mayr's equation, but the arc model is adapted by **Schavemaker and Van der Sluis** to

$$\frac{1}{g} \frac{dg}{dt} = \frac{1}{\tau} \cdot \left(\frac{v \cdot i}{\max\{V_{\text{arc}} \cdot |i|, P_0 + P_1 v \cdot i\}} - 1 \right). \quad (2.15)$$

P_0 and P_1 are cooling power constants and T is the arc time constant. V_{arc} is the constant arc voltage in the high current area. If the value of V_{arc} is zero, KEMA will transform into Mayr's equation. The model represents Cassie's model during the high current, while nearby the zero current the modified Mayr model is dominant. That feature is provided by the "max" statement in the equation (2.15). The following parameter values have been determined from a least square fit of KEMA experimental results. The considered parameters for SF₆ circuit breakers rated at 245 kV / 50 kA / 50 Hz are⁷⁶

$$T = 0.27 \mu\text{s}$$

$$P_0 = 15917 \text{ W}$$

$$P_1 = 0.994 \text{ W}$$

⁷⁴ cf. REECE, M.P. (1985), p. 41f.

⁷⁵ cf. SCHAVEMAKER, P.; VAN DER SLUIS, L. (2000) in DARWISH, H.; ELKALASHY, N. (2003), p. 5

Note that there must be an error in the above mentioned equation. Correctly there should be an addition or subtraction in the equation's part " $P_1 v \cdot i$ ". Otherwise the units are not in accordance with each other.

⁷⁶ cf. SCHAVEMAKER, P.; VAN DER SLUIS, L. (2000) in DARWISH, H.; ELKALASHY, N. (2003), p. 5

3 Modeling

This chapter is about the modeling process of the circuit to be analyzed. The structure of the overall network is shown in Figure 10. The modeling of the circuit occurs in two phases:

- Modeling of the overall structure
- Modeling of circuit breaker and electric arc

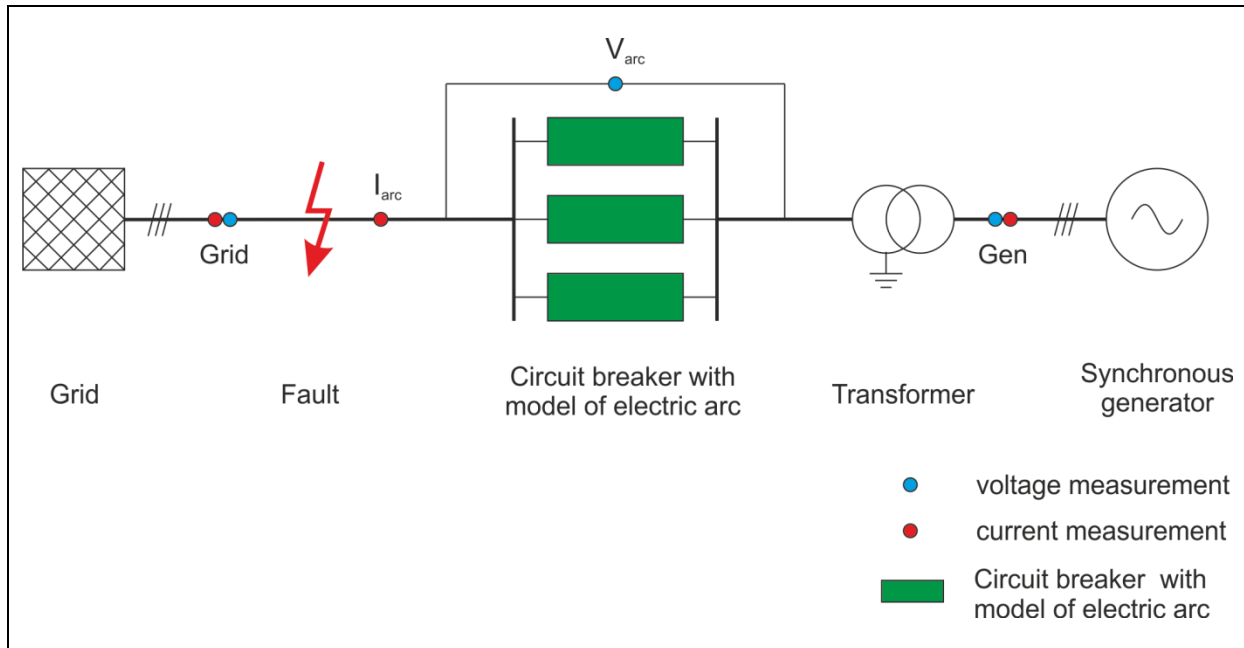


Figure 10: Equivalent network

To execute the modeling of the on hand overall network and to do the numeric simulation there are various application software tools. The electromagnetics transient program EMTP-RV is chosen because of its international acceptance and use.

“EMTP-RV is a professional software for simulation and analysis of transients in power systems”⁷⁷

In addition to that EMTP-RV offers high flexibility to solve different assignments of tasks, especially concerning transients in power systems and proved successfully as such a suitable tool for these types of analyses.

All numeric calculation, analyses and plots were done by using the software MATLAB R2008a. MATLAB is a product of MathWorks® and a common software to do technical and scientific calculations.

⁷⁷ EMTP-RV (2013)

3.1 Modeling of structure

As shown in Figure 10 the overall structure consists of four basic elements (by excluding the circuit breaker with model of the electric arc), which are specified in the following, and a few points of measurement.

Grid

The grid is modeled by a voltage source with source impedance. The wye connection is solidly grounded. A load-flow bus (type: slack bus) arranges a stable voltage at node "Grid" (cf. Figure 10).

V	380	kV _{RMS,LL}
f	50	Hz
S _{SC,1pol}	5000	MVA
S _{SC,3pol}	7000	MVA
X/R	12	---

Table 3: Parameters of element grid

Fault

The section fault is modeled with ideal switches and defined closing times to build several types of faults (line-to-earth faults, short-circuits, etc.). In the on hand Master's thesis there is only a three phase short-circuit fault with and without earth connection used.

Transformer

The transformer-block is composed of non-ideal transformer units based on the ideal transformer. The voltage level is 380 kV_{RMS,LL} on high tension and 13,8 kV_{RMS,LL} on low tension.

Voltage ratio	380/13,8	---
f _{rT}	50	Hz
S _{rT}	223	MVA
u _k	14.5	%
r _k	0.29	%
X/R on high tension/low tension	1:1	---

Table 4: Parameters of element transformer

The winding connection of the transformer is YNd5 (with a solidly grounded wye connection). The saturation is untended. Furthermore losses such as iron losses and hysteresis losses

are also untended. The following figure shows the correct circuitry of a transformer of type YNd5 (wye connection solidly grounded) or Yd5 (wye connection without ground connection).

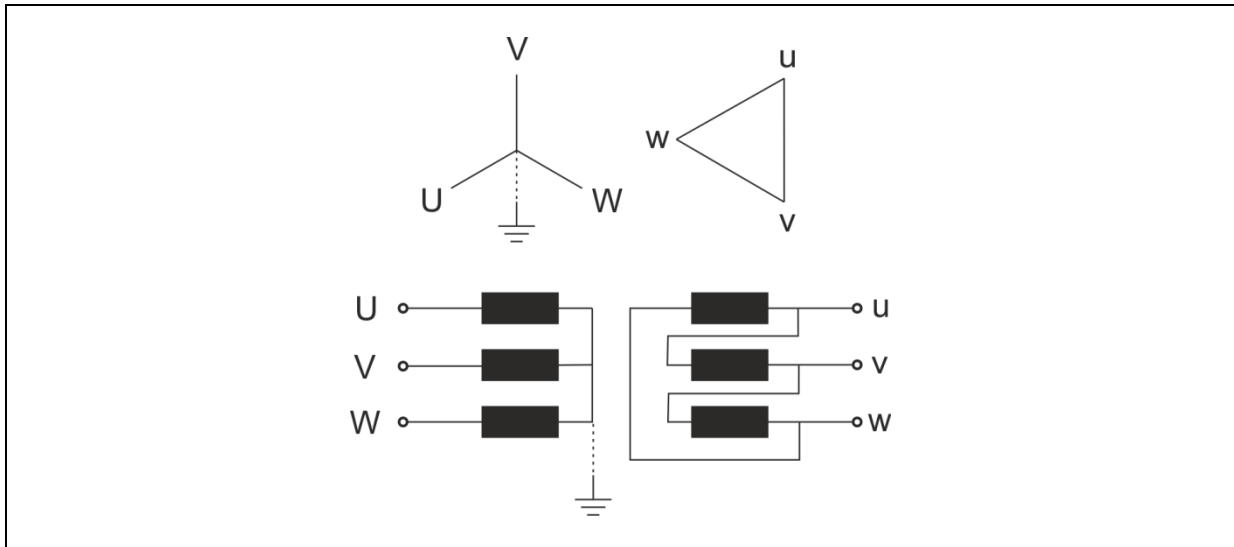


Figure 11: Connection symbol of Yd5/YNd5-transformer

In addition to the ratio $\frac{\sqrt{3} \cdot w_1}{w_2}$, an YNd5 transformer is characterized by a phase rotation of $5 \cdot 30^\circ = 150^\circ$. These types of transformers are commonly used in electric networks.

Synchronous generator

The parameters of the synchronous generator can be seen in Table 5.

V_{RG}	13,8	kV _{RMS,LL}	f	50	Hz
S_{RG}	223	MVA	cos φ	0.9	--
Speed	187,5	rpm	I_f	1562	A
T_a	0.33	s	R_a	0.00163	p.u.
X_2	0.215	p.u.	X_0	0.1	p.u.
X_d	1.06	p.u.	X_q	0.71	p.u.
X_{potier}	0.17	p.u.	H	4.4	--
X_d'	0.29	p.u.	X_d''	0.225	p.u.
X_q'	0.71	p.u.	X_q''	0.206	p.u.
T_d'	2.5	s	T_d''	0.076	s
T_q'	0	s	T_q''	0.07	s
T_{d0}'	9.2	s	T_{d0}''	0.0098	s
T_{q0}'	0	s	T_{q0}''	0.25	s

Table 5: Parameters of element synchronous generator

The generator is modeled by the block for synchronous machines (library “machines”). On basis of a load-flow bus (type: PQ control) it’s possible to set various generator operating points, which have an influence of voltage and current profiles at node “Gen” (cf. Figure 10).

The generator is a salient-pole machine with field winding and damper winding on d-axis and damper winding on q-axis. The saturation of the machine is untended; the armature winding is connected in wye (floating).

Measurements

To realize the measurements the library meters provides various helpful tools, like “i scope and observe” or “v scope (1 pin)” and “v scope (2 pins)”.

Calculation of range of expected short-circuit currents

The following calculation is to assess the range of the expected short-circuit currents.

The rated current I_{rG} of a synchronous generator is calculated by the rated power S_{rG} and the rated voltage V_{rG} .

$$I_{rG} = \frac{S_{rG}}{\sqrt{3} \cdot V_{rG}} \quad (3.1)$$

The result in this on hand case is

$$I_{rG} = \frac{223 \text{ MVA}}{\sqrt{3} \cdot 13.8 \text{ kV}} = 9.33 \text{ kA} . \quad (3.2)$$

To calculate the initial (sub-transient) short-circuit current I_c'' it is necessary to know the total sub-transient short-circuit impedance Z_{cG} , which could be determined as

$$Z_{cG} = \frac{x_d'' + x_q''}{2} \cdot \frac{(U_{rG})^2}{S_{rG}} , \quad (3.3)$$

whereby the related value of the impedance is the average of the sub-transient short-circuit impedances in both direct and quadrature axes.

By inserting the above given values the result is

$$Z_{cG} = \frac{0.225 + 0.206}{2} \cdot \frac{(13.8 \text{ kV})^2}{223 \text{ MVA}} = 0.18 \Omega . \quad (3.4)$$

The expected initial value of the short-circuit current I_{cG}'' on the low-voltage side can be calculated by the short-circuit impedance Z_{cG} to

$$I_{cG}'' = 60.96 \text{ kA} . \quad (3.5)$$

This means an increase of the short-circuit current compared to the rated current of nearly six times. In the on hand Master’s thesis the circuit breaker operates on high tension.

Therefore the current to be considered through the circuit breaker has to be calculated on high tension (cf. Figure 10).

The transformer's short-circuit impedance can be calculated to

$$Z_{cT} = u_k \cdot \frac{(U_{rT})^2}{S_{rT}} . \quad (3.6)$$

In this case a value of

$$Z_{cT} = 0.145 \cdot \frac{(380 \text{ kV})^2}{223 \text{ MVA}} = 93.89 \Omega , \quad (3.7)$$

could be estimated related on the high voltage side.

To determine the total effective impedance the short-circuit impedance of the synchronous generator has to be converted on high voltage side, like following shows, to

$$Z'_{cG} = Z_{cG} \cdot \left(\frac{380 \text{ kV}}{13.8 \text{ kV}} \right)^2 = 0.18 \Omega \cdot \left(\frac{380 \text{ kV}}{13.8 \text{ kV}} \right)^2 = 136.48 \Omega . \quad (3.8)$$

With the sum of the values of the transformer's short-circuit impedance and the converted synchronous generator's short-circuit impedance an estimated initial value of the short-circuit current I_c on high voltage side (at circuit breaker) can be calculated.

$$Z_{\text{sum}} = Z_{cT} + Z'_{cG} = 93.89 \Omega + 136.48 \Omega = 230.37 \Omega \quad (3.9)$$

$$I''_c = \frac{U_{rT}}{\sqrt{3} \cdot Z_{\text{sum}}} \cdot 1.1 . \quad (3.10)$$

$$I''_c = \frac{380 \text{ kV}}{\sqrt{3} \cdot 230.37 \Omega} \cdot 1.1 = 1.05 \text{ kA} . \quad (3.11)$$

The short-circuit current which should be interrupted by the high voltage circuit breaker is in a range of about 1 kA. Assigning the value of the short-circuit current it should not be a problem for circuit breakers like SF₆ circuit breakers to break such current ranges. According to CRATAN, V. (1999, 2006, 2012) SF₆ circuit breakers are built for currents up to 63 and 80 kA.⁷⁸

⁷⁸ CRATAN, V. (1999, 2006, 2012), p. 551

3.2 Modeling of electric arc

In this chapter the implementations of the used arc models in the software EMTP-RV are described. The following models are considered in the on hand Master's thesis:

- Model with constant d.c. arc voltage
- Cassie's model of electric arc
- Mayr's model of electric arc
- Combination of Cassie's and Mayr's arc model

Model with constant d.c. arc voltage

The model with constant d.c. voltage is characterized by the constant arc voltage, which applies between $t_{\text{contactseparation}}$ and $t_{\text{firstzerocross}}$, which is the time period of arc lightening. The typical characteristic of the constant d.c. arc voltage is diagrammed in Figure 12.

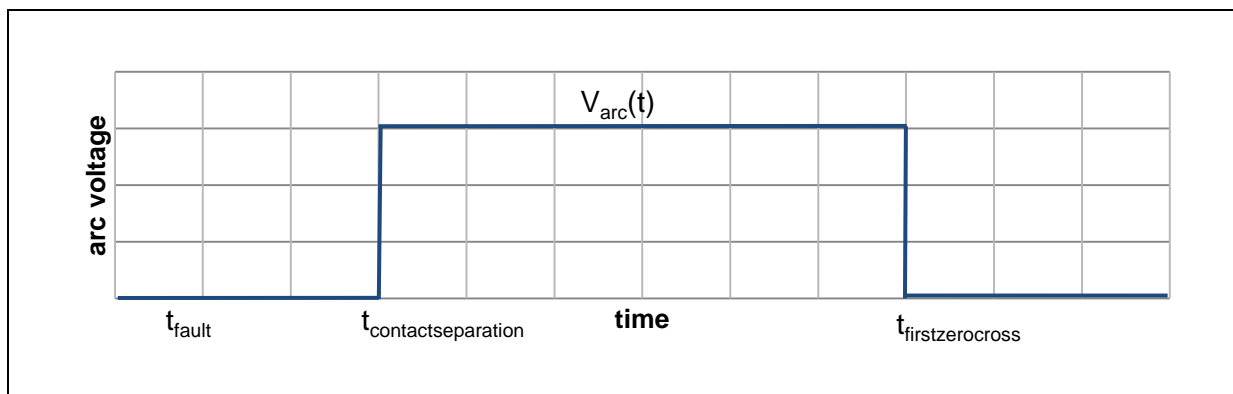


Figure 12: Schematic diagram of arc voltage if arc voltage is a constant d.c. voltage

Start of the arc voltage is 40 ms after the fault occurs ($t_{\text{contactseparation}}$), $t_{\text{firstzerocross}}$ is the point where the circuit breaker contacts are separated, the electric arc is extinguished and the current is zero. The model is realized with two ideal switches, which operate contrary, and a DC voltage source. The voltage level can easily be set by the DC voltage source.

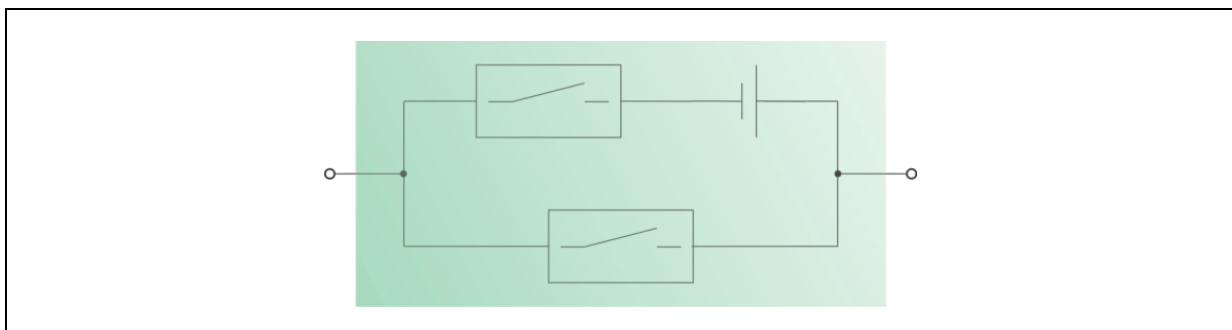


Figure 13: Implementation of model with constant d.c. arc voltage

Cassie's equation

Cassie's equation is composed of various useful elements of library "control". The library "nonlinear" provides the element "R nonlinear controlled", which is used to insert the equation into the overall network (please also refer to chapter 2.3.2).

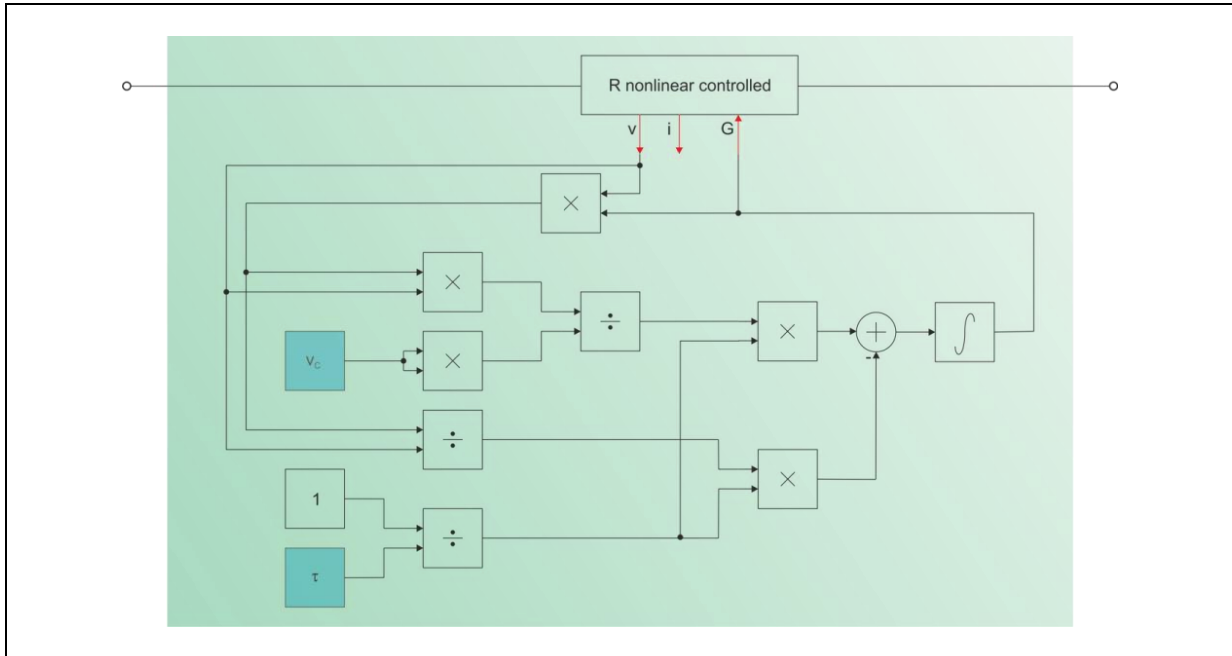


Figure 14: Implementation of Cassie's equation

As can be seen in the figure above fundamental operations of arithmetic are sufficient, except an integrator element, to implement Cassie's equation. The same is guilty for the implementation of Mayr's equation or the combined Cassie-Mayr equation. The parameters V_c and T can be set as constants. The integrator is without any limits. To avoid divisions by zero, the current through the arc is calculated by the arc voltage v and the arc conductance G . The current pin i is not used.

Mayr's equation

Mayr's equation is like Cassie's equation composed of various useful elements of library "control". The library "nonlinear" provides the element "R nonlinear controlled", which is used to insert the equation into the overall network (please also refer to chapter 2.3.2). The current in Mayr's model is (as in Cassie's equation above) calculated from the voltage and the electric conductance.

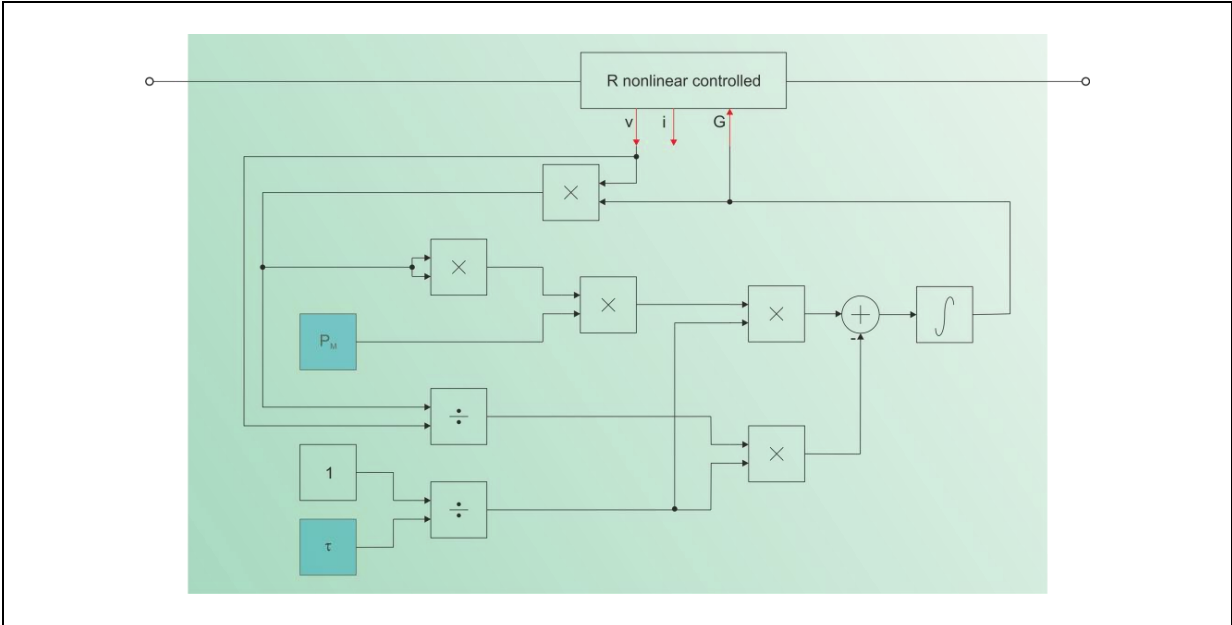


Figure 15: Implementation of Mayr's equation

Combined Cassie-Mayr equation

As described in chapter 2.3.2 the combined Cassie-Mayr equation is the sum of both reactances Cassie and Mayr. The block diagram can be seen in the following figure.

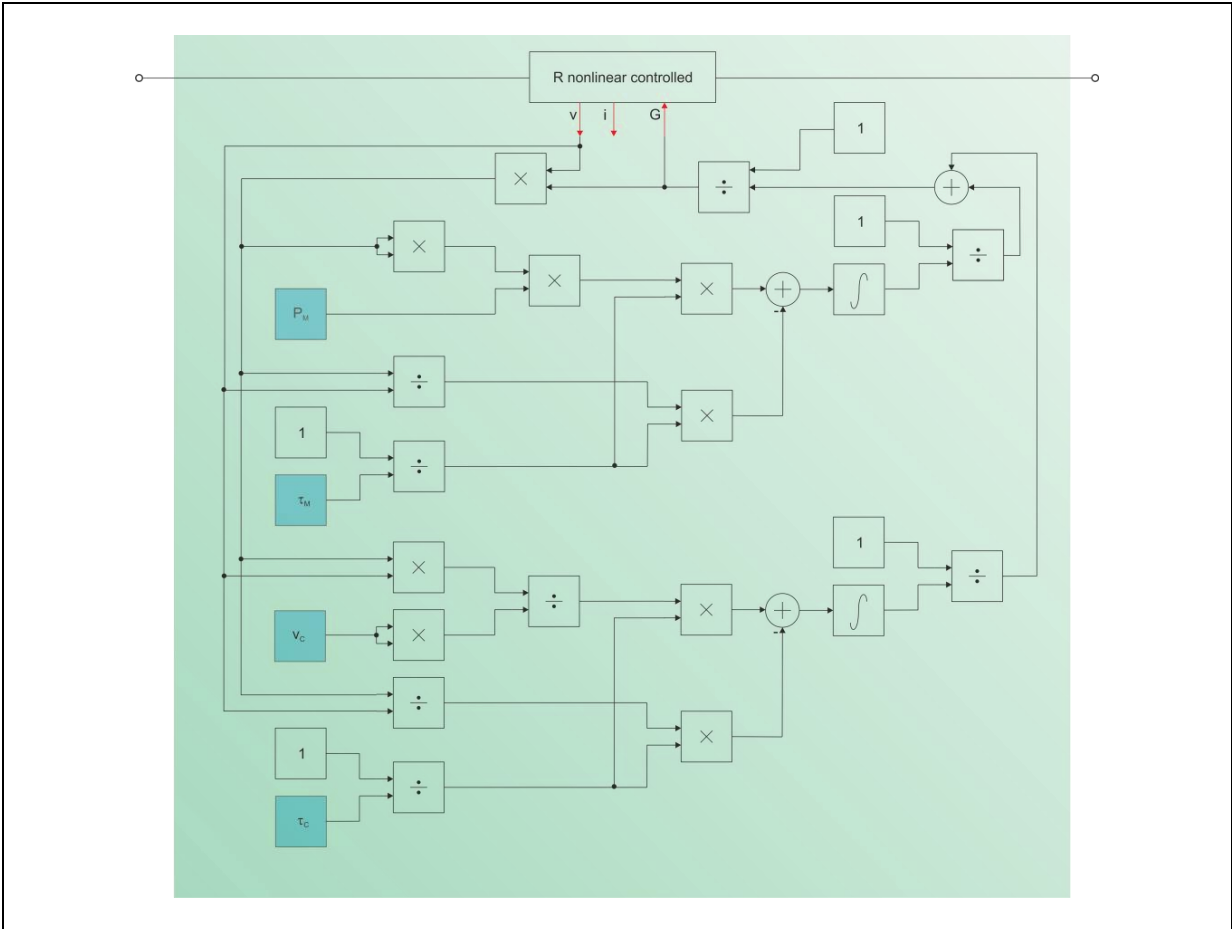


Figure 16: Implementation of the combined Cassie-Mayr equation

4 Results and discussion

This chapter is concerned with all kinds of analyses belonging to the on hand Master's thesis, including

- worst-case point on wave calculation with respect to the DC-component
- selection of outlined operating points
- comparison of the arc models in a single-phase circuit
- evaluation of results using a single-phase circuit
- implementation of relevant arc models in a three phase circuit
- discussion about the impact of arc voltage on zero-crossing of current considering the wye-connection of the transformer
- discussion about the impact of arc voltage on zero-crossing of current considering the ground-connection of the fault

4.1 Worst-case point on wave with respect to the DC-component

Before starting with the analyses the worst-case point on wave with respect to the DC-component has to be found. It is calculated for the nominal rating point of the synchronous machine, but also valid for the other outlined operating points. The variation of point on wave happens in steps of 9° (equates to steps of 0.5 ms) over a half-wave. Starting point is at zero-crossing of phase-to-earth voltage in phase A of generator voltage, time $t_0 = 0$ ms (cf. Figure 17). As fault there is chosen a three-phase short-circuit (without ground connection). The interesting factor is the current's DC-component in point of contact separation (estimated 40 ms after fault).

The following equations show a step-by-step calculation of the current's DC-component.

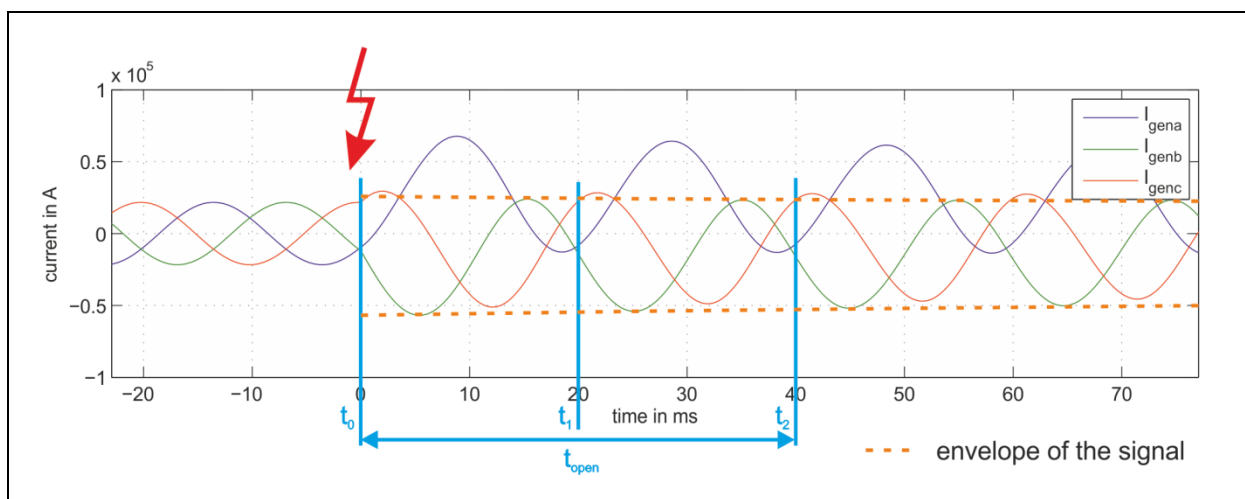


Figure 17: Chart of signal sequences including the naming

$$t_2 = t_0 + t_{\text{contactseparation}} \quad (4.1)$$

$$t_1 = t_2 - \frac{1}{f} \quad (4.2)$$

$$\Delta T = t_2 - t_1 \quad (4.3)$$

$$i_{DC} = \frac{1}{\Delta T} \cdot \int_{t_1}^{t_2} i(t) dt \quad (4.4)$$

$$i_{AC} = \sqrt{\frac{1}{\Delta T} \cdot \int_{t_1}^{t_2} [i(t) - i_{DC}]^2 dt} \quad (4.5)$$

$$i_{DC,rel} = \frac{i_{DC}}{\sqrt{2} \cdot i_{AC}} \cdot 100 \% \quad (4.6)$$

Figure 18 reflects the periodic characteristic of the maxima in the different phases in steps of 60°, as expected, the corresponding table is provided in the appendix.

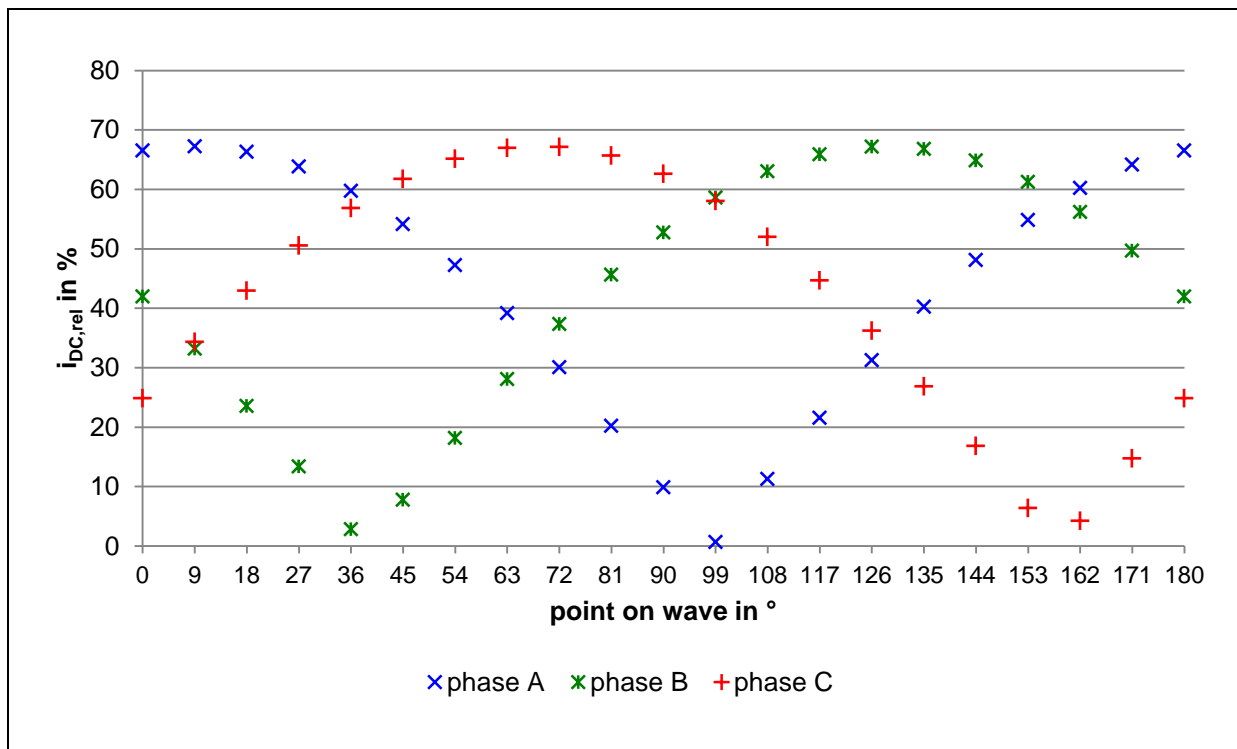


Figure 18: Relative DC-component of phase current in different phases

It is also shown, that the DC-component is highest at the voltage's zero-crossings of the different phases (at 0°, about 60° and about 120°) as described in chapter 2.2.2. The lowest DC-component (nearly 0 % in the figure above) appears when the phase-to-earth voltage is at maximum peak. It has to be considered that the calculation is only an approximation because of the discrete availability of the signal, so there could be little differences between the figure above and the theoretic analyses.

For further analyses the point on wave is set at 0°. The starting point is, like above mentioned, the point of time where the voltage zero-crossing of phase A in the rising edge appears. The worst case point on wave for a three-phase fault concerning the DC-component is (according to chapter 2.2.2) if the phase voltage crosses zero in rising edge.

4.2 Selection of operating points

For the selection of the operating points the uninfluenced short-circuit signal sequences of all operating points are needed. The assignment of tasks is to use the operating points 1, 2 and 6 in any case and in addition to that to identify the worst-case concerning the DC-component and the point of time of current's first zero-crossing out of the operating points 3, 4 and 5.

The current's DC-component is calculated as in chapter 4.1 executed. The calculation results are shown in Table 6.

Operating point	$i_{DC,rel}$ in %			$t_{firstzerocross}$ in ms		
	Phase A	Phase B	Phase C	Phase A	Phase B	Phase C
1	95,61	57,68	37,32	64,71	63,18	70,49
2	80,13	49,31	31,15	64,24	75,37	69,46
3	114,47	71,08	43,94	139,55	75,51	68,35
4	188,99	115,63	72,57	400,00	400,00	64,00
5	99,42	60,80	39,08	63,58	76,51	69,86
6	176,41	106,81	70,84	282,79	99,62	64,02

Table 6: DC-component of current and point of time of current's first zero-cross in each phase in due consideration of different operating points

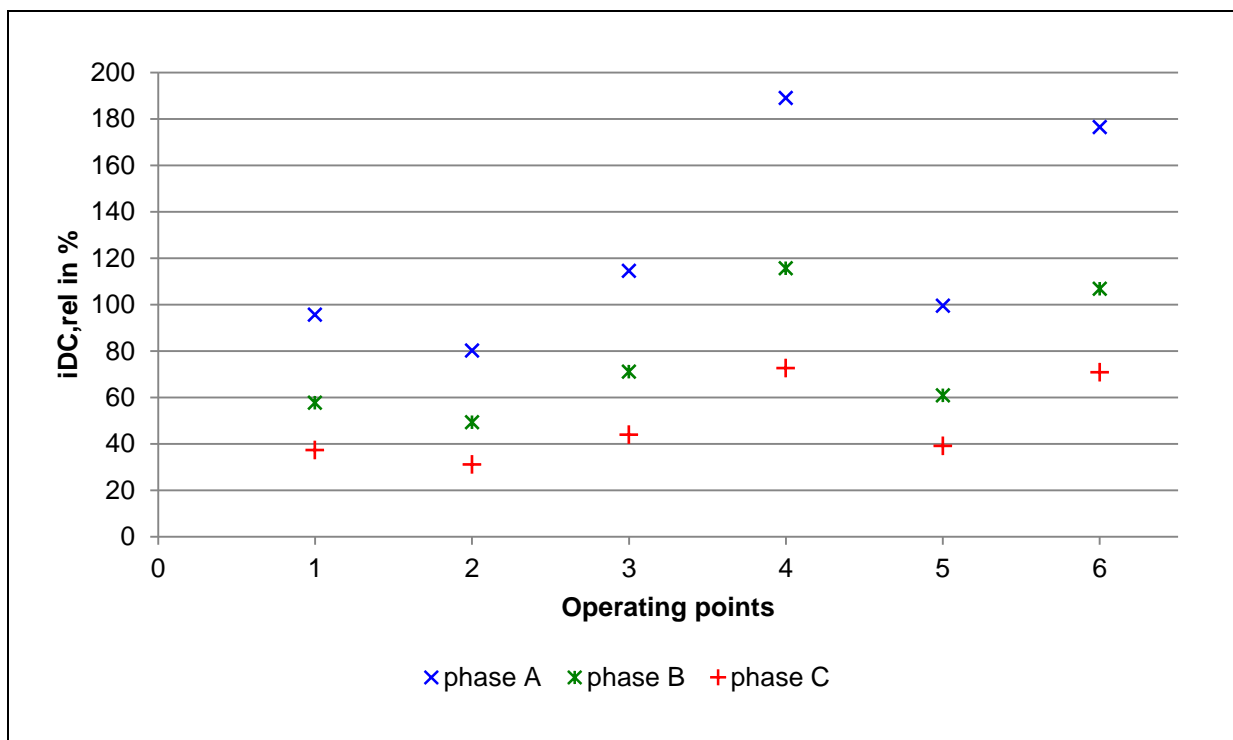


Figure 19: Relative DC-component of current in each phase in due consideration of different operating points

As shown in Figure 19, there is a wide difference concerning the relative DC-components. On the one hand there are differences between the three phases in one operating point, in which phase A is the most disadvantaged phase of all. This is valid for all considered operating points. On the other hand there are also differences between the six operating points.

While the operating points 1 (open-circuit point) and 2 (nominal rating point) show a relative DC-component of about 100 % (maximum value), the other operating points have a clearly higher value of DC-component, expect operating point 5. But it has to be considered, that operating point 5 is at minimal turbine output and under-excited rated power factor ($p = 0.3$ p.u., $q = -0.25$ p.u.), in opposition to the other points, where active power p or reactive power q have values of at least 0.9 (expect open-circuit point).

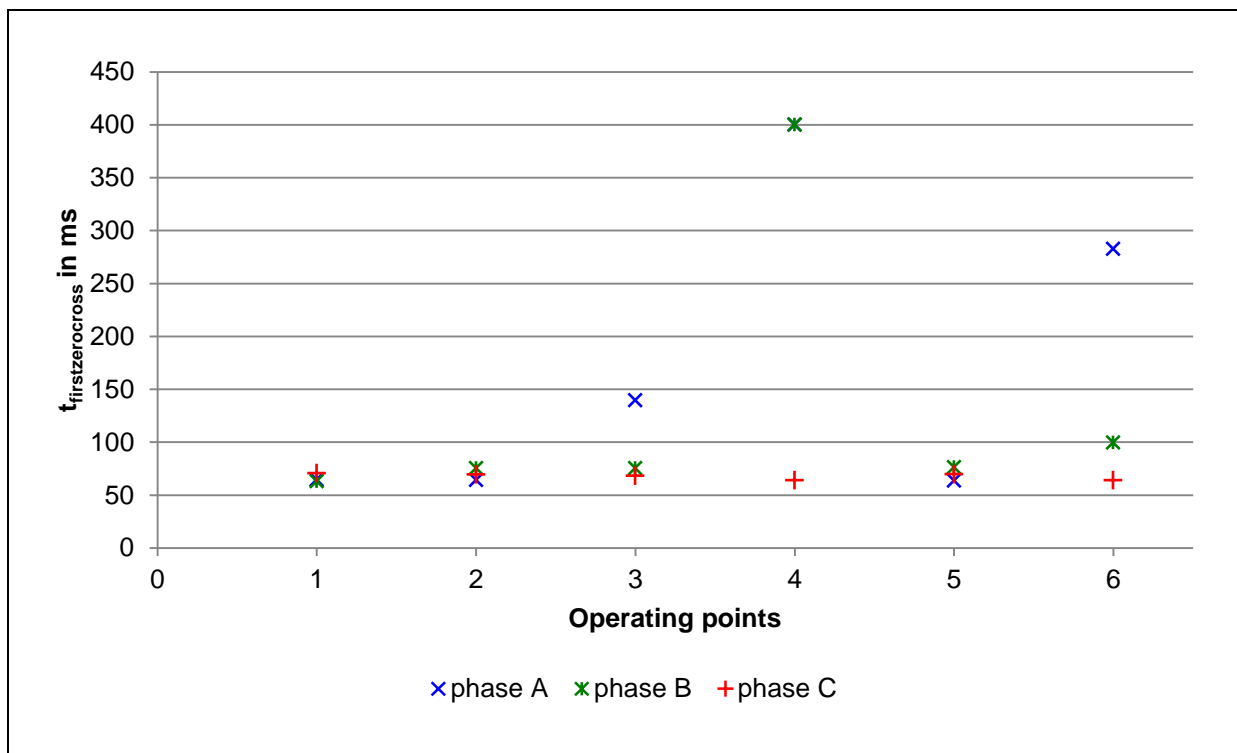


Figure 20: Point of time of current's first zero-crossing in each phase in due consideration of different operating points

It's the same story in both DC-component and current's zero-crossing: The point of time of current's first zero-crossing in the operating points 1 and 2 is immediately after the point of time of contact separation (40 ms). The similar pattern can be seen at operating point 5. In operating point 3 the point of first current's zero-crossing appears about twice later in phase A; the phases B and C show the first zero-crossing of current immediately after contact separation. As a result only the operating points 4 and 6 have clearly later points of first zero-crossings in some phases.

There is an evident difference of the relative DC-component and the first zero-crossing of current between the operating points 3, 4 and 5, whereas operating point 4 is clearly at a disadvantage. The DC-component of phase A at operating point 4 is nearly twice of the DC-component in the same phase at the operating points 3 and 5. Therefore operating point 4 is

chosen as worst-case operating point out of the operating points 3, 4 and 5. For further analyses the points 1, 2, 4 and 6 are identified as relevant initial conditions.

4.3 Comparison of arc models, single-phase

Before implementing the different arc models (described in chapter 2.3.2) in the structure shown in Figure 3, it is useful to test the arc models in a one phase test circuit and verify their availability.

Therefore a single-phase test circuit with a source and different types of loads in the system are built up.

Pure resistive test circuit with resistance R

True for all models is the circuit breaker opening time, $t_{\text{contactseparation}} = 20$ ms.

To compare the different arc models in single-phase a test circuit with a superposed voltage signal, a circuit breaker model, a resistance R, an amperemeter for current detection and a voltmeter for arc voltage measurement is built up as shown in Figure 21.

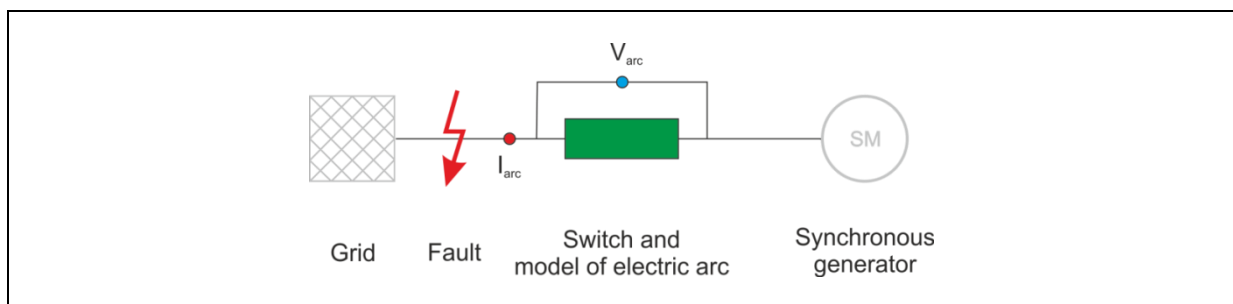


Figure 21: Equivalent network

The voltage's and the current's decaying waves with missing zero-crossings are diagrammed in Figure 22, a similar decaying characteristic is typical for short-circuit currents of synchronous generators.

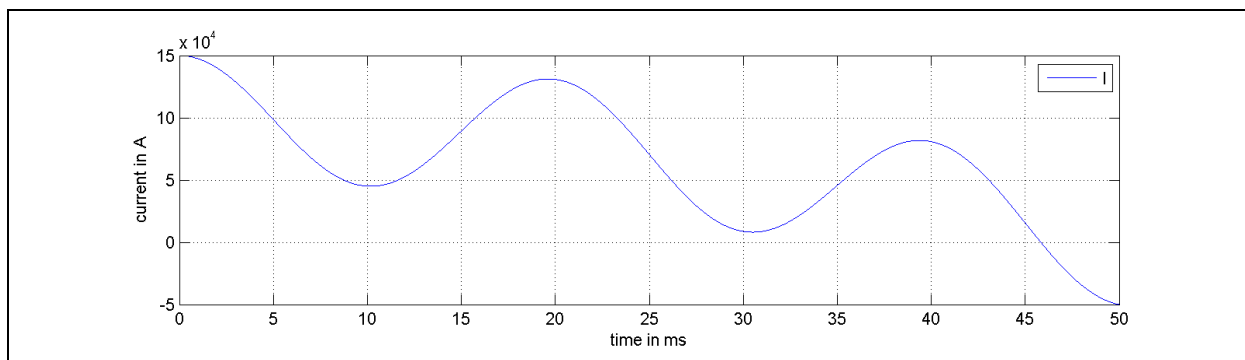


Figure 22: Reference current basic signal

The following figures show the signal sequences using different arc models. Figure 23 shows only the model with a constant d.c. arc voltage of different values. The corresponding arc model parameters and calculated values may be seen in Table 7.

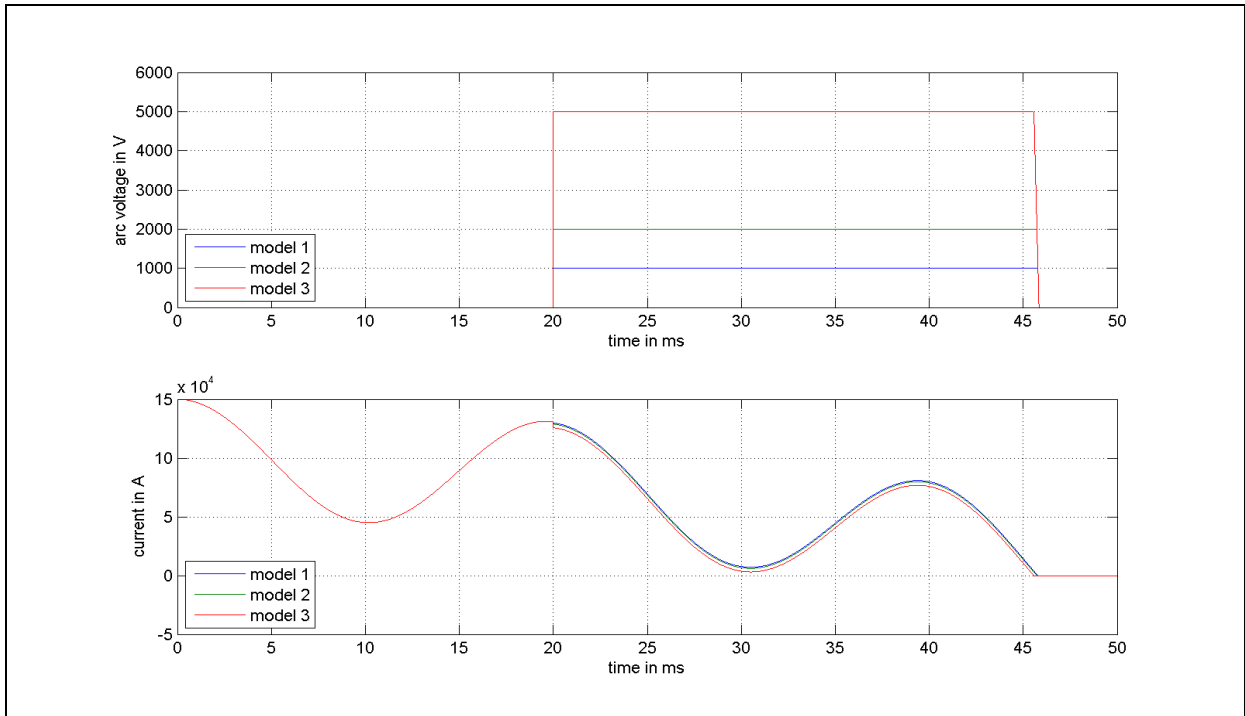


Figure 23: Signal sequences at different arc voltages by using the model with constant d.c. arc voltage

In Figure 24 you can see the comparison of arc voltage and current profile between different used arc models.

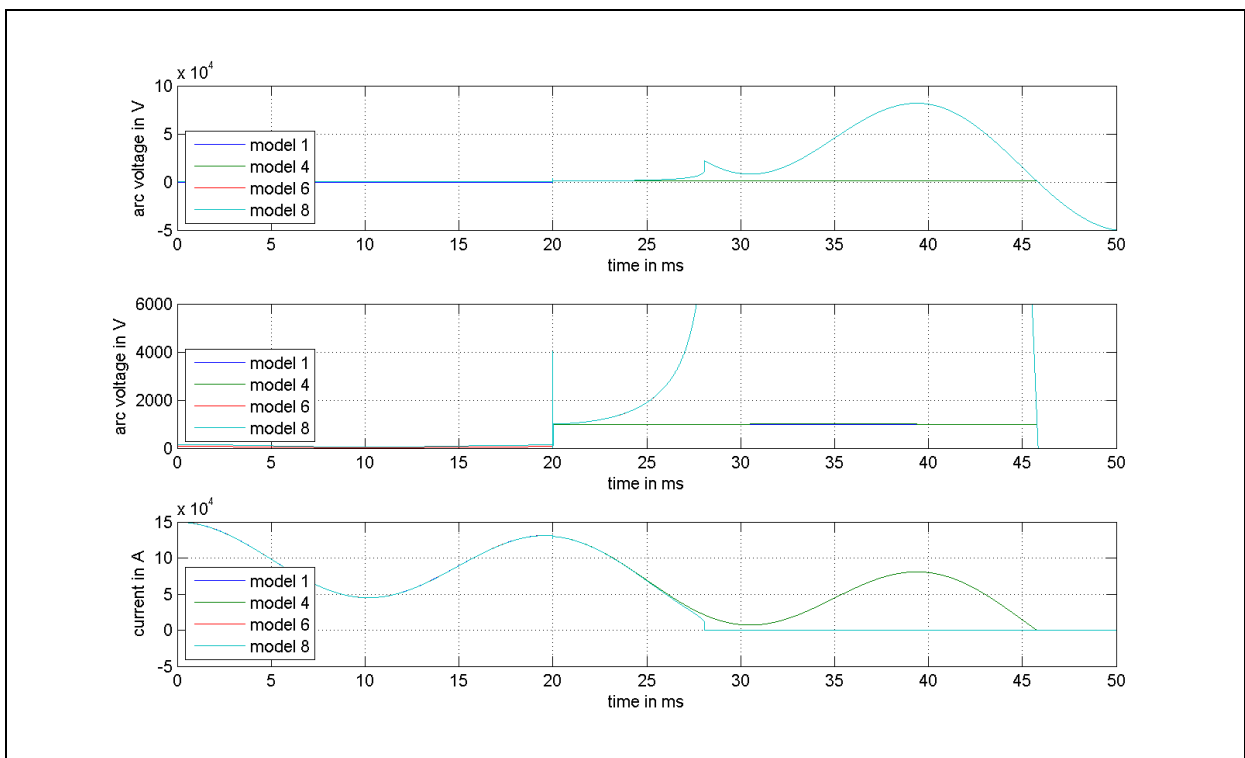


Figure 24: Comparison of arc voltages and shape of currents of different arc models

No.	Type	Parameters	Time of first zero-crossing in ms	Time difference to ideal CB in ms	Time difference to ideal CB in %
0	Ideal circuit breaker	No parameters needed	45,84	0,00	0,00
1	Model with constant d.c. arc voltage	$V_{DC} = 1000 \text{ V}$	45,78	0,05	0,12
2	Model with constant d.c. arc voltage	$V_{DC} = 2000 \text{ V}$	45,73	0,11	0,24
3	Model with constant d.c. arc voltage	$V_{DC} = 5000 \text{ V}$	45,57	0,27	0,59
4	Cassie-equation	$T_C = 1 \mu\text{s}, V_C = 1000 \text{ V}$	45,81	0,03	0,06
5	Cassie-equation	$T_C = 10 \mu\text{s}, V_C = 1000 \text{ V}$	45,84	0,00	0,00
6	Mayr-equation	$T_M = 1 \mu\text{s}, P_M = 65 \text{ MW}$	28,09	17,75	38,72
7	Mayr-equation	$T_M = 10 \mu\text{s}, P_M = 65 \text{ MW}$	28,36	17,48	38,13
8	Combined Cassie-Mayr-model	$T_C = 1 \mu\text{s}, V_C = 1000 \text{ V}$ $T_M = 1 \mu\text{s}, P_M = 65 \text{ MW}$	28,09	17,75	38,72
9	Combined Cassie-Mayr-model	$T_C = 10 \mu\text{s}, V_C = 1000 \text{ V}$ $T_M = 10 \mu\text{s}, P_M = 65 \text{ MW}$	28,36	17,48	38,13

Table 7: Comparison of different models concerning time of zero-crossing

Under inductive load test circuit with impedance X

True for all models is the circuit breaker opening time, $t_{\text{contactseparation}} = 20 \text{ ms}$.

The different arc models are also used in an inductive test circuit with a superposed source signal, circuit breaker model, impedance X, an amperemeter for current detection and a voltmeter for arc voltage measurement (as shown in Figure 25).

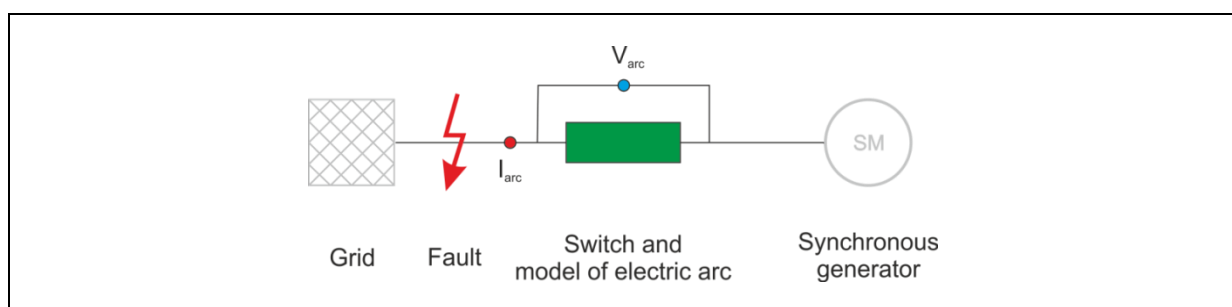


Figure 25: Equivalent network

The resultant source signal is a superposition of two signals, the impedance is $X = 24 \Omega + j205 \Omega$

The resultant current signal has an rms-amplitude of about 1 kA which is according to the nominal short-circuit current in the network shown in Figure 10.

Table 8 shows the used types of arc models and the corresponding arc model parameters. Furthermore the results of point of time of current's first zero-crossing can be seen.

No.	Type	Parameters	Time of first zero-crossing in ms	Time difference to ideal circuit breaker in ms	Time difference to ideal circuit breaker in %
0	Ideal circuit breaker	No parameters needed	95,38	0,00	0,00
1	Model with constant d.c. arc voltage	$V_{DC} = 1000 \text{ V}$	95,07	0,31	0,32
2	Model with constant d.c. arc voltage	$V_{DC} = 2000 \text{ V}$	94,80	0,58	0,61
3	Model with constant d.c. arc voltage	$V_{DC} = 5000 \text{ V}$	94,03	1,35	1,42
4	Cassie-equation	$T_C = 1 \mu\text{s}, V_C = 1000 \text{ V}$	95,07	0,31	0,32
5	Cassie-equation	$T_C = 10 \mu\text{s}, V_C = 1000 \text{ V}$	95,07	0,31	0,32
6	Cassie-equation	$T_C = 1 \mu\text{s}, V_C = 2000 \text{ V}$	94,80	0,58	0,61
7	Cassie-equation	$T_C = 10 \mu\text{s}, V_C = 2000 \text{ V}$	94,80	0,58	0,61
8	Mayr-equation	$T_M = 1 \mu\text{s}, P_0 = 1,1 \text{ MW}$	94,55	0,83	0,87
9	Mayr-equation	$T_M = 10 \mu\text{s}, P_0 = 1,1 \text{ MW}$	94,58	0,80	0,83
10	Mayr-equation	$T_M = 1 \mu\text{s}, P_0 = 2,2 \text{ MW}$	93,95	1,43	1,50
11	Mayr-equation	$T_M = 10 \mu\text{s}, P_0 = 2,2 \text{ MW}$	93,99	1,39	1,46
12	Combined Cassie-Mayr-model	$T_C = 1 \mu\text{s}, V_C = 1000 \text{ V}$ $T_M = 1 \mu\text{s}, P_0 = 1,1 \text{ MW}$	93,99	1,39	1,46
13	Combined Cassie-Mayr-model	$T_C = 10 \mu\text{s}, V_C = 1000 \text{ V}$ $T_M = 10 \mu\text{s}, P_0 = 1,1 \text{ MW}$	94,59	0,80	0,83
14	Combined Cassie-Mayr-model	$T_C = 10 \mu\text{s}, V_C = 2000 \text{ V}$ $T_M = 10 \mu\text{s}, P_0 = 2,2 \text{ MW}$	93,99	1,39	1,46

Table 8: Comparison of different models concerning time of zero-crossing

The following figures show the signal sequences of the different arc voltages and currents by using different models and various parameters. The parameters can be seen in Table 8. Figure 26 shows the different signal sequences for different V_{DC} using the model with constant d.c. arc voltage. It can be seen that the arc voltage is constant during the time while the arc is burning.

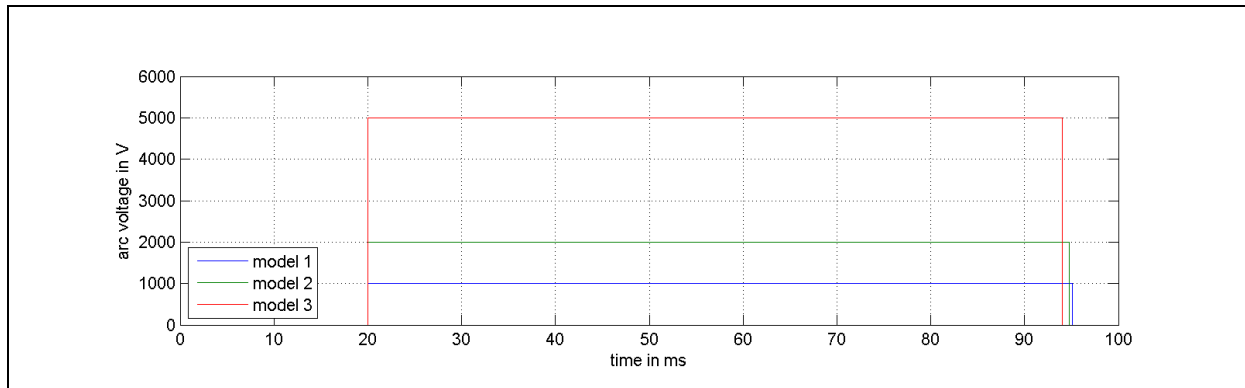


Figure 26: Signal sequences at different arc voltages, model with constant d.c. arc voltage

In Figure 27 different arc voltages by using Cassie's equation can be seen. It is visible, that Cassie's arc voltage is constant and similar to the arc voltages' characteristics shown in Figure 26.

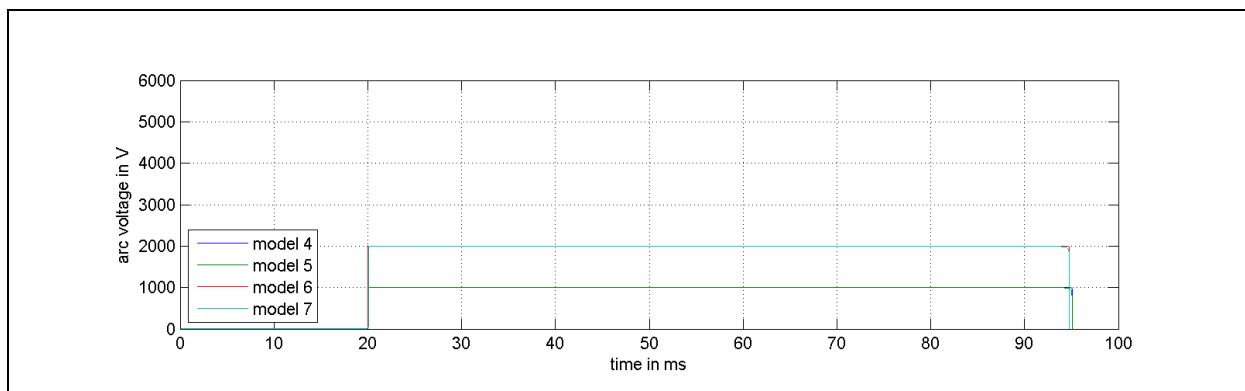


Figure 27: Signal sequences at different arc voltages by using Cassie's equation

In contrast, the arc voltage at Mayr's model depends among other things on the current. For that reason that the arc voltage is no longer a constant but has a characteristic as shown in Figure 28. Typical for the characteristic of Mayr's arc voltage is the rapid increase in the area around current's zero-crossing.

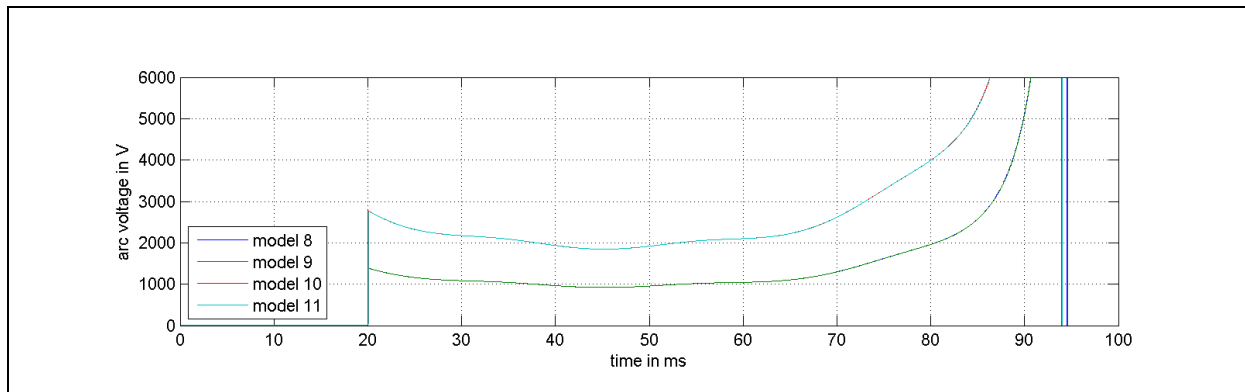


Figure 28: Signal sequences at different arc voltages by using Mayr's equation

The arc voltage resulting of the combined Cassie-Mayr equation is in a large part similar to the arc voltage resulting out of Mayr's equation. Characterizing is also the overshoot at the beginning, which can be seen in Figure 29.

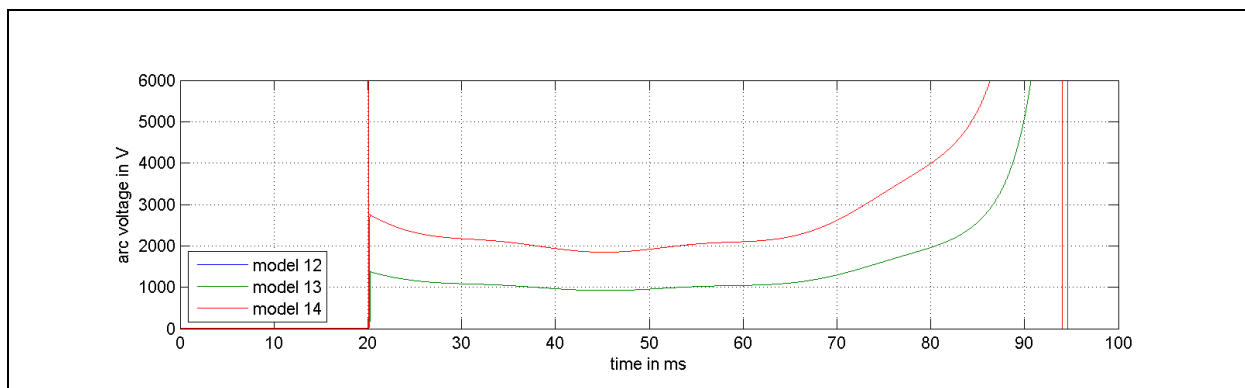


Figure 29: Signal sequences at different arc voltages by using the Cassie-Mayr model

4.4 Evaluation of results, single-phase

A number of sources in a circuit with linear and time-invariant elements make an impact on the resultant total current in each defined point of the circuit, implied in the Helmholtz's theorem of superposition. Figure 30 shows the Helmholtz's theorem of superposition applied on any desired elementary circuit.

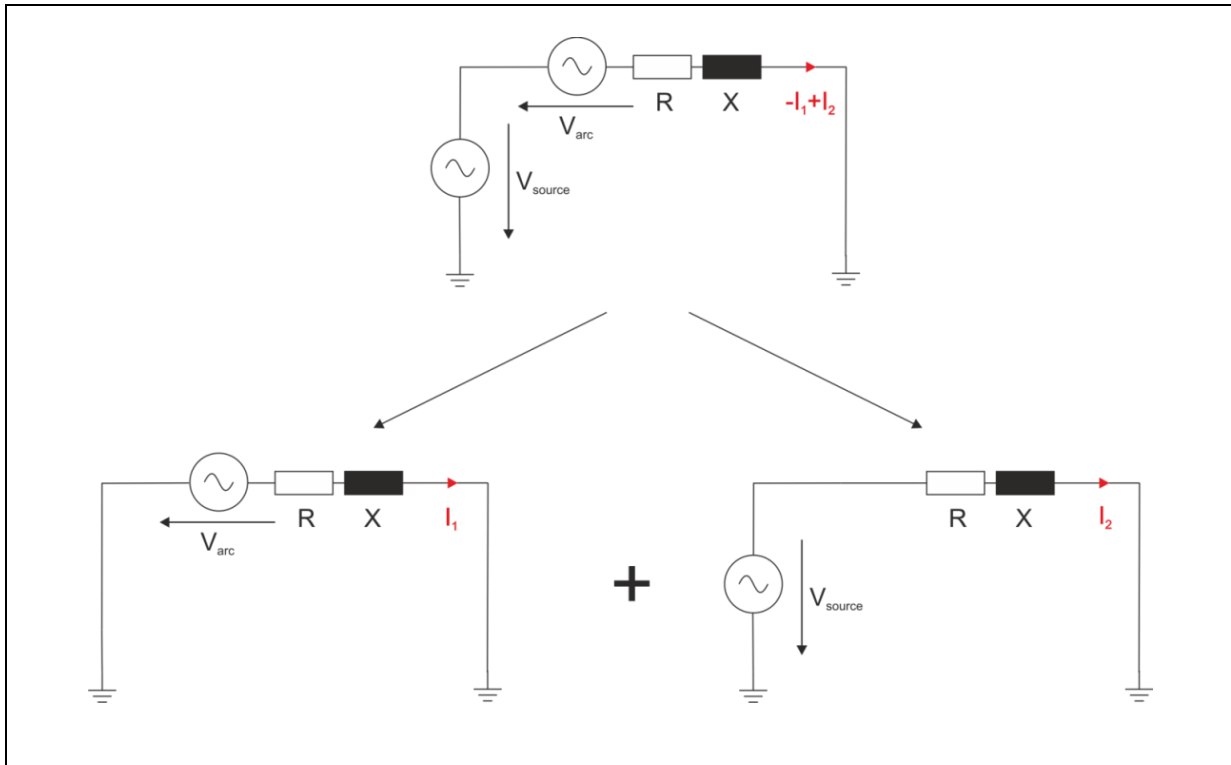


Figure 30: Schematic diagram of Helmholtz' superposition theorem

Based on Helmholtz' superposition theorem for linear electrical circuits the voltage of the power supply unit V_{source} and the counteracting arc voltage V_{arc} in the defined space of time in the figure above cause a resultant total current depending on these two voltages.

Characterizing for Mayr's model of electric arc is the fact, that the arc voltage is not constant over the lightning period (compared to Cassie's model). At the very end of the lightning period the arc voltage in Mayr's equation has a steep slope what causes a sharp decline of the current (cf. Figure 31).

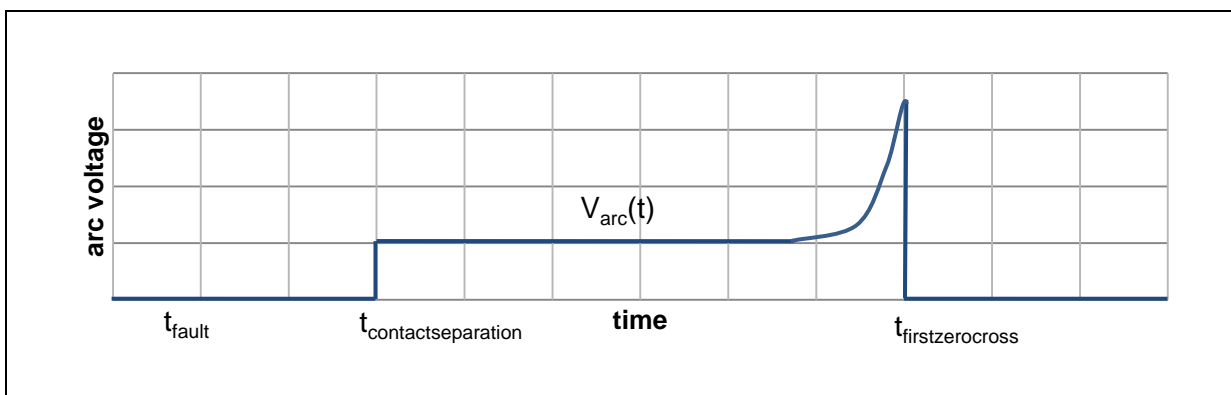


Figure 31: Characteristic of Mayr's arc voltage

Compared to a circuit with pure resistive load with a sharp decline of the current a circuit under inductive load doesn't show the effect of the sharp decline that clearly (cf. Figure 32).

Important is the look on scaling factor of the ordinate. While on the left-hand side picture the current goes to zero fast (higher di/dt), the current's rate of change is comparable smaller on the right-hand side picture.

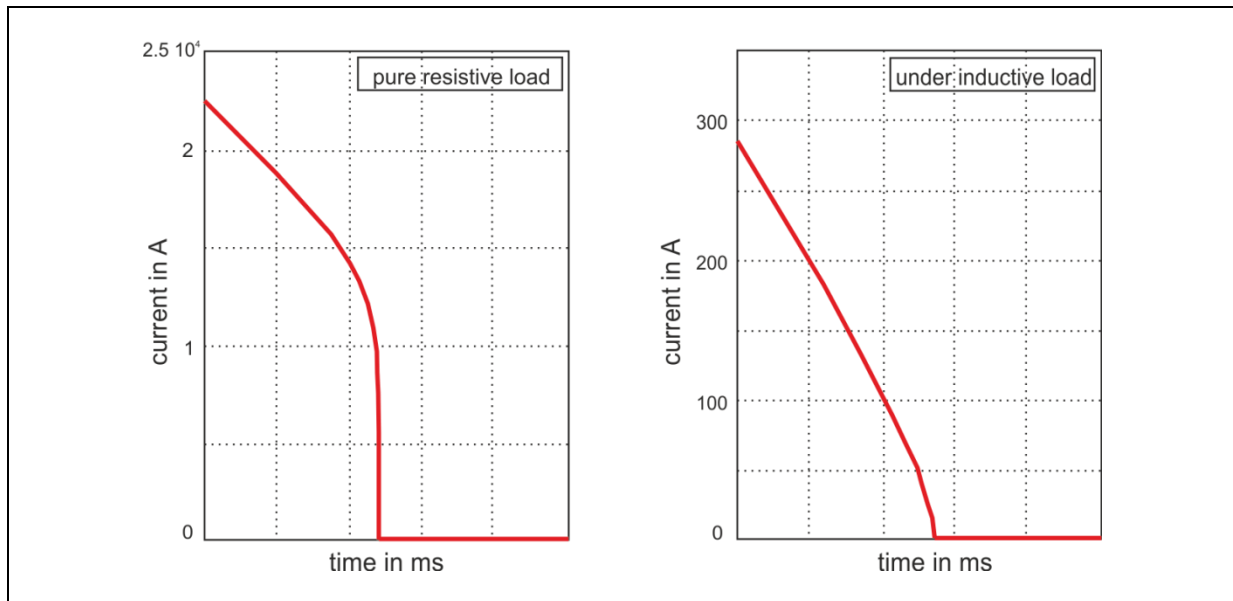


Figure 32: Sharp decline of the current in circuits with different load (pure resistive load and inductive load) and combined Cassie-Mayr-equation

This effect is caused by the signal shifts of voltage, arc voltage and current in different load cases (cf. Figure 33).

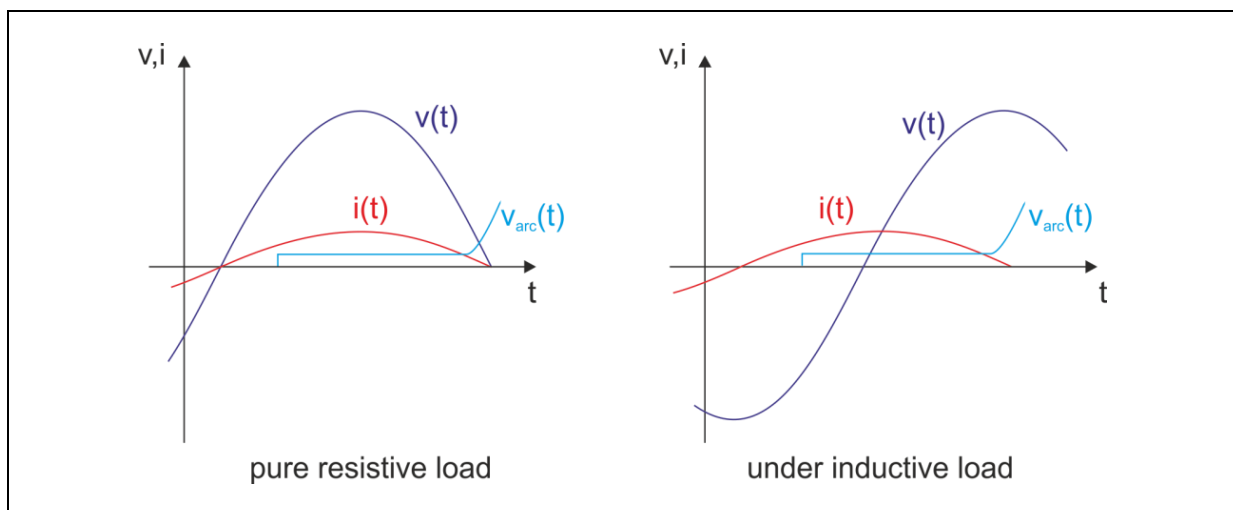


Figure 33: Signal characteristics (sketch) of circuits with different load

In case of inductive load the zero-crossing of $i(t)$ is at the same time as the maximum of the voltage $v(t)$ (cf. Figure 33, right-hand side sketch). The arc voltage $v_{\text{arc}}(t)$ battles a higher value of $v(t)$. The arc voltage $v_{\text{arc}}(t)$ is lower in relation to the voltage $v(t)$, what implicates a lower rate of change in $i(t)$ (cf. Figure 32, right-hand side figure). According to this aspect in case of pure resistive load the zero-crossing of $i(t)$ is contemporaneous with the zero-crossing of $v(t)$. So the arc voltage $v_{\text{arc}}(t)$ in that case battles a lower value of $v(t)$ compared to

the case of inductive load. The arc voltage $v_{\text{arc}}(t)$ is higher related to the voltage $v(t)$. That implicates a higher rate of change in $i(t)$, what can be seen on left-hand side in Figure 32. To establish a relation between the arc voltage V_{arc} and the total time constant T (of the overall circuit) it is helpful to replace the arc voltage source with a virtual resistance depending on the arc voltage and the current through the arc, according to Ohm's law (cf. Figure 34).

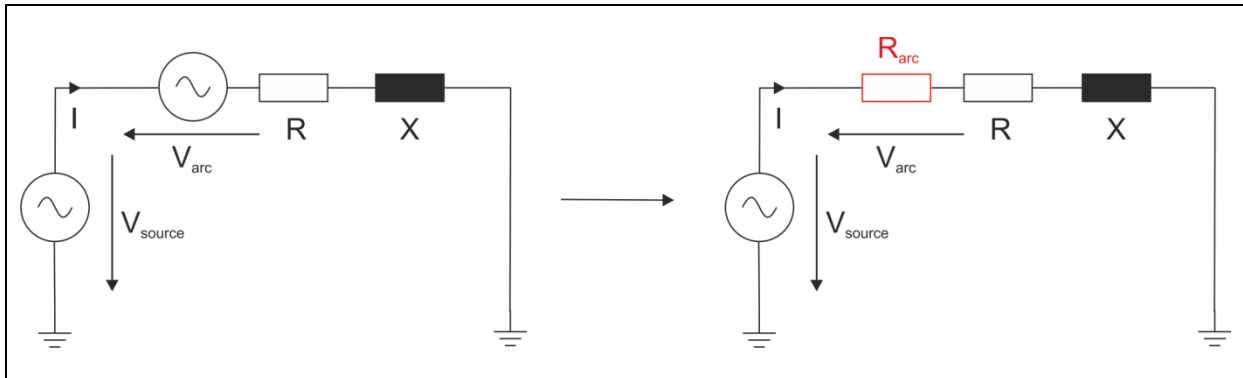


Figure 34: Representation of arc voltage as a virtual resistance

Different arc models cause different virtual arc resistances, depending on the value of the arc voltage. The higher the arc voltage, the higher the virtual arc resistance is.

In general circuits under inductive load have a time constant T , for which additionally holds

$$\tau = \frac{L}{R}. \quad (4.7)$$

If there is an additional (virtual) resistance R_{arc} (caused by the electric arc) the time constant T becomes to

$$\tau = \frac{L}{R+R_{\text{arc}}}. \quad (4.8)$$

That causes a reduction of the time constant, provided that the inductivity L is constant.

The following table shows the parameters used at the different models. Furthermore the points of time of currents' first zero-crossings and the virtual arc resistances R_{arc} are visible.

No.	Type	Parameters	Time of first zero-crossing in ms	Virtual arc resistance R_{arc} in Ω
0	Ideal circuit breaker	No parameters needed	95,38	0,00
1	Model with constant d.c. arc voltage	$V_{DC} = 1000 \text{ V}$	95,07	2,66
2	Model with constant d.c. arc voltage	$V_{DC} = 2000 \text{ V}$	94,80	8,58
3	Model with constant d.c. arc voltage	$V_{DC} = 5000 \text{ V}$	94,03	23,98
4	Cassie-equation	$T_C = 1 \mu\text{s}, V_C = 1000 \text{ V}$	95,07	2,66
5	Cassie-equation	$T_C = 10 \mu\text{s}, V_C = 1000 \text{ V}$	95,07	2,64
6	Cassie-equation	$T_C = 1 \mu\text{s}, V_C = 2000 \text{ V}$	94,80	8,18
7	Cassie-equation	$T_C = 10 \mu\text{s}, V_C = 2000 \text{ V}$	94,80	6,92
8	Mayr-equation	$T_M = 1 \mu\text{s}, P_M = 1,1 \text{ MW}$	94,55	192,48
9	Mayr-equation	$T_M = 10 \mu\text{s}, P_M = 1,1 \text{ MW}$	94,58	182,18
10	Mayr-equation	$T_M = 1 \mu\text{s}, P_M = 2,2 \text{ MW}$	93,95	191,32
11	Mayr-equation	$T_M = 10 \mu\text{s}, P_M = 2,2 \text{ MW}$	93,99	129,78
12	Combined Cassie-Mayr-model	$T_C = 1 \mu\text{s}, V_C = 1000 \text{ V}$ $T_M = 1 \mu\text{s}, P_0 = 1,1 \text{ MW}$	93,99	129,78
13	Combined Cassie-Mayr-model	$T_C = 10 \mu\text{s}, V_C = 1000 \text{ V}$ $T_M = 10 \mu\text{s}, P_0 = 1,1 \text{ MW}$	94,59	176,66
14	Combined Cassie-Mayr-model	$T_C = 10 \mu\text{s}, V_C = 2000 \text{ V}$ $T_M = 10 \mu\text{s}, P_0 = 2,2 \text{ MW}$	93,99	127,78

Table 9: Comparison of points of time of current's first zero-crossing and virtual arc resistances in different models

Figure 35 gives an overview of the point of current's first zero-crossing by using different arc models (described in Table 9). It may be seen that there are small differences concerning the point of time between using the different described models.

More significant than the differences in Figure 35 are those ones shown in Figure 36. There it is visible, that the virtual arc resistance, which is described above, is different by using different models of electric arc. The contrast is even higher by using a model consisting Mayr's equation (models no. 8-14) because of the characteristic of the arc voltage (cf. description of the different arc voltages in chapter 4.3).

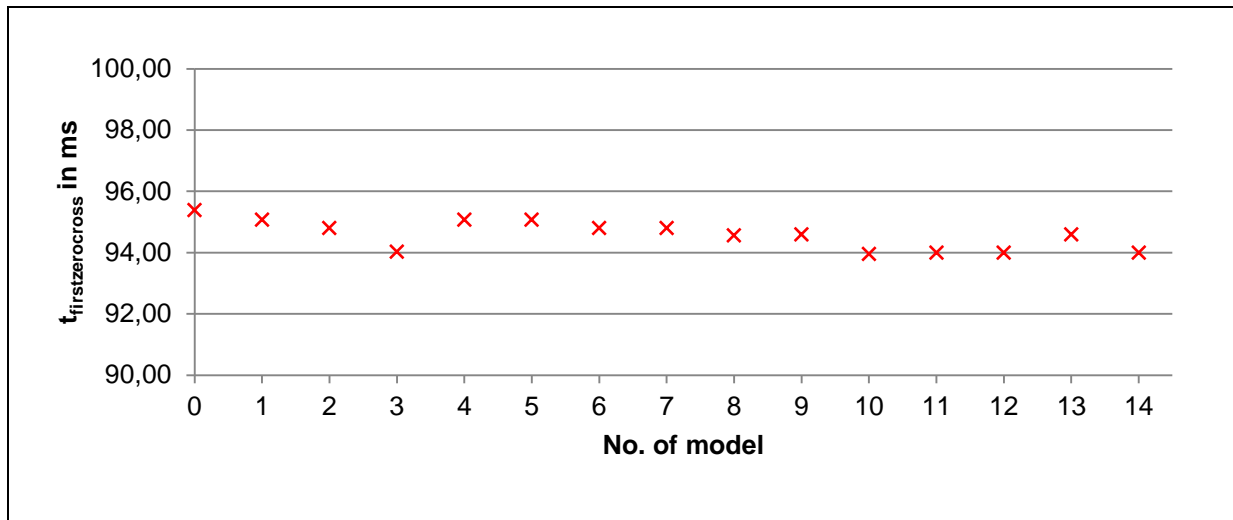


Figure 35: Comparison of point of time of current's first zero-crossing using different models

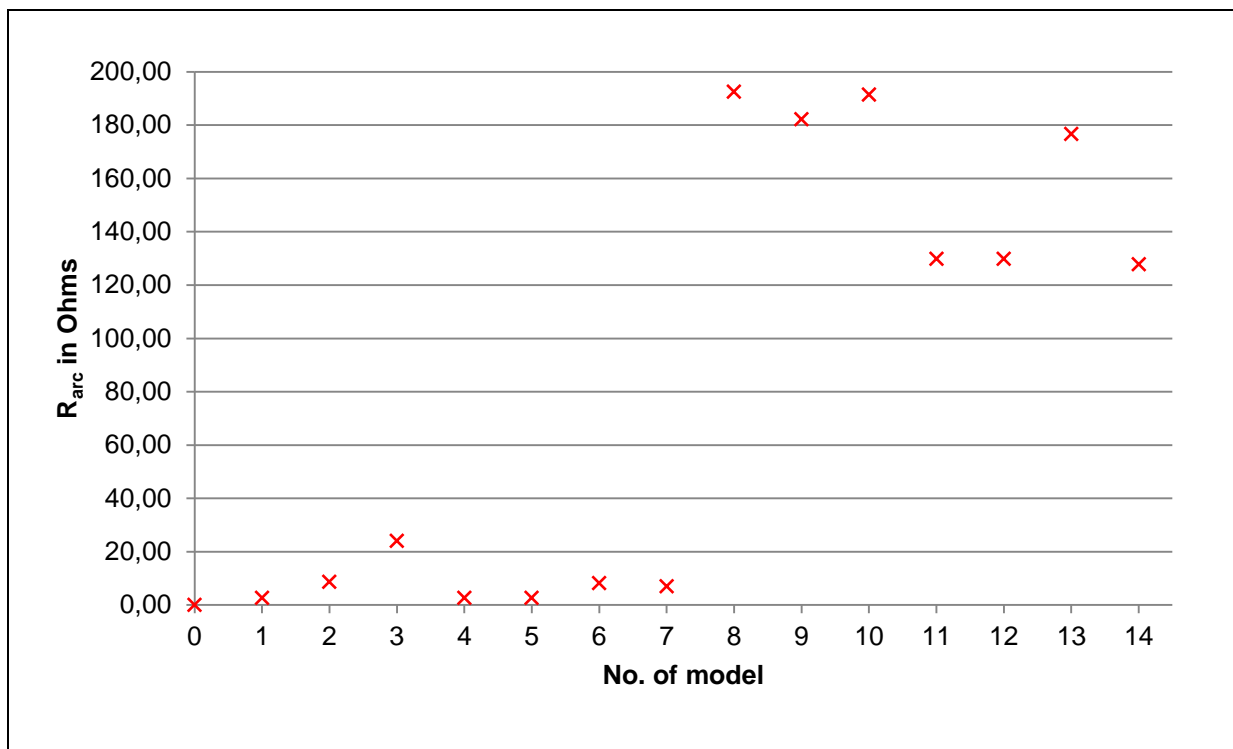


Figure 36: Comparison of virtual arc resistances using different models

Figure 37 shows the differences concerning the point of time of current's first zero-crossing by using both, the arc model and the virtual arc resistance, which is calculated in Table 9 and visible in Figure 36. There can be seen that the results for the model with constant d.c. arc voltage and Cassie's arc voltage are nearly identical, weather using the model (blue marks) or the virtual arc resistance (red marks). The differences in models no. 8-14 result from the fact that the virtual arc resistance by using Mayr's equation is definitely higher than by using Cassie's equation with a similar arc voltage. Therefore the results concerning point of time of current's first zero-cross by using the virtual arc resistances deviate from the results by using the model.

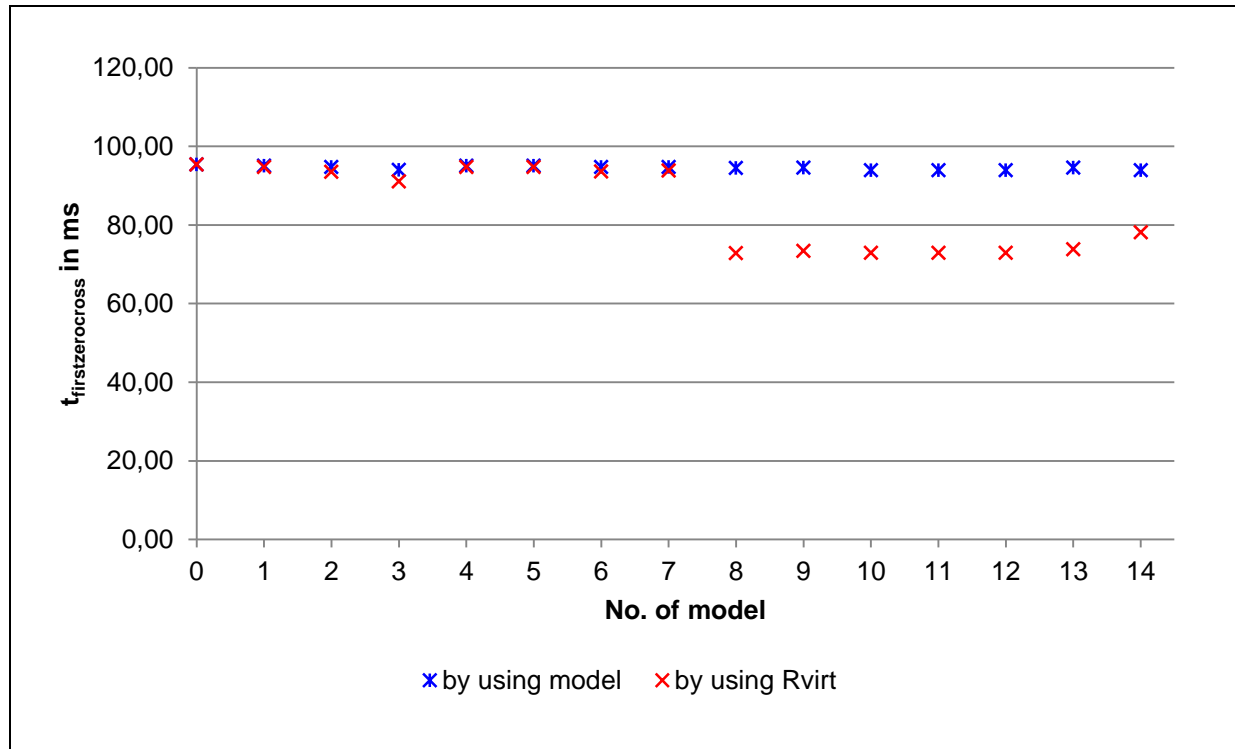


Figure 37: Comparison of current's first zero-crossing by using the model and the virtual arc resistance

To sum up, it could be captured that the model with constant d.c. arc voltage is a very simple model with only one parameter. The biggest advantage is that this parameter can be estimated well or is known because of several manufacturer information or data sheets of the circuit breakers. A disadvantage is that the arc voltage is not reproduced exactly, but it has to be considered if that is necessary for the calculation and studies.

The Cassie equation is very similar to the model with constant d.c. arc voltage concerning the characteristic of the arc voltage. As described in chapter 2.3.2, Cassie's equation reproduces the current characteristic for higher currents. As shown in some figures above (e.g. Figure 27) the characteristic of the modeled arc voltage is very similar to the characteristic of the one by using the model with constant d.c. arc voltage. Therefore it is not useful to implement Cassie's equation for basic studies concerning the arc voltage and its impact on the current characteristics. The model with constant d.c. arc voltage delivers similar results and is easier to realize and implement.

Mayr's equation is better used to simulate the current in regions around the zero-crossing point (low current levels). While the parameter V_C in Cassie's equation may be estimated in an easier way, it needs some additional work to find a correct parameter P_0 , which represents the power losses in Mayr's equation (e.g. estimating a veritable range of power losses first). For studies concerning the influence of the arc voltage on the current characteristic Mayr's equation is only usable if the current characteristic around zero is needed in an exact way. Otherwise Mayr's equation – compared to the above mentioned models – is not that usable to investigate the influence in higher current levels, because the

bigger amount of influence should have happened, when Mayr's equation takes an effect on the characteristic of the current. Furthermore it has to be considered if it is necessary to implement a differential equation for basic studies on the influence of the electric arc on the current's characteristics.

The combined Cassie-Mayr equation is similar to Mayr's equation concerning the characteristic of the modeled arc voltage and its influence on the current characteristic. For initial assessments it's not helpful to implement two independent differential equations which work in series. It is also noted in chapter 2.3.2 that the combined Cassie-Mayr model is not founded physically. The equation is only a mathematic model. For basic investigations of the electric arc and its influence on the current it certainly does not indicate that differential equations are implemented in a numeric model. The model with a constant d.c. arc voltage is fully adequate. For further studies and exacter investigations it can't be ensured that the combined model of Cassie and Mayr is the perfect solution. More probably than not a more complex model of electric arc has to be chosen to get results of the desired quality.

For further studies concerning the point in time of current's zero-crossing it is enough to use the model with constant d.c. arc voltage. Furthermore Mayr's equation is implemented in the three-phase structure for more detailed results concerning the influence of the arc voltage on point of current's zero-crossing.

4.5 Implementation of relevant arc models, three-phase

As relevant arc model the model with constant d.c. arc voltage is chosen, because of the above mentioned arguments. To compare the results of using an easy and a complex model Mayr's equation is also implemented and investigated.

The point of time of the fault is set at $t_{\text{fault}} = 0$ ms. The point of time of circuit breaker's contact separation is set on $t_{\text{contactseparation}} = 40$ ms.

4.5.1 Model with constant d.c. arc voltage

The following figure shows the uninfluenced signal sequences by the initial condition of operating point 4 at synchronous generator. In Figure 38 you may see the characteristics of the signals on measure points V_{arc} and I_{arc} (cf. Figure 10) on high tension. The three-phase short-circuit appears at a time of 0 ms, there is no separation of contacts, so the fault occurs over 400 ms and longer.

In contrary to Figure 38, Figure 39 shows the signal sequences (at same initial conditions) if an ideal circuit breaker opens 40 ms after the fault appears (time of contact separation is at 40 ms).

Note: There is no arc voltage modeled. The occurring voltage in phase C is the potential difference between the fault's side of the circuit breaker and the signal after the circuit breaker (which is turned off). A comparison with the associated current profile below is helpful in this case.

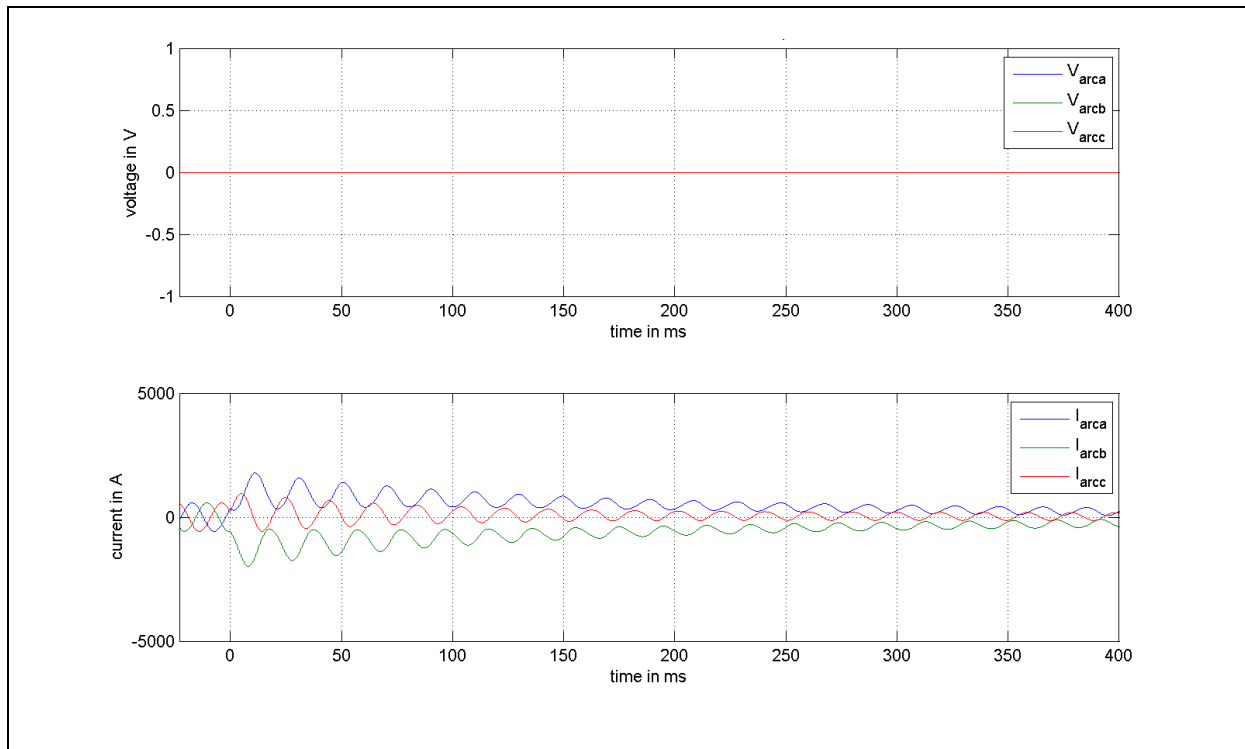


Figure 38: OP 4: uninfluenced signal sequences V_{arc} and I_{arc}

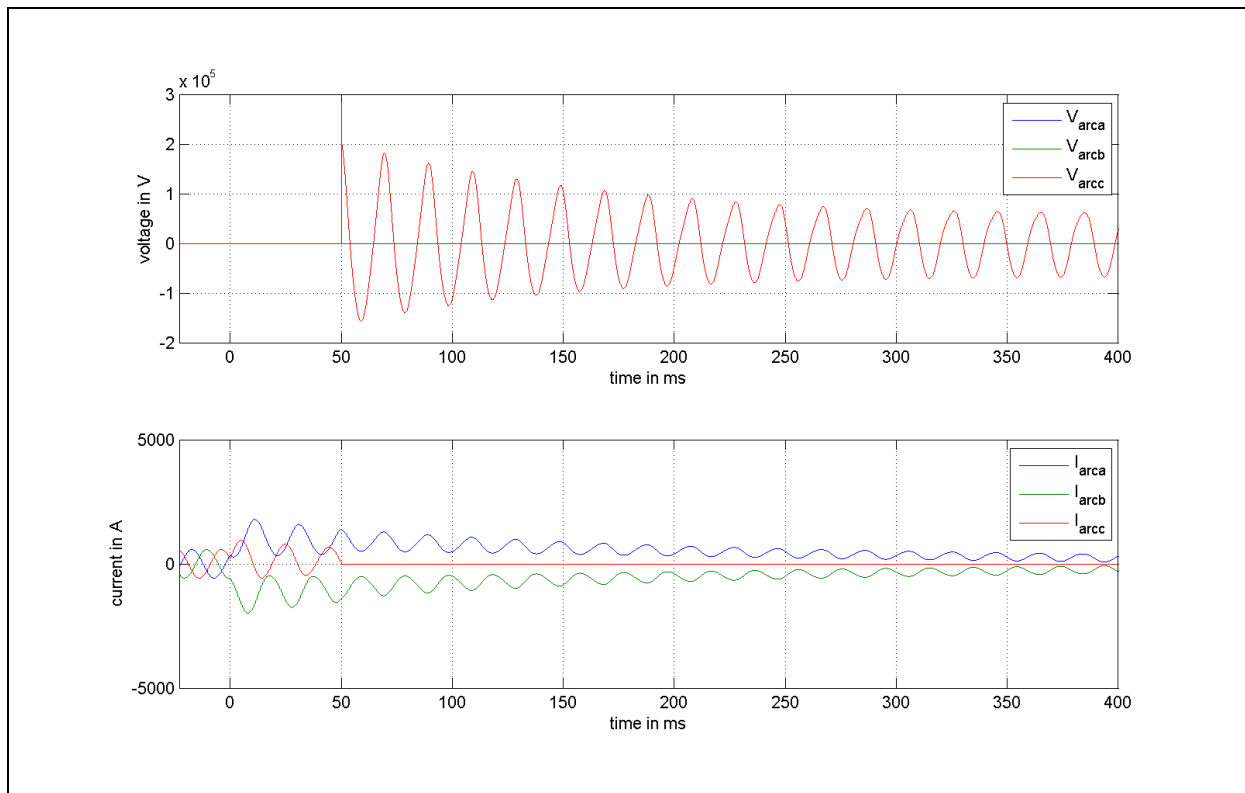


Figure 39: OP 4: signal sequences V_{arc} and I_{arc} – ideal circuit breaker, $t_{contactseparation} = 40$ ms, YNd5-Transformer

Figure 41 shows the same as Figure 40 does, but with a different arc voltage's range. So you may have a look on the more or less detailed characteristics of the arc voltages in the different phases.

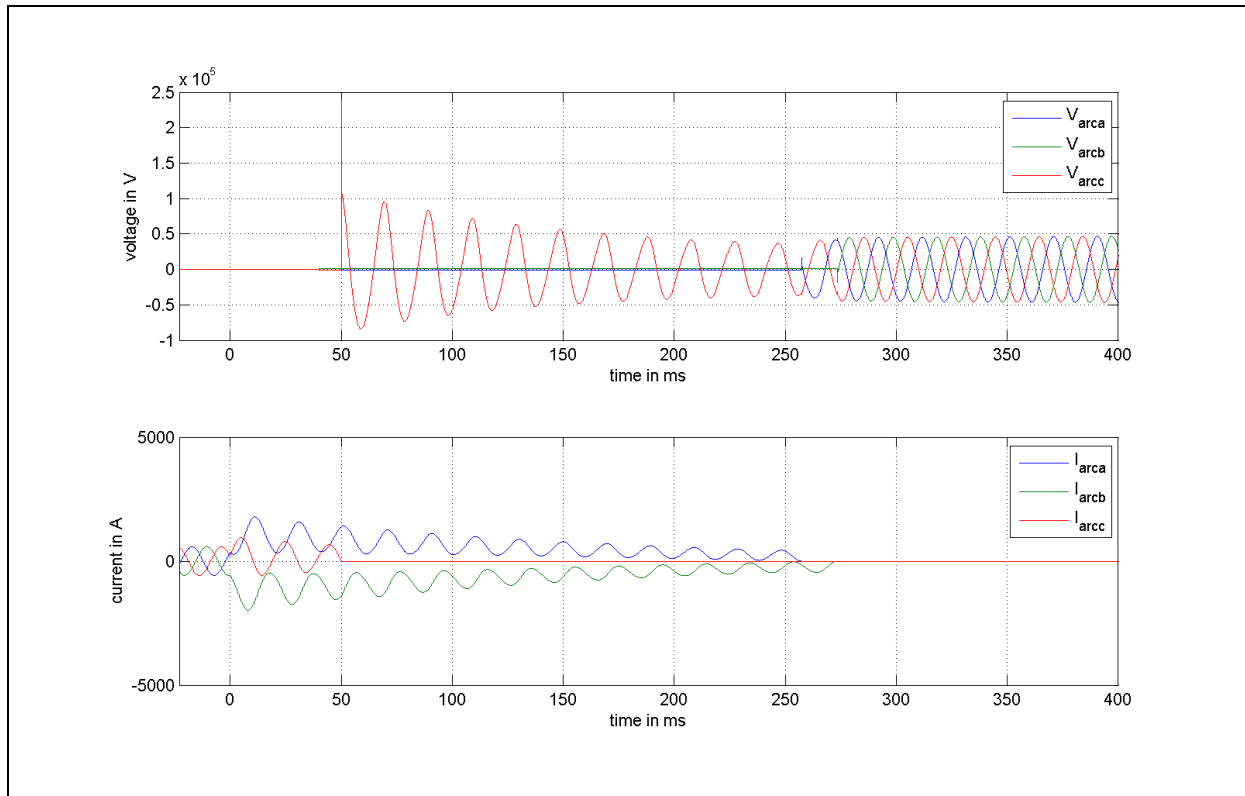


Figure 40: OP 4: signal sequences V_{arc} and I_{arc} – model with $V_{DC} = 1000$ V, $t_{contactseparation} = 40$ ms

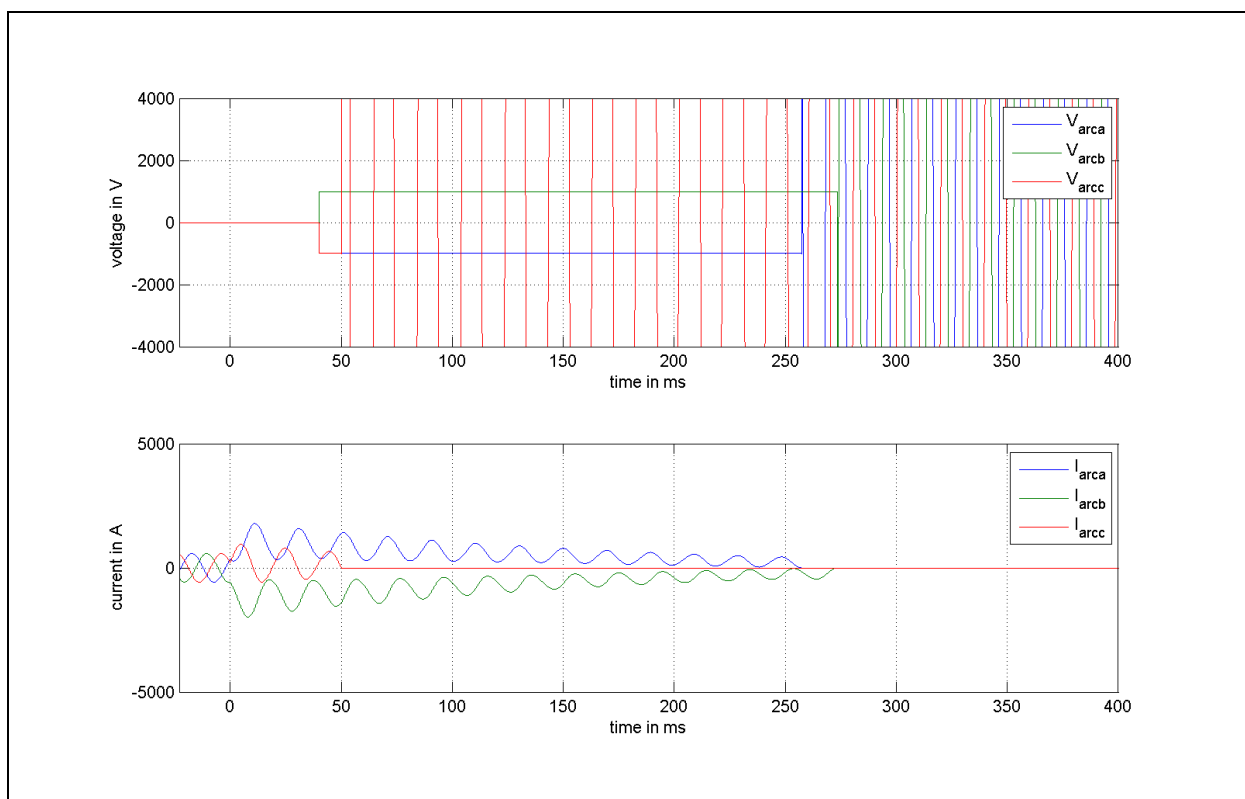


Figure 41: OP 4: signal sequences V_{arc} and I_{arc} – model with $V_{DC} = 1000$ V, $t_{contactseparation} = 40$ ms – zoom in at arc voltage

The following tables (Table 10, Table 11 and Table 12) show the calculated values of the relative DC-component of the current and the point of time of current first zero-crossing in each phase and in the concerned operating points (OP 1, OP 2, OP 4, OP 6). The current's relative DC-component is listed in percent; the point of time of current's first zero-crossing in each phase and each concerned operating point is listed in ms. The tables and the figure below (Figure 42) show that phase B is the most disadvantaged phase concerning the relative DC-component of the current and concerning the point of time of current's first zero-crossing.

Operating Point	$i_{DC,rel}$ in %			$t_{firstcurrentzero}$ in ms		
	Phase A	Phase B	Phase C	Phase A	Phase B	Phase C
OP 1	77,18	88,08	12,17	44,47	40,45	40,08
OP 2	64,68	74,49	10,73	43,61	54,66	48,71
OP 4	152,04	174,79	25,91	257,38	273,36	50,12
OP 6	144,40	161,73	22,53	101,78	137,84	51,18

Table 10: Relative current's DC-component and point of time of current's first zero-crossing – model with $V_{arc} = 1000$ V

Operating Point	$i_{DC,rel}$ in %			$t_{firstcurrentzero}$ in ms		
	Phase A	Phase B	Phase C	Phase A	Phase B	Phase C
OP 1	77,18	88,08	12,17	44,45	40,45	40,08
OP 2	64,49	74,49	10,73	43,59	54,60	48,68
OP 4	151,98	174,76	25,90	178,89	212,78	50,03
OP 6	144,25	161,65	22,50	81,83	117,51	51,08

Table 11: Relative current's DC-component and point of time of current's first zero-crossing – model with $V_{arc} = 2000$ V

Operating Point	$i_{DC,rel}$ in %			$t_{firstcurrentzero}$ in ms		
	Phase A	Phase B	Phase C	Phase A	Phase B	Phase C
OP 1	77,18	88,08	12,17	41,76	41,76	40,08
OP 2	64,49	74,49	10,73	43,58	52,01	52,01
OP 4	151,94	174,59	25,89	117,35	117,35	49,96
OP 6	144,14	161,17	22,47	98,55	98,55	50,99

Table 12: Relative current's DC-component and point of time of current's first zero-crossing – model with $V_{arc} = 5000$ V

Figure 42 shows an overall comparison of most disadvantaged phases considering first current zero-crossings of all investigated operating points. As also described in chapter 4.3 there is a relation between the value of arc voltage and the point of time of current zero-crossing in each phase. The higher the arc voltage is, the earlier the point of first zero-crossing (even in the most disadvantaged phase) occurs.

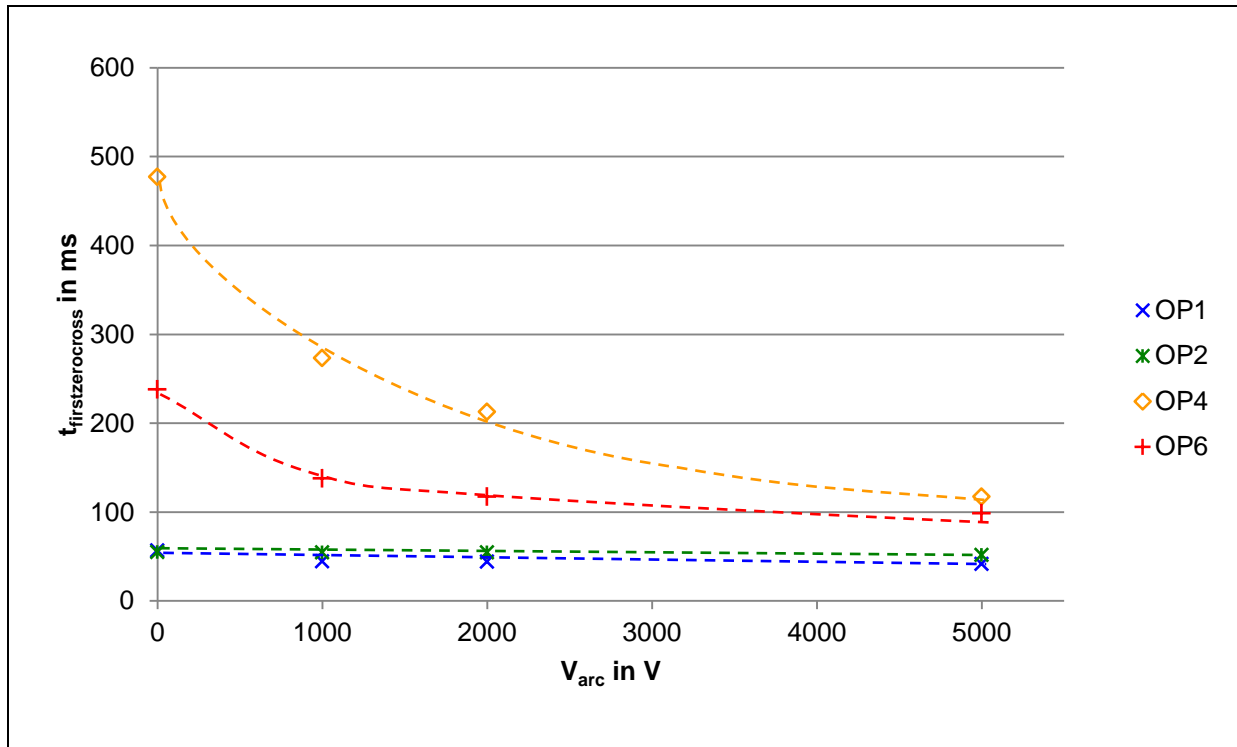


Figure 42: Overall comparison of point of current's first zero-crossing in most disadvantaged phases by using the model with constant d.c. arc voltage

The overall comparison in Figure 42 shows a possible relation between the value of the arc voltage and the point of time of first zero-crossing, especially in operating points with load. At open-circuit point and nominal rating point there's almost no relation between these parameters. But if the synchronous generator is in under-excited mode, the influence of the arc voltage on the decay characteristics becomes visible. The higher the arc voltage is, the earlier the point of time of current's first zero-crossing appears. In the figure above the arc voltage increases from the left to the right from 0 V in steps to 5000 V, whereby an arc voltage of 0 V means, that there is modeled an ideal circuit breaker.

As shown in chapter 4.4 the arc voltage could be replaced by a virtual resistance, depending on the arc voltage and the current (Ohm's law). The signal sequence of the virtual resistance according to the case shown in Figure 40 is pictured in the following figure. The dotted line symbolizes the calculated average of the arc resistance R_{mean} .

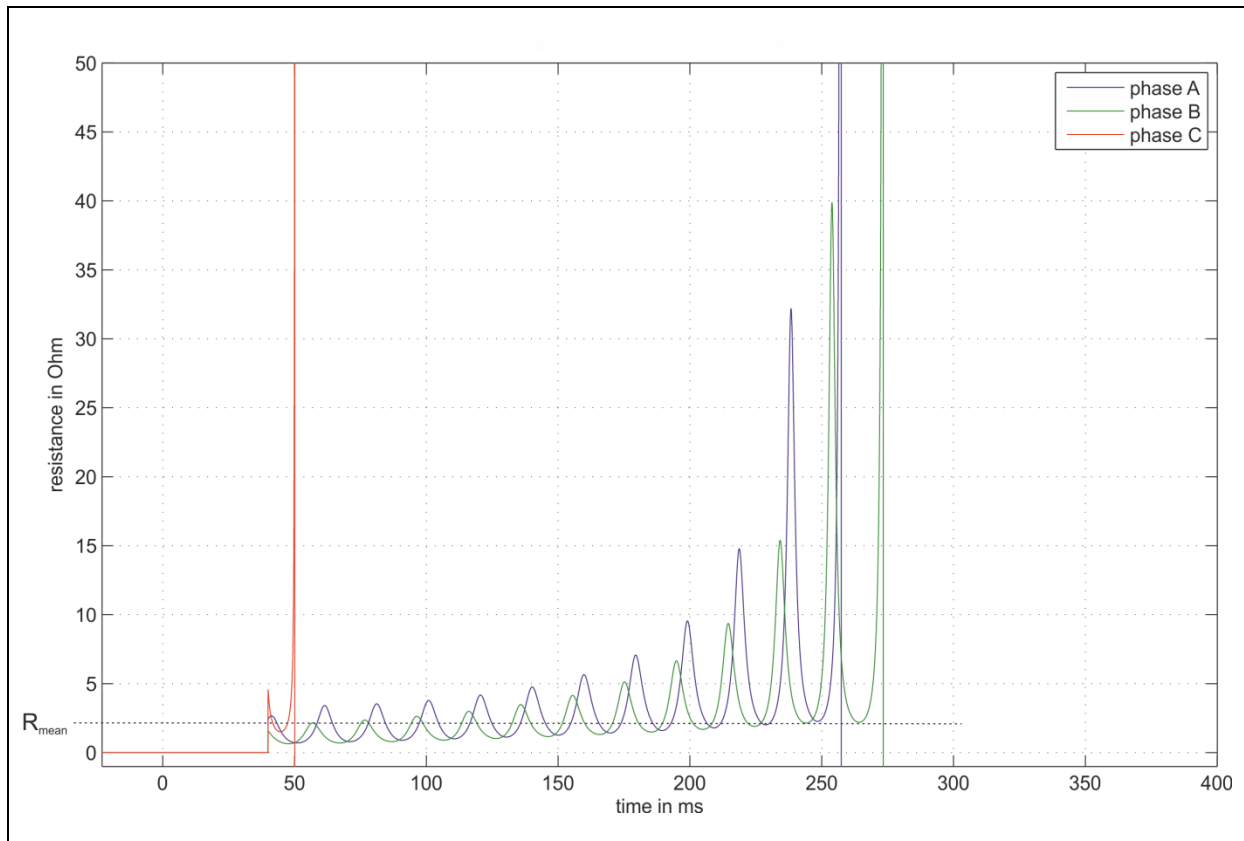


Figure 43: OP 4: arc resistance R_{arc} in all phases – model with $V_{DC} = 1000$ V, $t_{contactseparation} = 40$ ms

The signal sequences of the arc resistances by using different values of arc voltages at are similar to Figure 43. The figure below (Figure 44) gives an overview of the different calculated values of the arc resistances. Additionally the figure shows which arc resistances are necessary to get the same results of current's first zero-crossing (in most disadvantaged phases) as by using the model of electric arc.

The series $R_{arc,virt}$ (green one) in Figure 44 represents the calculated averages of the virtual arc resistances. The blue marked series stands for the determined arc resistances which lead to the same results concerning point of time of current's first zero-crossing as by using the model of electric arc. But as could be seen in the figure below the blue marks are consistent with the green ones to a large extent.

Figure 45 shows a comparison of using both concerning the current's first zero-crossing point of time. The blue markers show the point of time of first current zero-crossing by using the arc model with constant d.c. arc voltages and the virtual arc resistances which result in the same points of time. The green markers show the point of time of current's first zero-crossing by using the calculated averages of arc resistances. Similar to Figure 44 there are nearly no differences between the resistance values at the same arc voltage level.

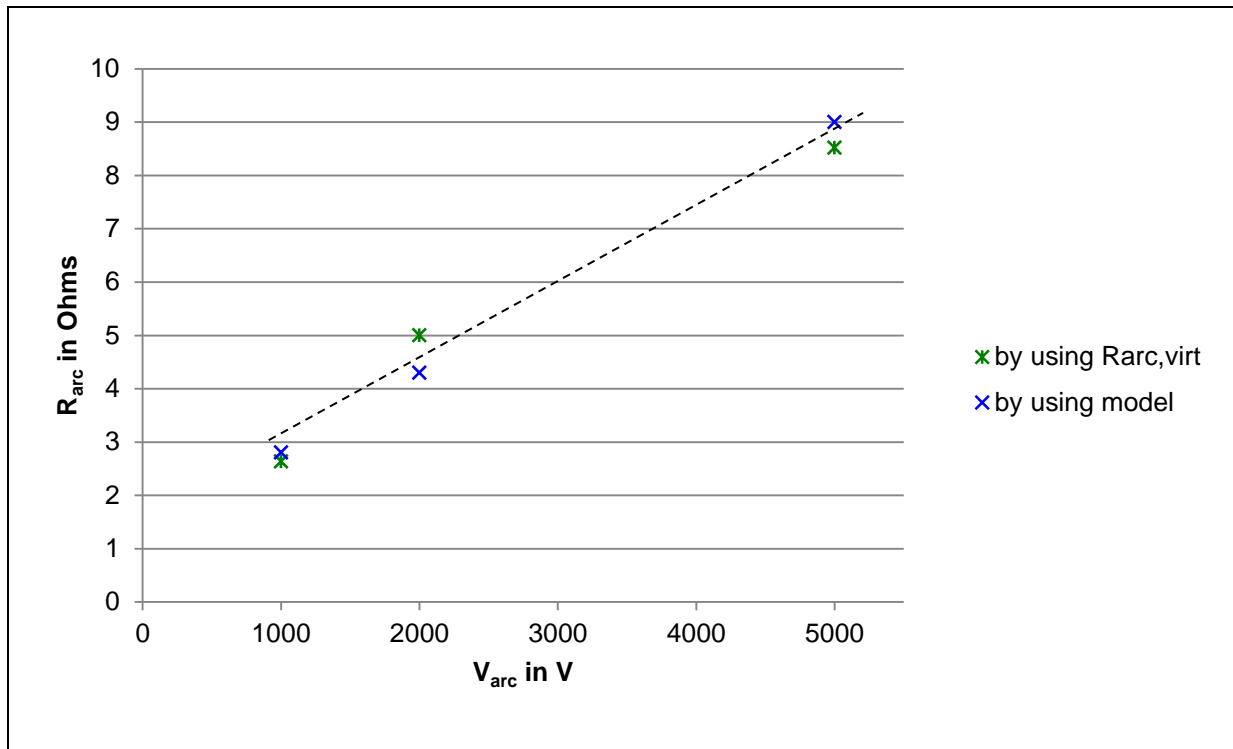


Figure 44: OP 4: actual virtual arc resistances by using different arc voltages (green) compared to the virtual arc resistances which are needed to get the same results as by using the model (blue)

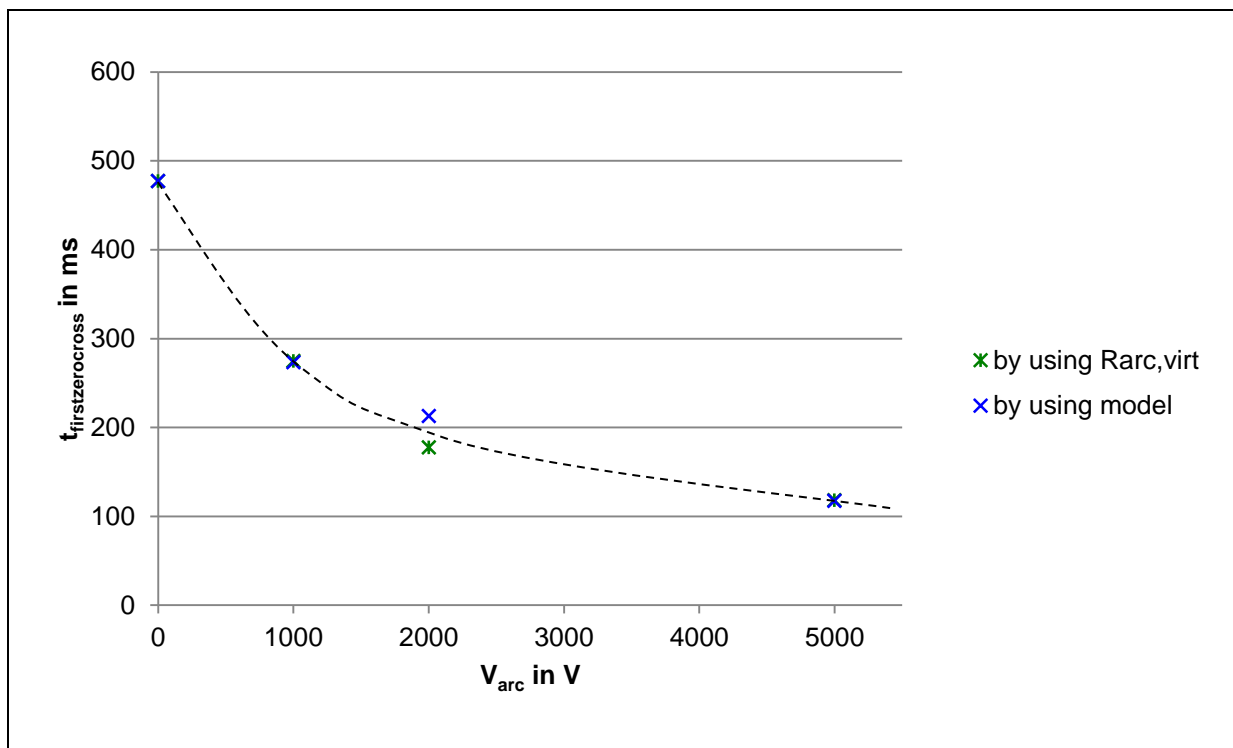


Figure 45: OP 4: point of time of current's first zero-crossing by using different values of virtual arc resistances (depending on the arc voltages)

4.5.2 Mayr's equation

The uninfluenced signal sequences and the signal sequences by using an ideal circuit breaker for comparison can be seen in chapter 4.5.1 (Figure 38, Figure 39).

The parameters in Mayr's equation are chosen to get resulting arc voltages which are almost the same level in their average as the chosen arc voltages of the model with constant d.c. arc voltage (1 kV, 2 kV and 5 kV).

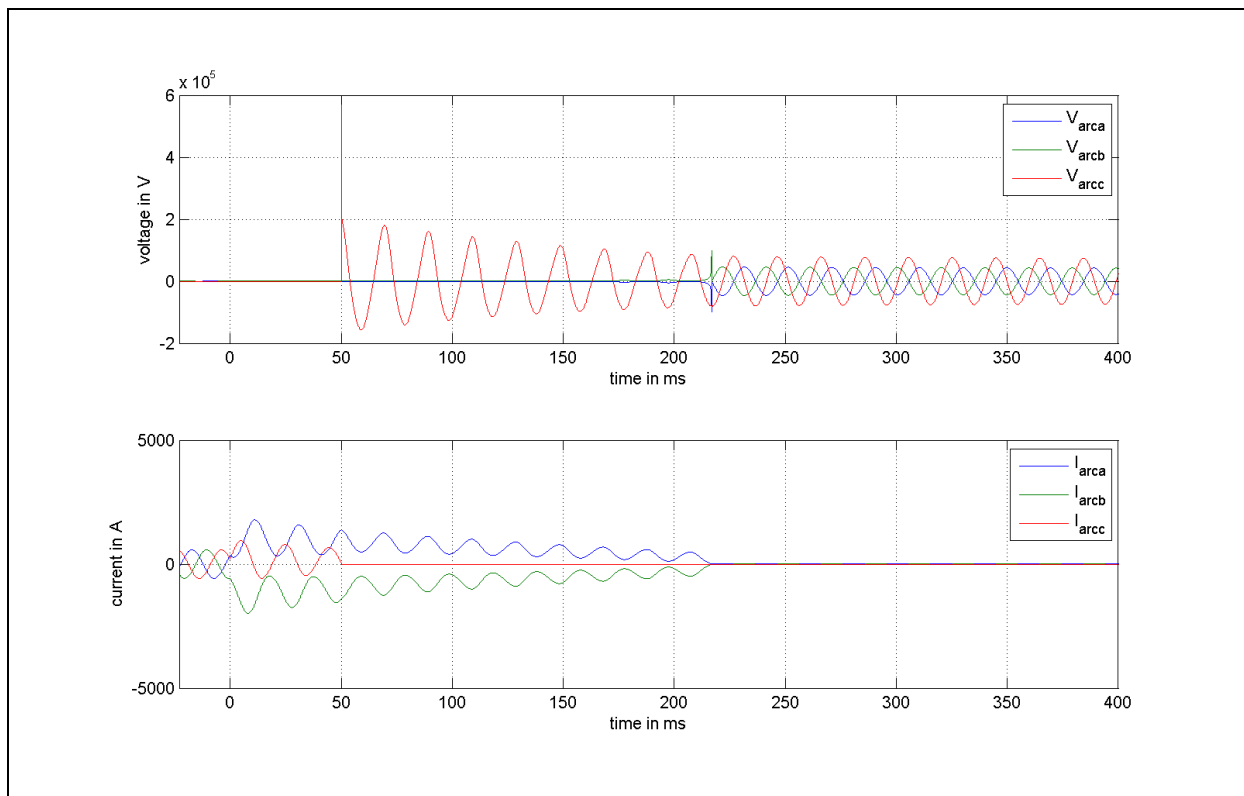


Figure 46: OP 4: signal sequences V_{arc} and I_{arc} – Mayr's equation with an average arc voltage of about 1000 V, $t_{contactseparation} = 40$ ms

Figure 46 shows the signal sequences at the circuit breaker model by using Mayr's equation with an average arc voltage of about 1000 V. The initial condition is operating point 4. To get an overview of the arc voltage, the following figure, Figure 47, shows the same signal sequences but the scaling of the arc voltage is different. So you may have a look on the more or less detailed characteristics of the arc voltages in the different phases. However, what is striking is the fact, that the arc voltage is not constant over the chosen time section, compared to the model with constant d.c. arc voltage. At minimal turning points of the current signal the arc voltages increase on local maxima, which cause waved characteristics of the arc voltage signal (cf. Figure 47). An effect, which can also be noticed by using Mayr's equation, is that the point of first current zero-crossing is much earlier than by using only an ideal switch. But it is in the same area as by using the model with constant d.c. arc voltage (cf. chapter 4.5.3).

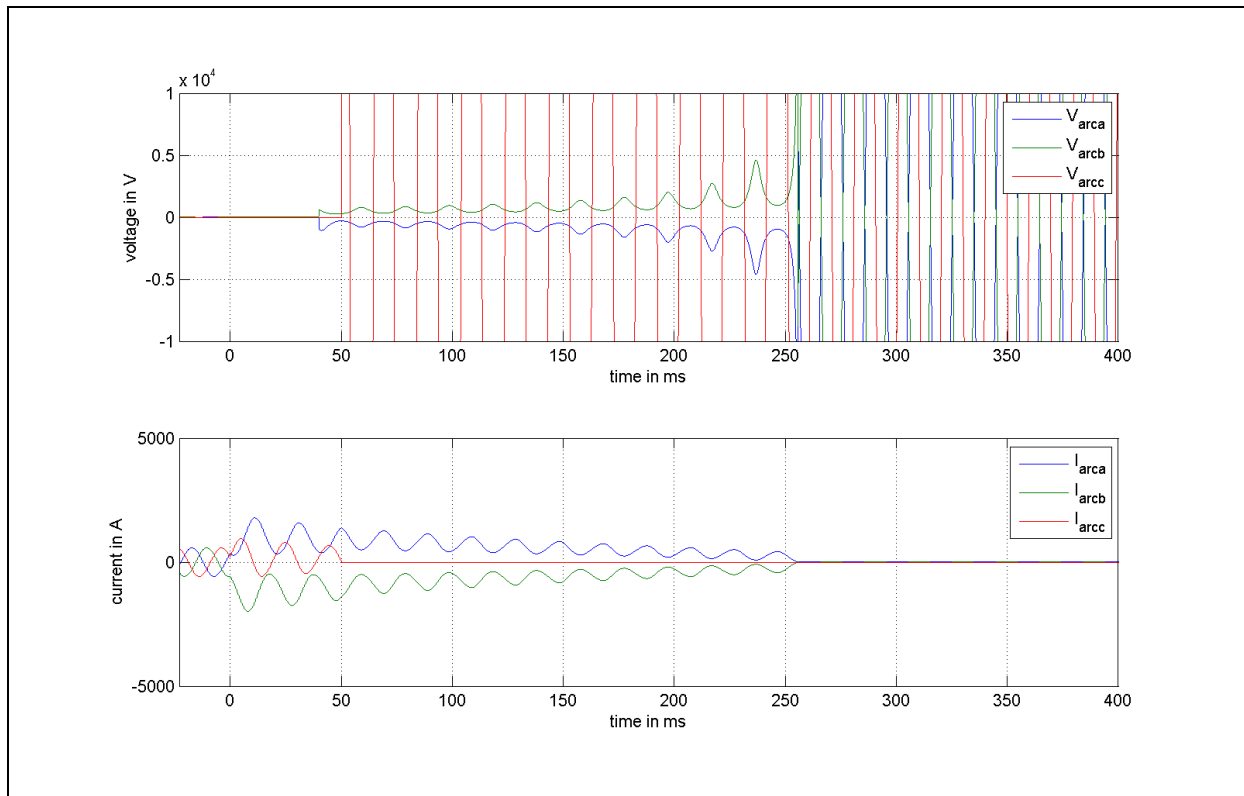


Figure 47: OP 4: signal sequences V_{arc} and I_{arc} – Mayr's equation with an arc voltage of about 1000 V, $t_{contactseparation} = 40$ ms, zoom in at arc voltage

The following tables (Table 13, Table 14 and Table 15) show the calculated values of the relative DC-component of the current and the point of time of current's first zero-crossing in each phase and in the concerned operating points (OP 1, OP 2, OP 4, OP 6). The current's relative DC-component is listed in percent; the point of time of current's first zero-crossing in each phase and each concerned operating point is listed in ms. The tables and the figure below (Figure 42) show that the phases A and B are the most disadvantaged phases concerning the point of time of current first zero-crossing.

Notable by using Mayr's model of electric arc are the points of time of currents first zero-crossings in all operating points. The circuit acts if a fault with ground connection occurs. If the current in phase C reaches the point of zero-crossing phase A and B are symmetric (cf. Figure 46 and Figure 47)

Operating Point	$t_{firstcurrentzero}$ in ms		
	Phase A	Phase B	Phase C
OP 1	41,67	41,67	40,08
OP 2	56,62	56,62	43,61
OP 4	255,71	255,71	50,22
OP 6	159,62	159,62	51,29

Table 13: Points of time of current first zero-crossings – model with $V_{arc} \approx 1000$ V

Operating Point	$t_{\text{firstcurrentzero}}$ in ms		
	Phase A	Phase B	Phase C
OP 1	41,53	41,53	40,08
OP 2	56,62	56,62	43,61
OP 4	196,00	196,00	50,22
OP 6	138,55	138,55	51,30

Table 14: Points of time of current first zero-crossings – model with $V_{\text{arc}} \approx 2000$ V

Operating Point	$t_{\text{firstcurrentzero}}$ in ms		
	Phase A	Phase B	Phase C
OP 1	41,18	41,18	40,08
OP 2	56,62	56,62	43,61
OP 4	134,87	134,87	50,24
OP 6	99,00	99,00	51,33

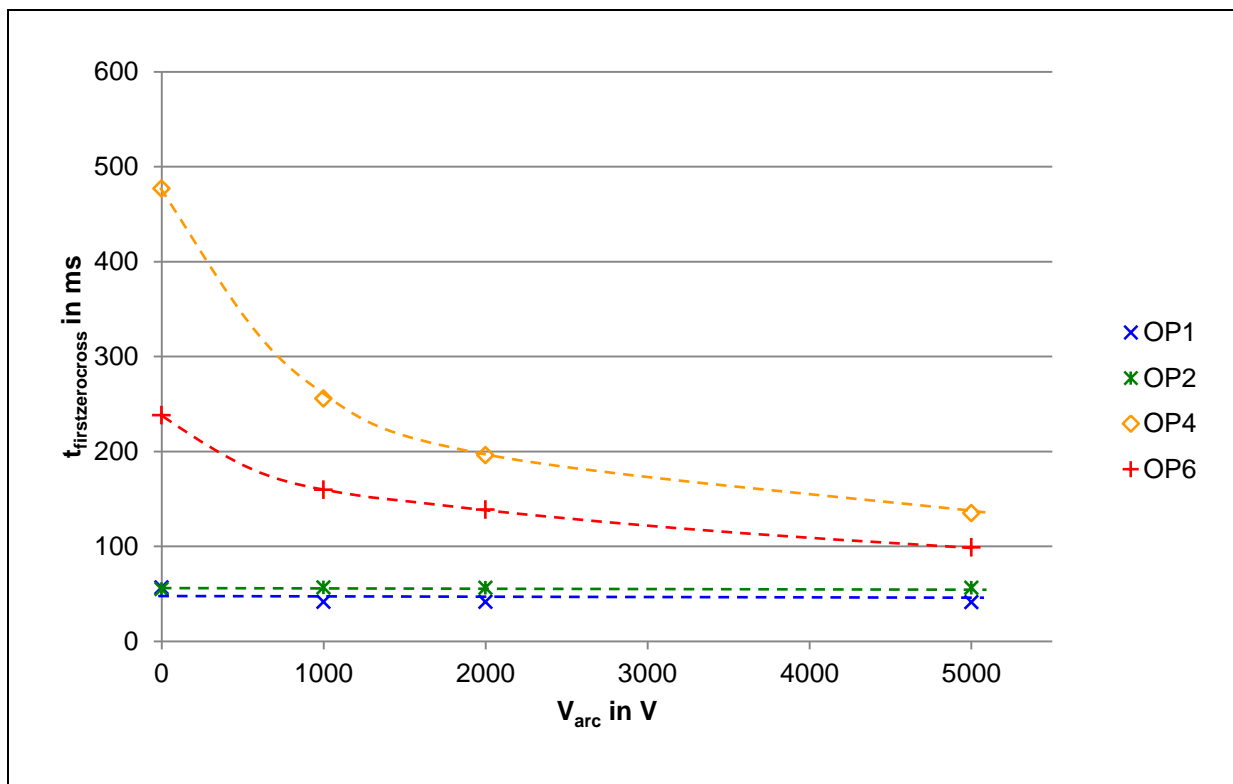
Table 15: Points of time of current first zero-crossings – model with $V_{\text{arc}} \approx 5000$ V

Figure 48: Overall comparison of points of time of current first zero-crossings in most disadvantaged phases by using Mayr's equation

The overall comparison in Figure 48 shows a possible relation between the level of the arc voltage and the point of time of first zero-crossing, especially in operating points with load. It is a similar figure to Figure 42 in the chapter about the model with constant d.c. arc voltage. At open-circuit point and nominal rating point there's almost no visible relation between these parameters. But if the synchronous generator is in under-excited mode the influence of the arc voltage on the decay characteristic becomes visible. The higher the arc voltage is, the earlier the point of time of current's first zero-crossing appears. In the figure above the arc voltage increases from the left to the right from 0 V in various steps to 5000 V, whereby an arc voltage of 0 V means, that there is modeled an ideal circuit breaker.

As shown in chapter 4.4 the arc voltage could be replaced by a virtual arc resistance, depending on the arc voltage and the current (Ohm's law). The signal sequence of the virtual resistance according to the case shown in Figure 49 is pictured in the following figure. The dotted line symbolizes the calculated average of the virtual arc resistance R_{mean} .

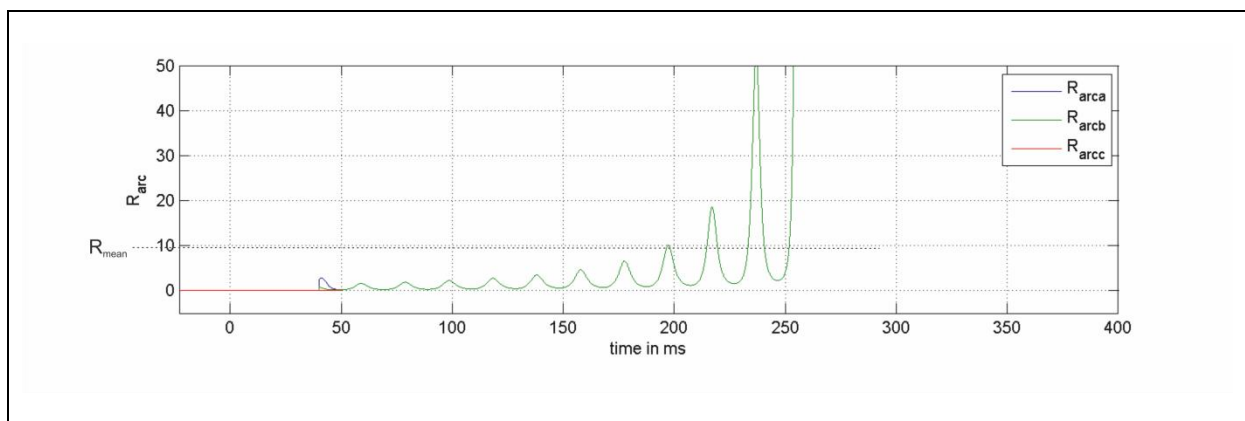


Figure 49: OP 4: arc resistance R_{arc} in all phases – Mayr's equation with an arc voltage of about 1000 V, $t_{contactseparation} = 40$ ms

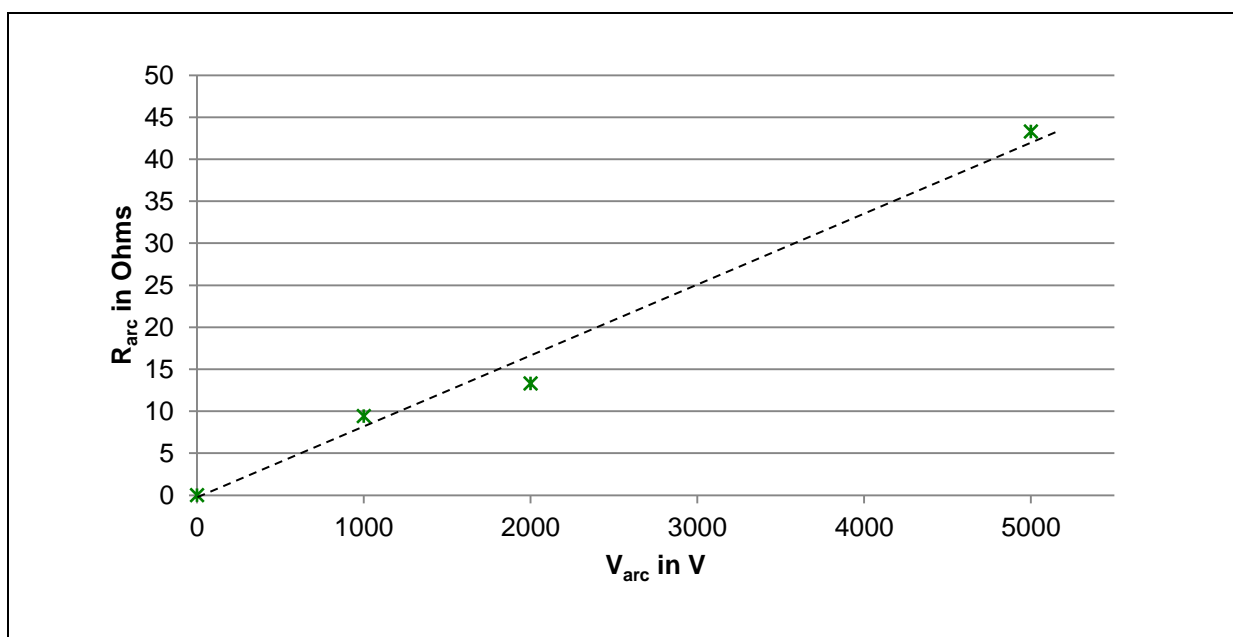


Figure 50: OP 4: virtual arc resistances by using different arc voltages

The figure above shows the virtual arc resistances by using Mayr's equation at different arc voltages in operating point 4. It can be seen that the higher the arc voltage, the higher the virtual equivalent arc resistance is. This is the same effect as described in chapter 4.5.1 by using the model with constant d.c. arc voltage.

4.5.3 Comparison of model with constant d.c. arc voltage and model with Mayr's equation

To investigate the influence of a more complex arc model on the characteristic of the arc voltage and furthermore on the current characteristic, it is needed to compare the results of chapters 4.5.1 (model with constant d.c. arc voltage) and 4.5.2 (Mayr's model of electric arc).

Concerning the point of time of current first zero-crossing the following figure shows the differences between using the model with constant d.c. arc voltage and using the model with Mayr's equation.

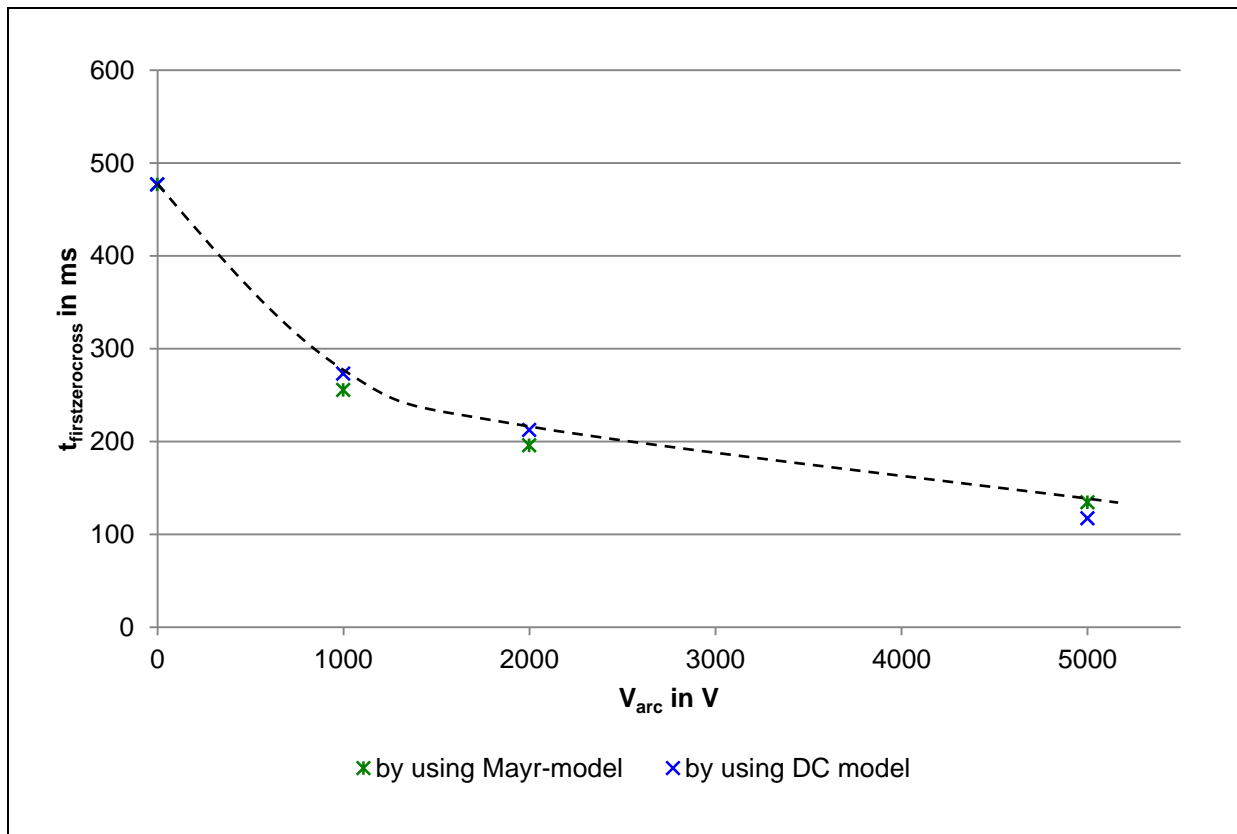


Figure 51: OP 4: Comparison of point of time of current's first zero-crossing in most disadvantaged phases

The green marks in Figure 51 represent the point of time of current's first zero-crossing in most disadvantaged phases by using Mayr's equation. The blue marks in the figure above represent the values by using the model with constant d.c. arc voltage. In the figure above is shown that there is only a small difference (about one signal period) between the results concerning the time of current's first zero-crossing.

The result of a comparison concerning the virtual arc resistance is not equivalent. As described in chapter 2.3.2 Mayr's equation is more usable to model the signal sequences in lower current regions. Therefore the virtual arc resistance increases many times in the same areas like the characteristic of the arc voltage do. As a result the average of the virtual arc voltage over a period of arcing time is higher by using Mayr's equation than by using the model with constant d.c. arc voltage (cf. Figure 52).

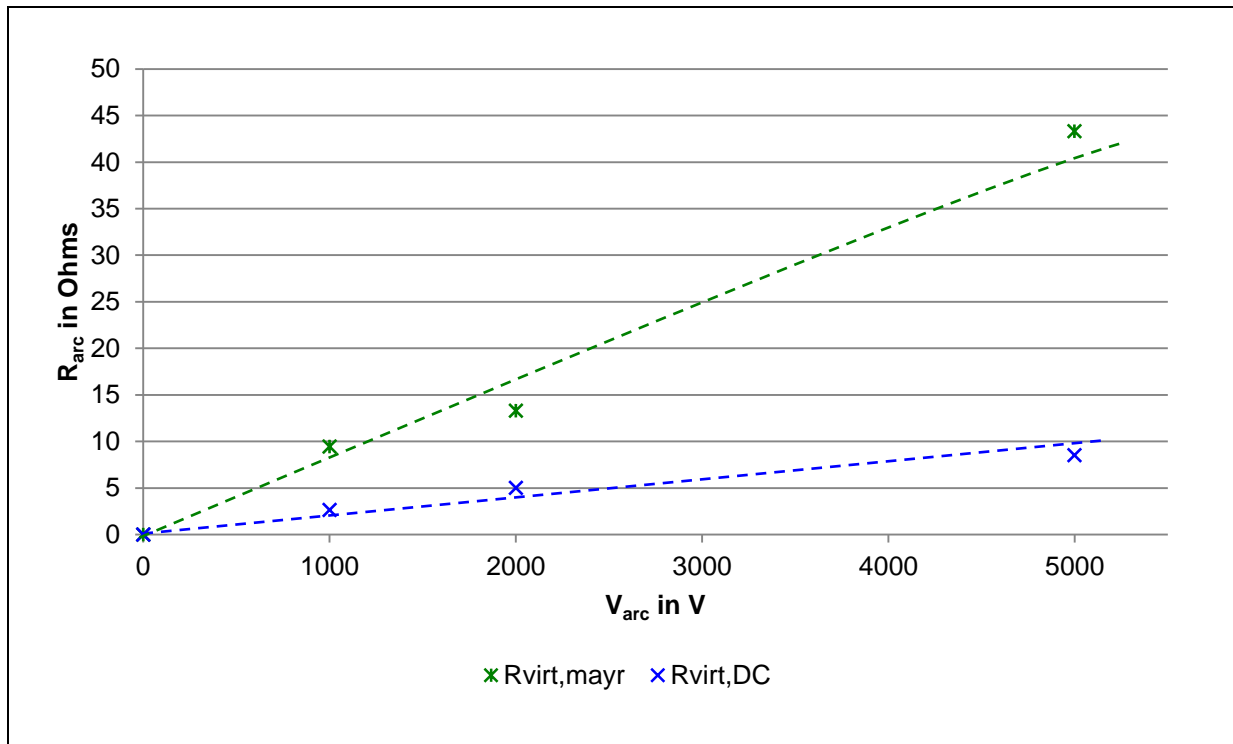


Figure 52: OP 4: comparison of virtual arc resistance by using different arc models

As a conclusion it can be said that it is enough to replicate the electric arc by the model with constant d.c. arc voltage for a first estimation. The differences concerning the point of time of current's first zero-crossing are in a range of about one signal period at the on hand conditions and for the chosen parameters. For further studies of the arc's influence on the current's characteristics Mayr's equation is only a first indicator.

4.6 Impact of arc voltage on zero-crossing of current considering the wye connection of the transformer

For this analysis two different types of transformers are needed:

- Transformer YNd5, wye connection is solidly grounded
- Transformer Yd5, wye connection is isolated

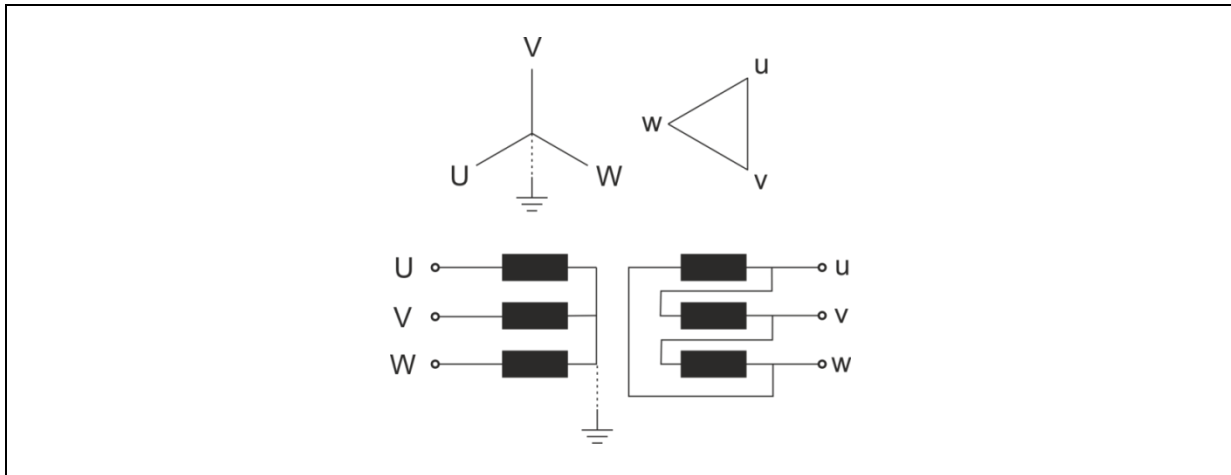


Figure 53: Connection symbol of Yd5/YNd5-transformer

Figure 54 shows the signal sequences by using an Yd5-tranformer and constant arc voltage.

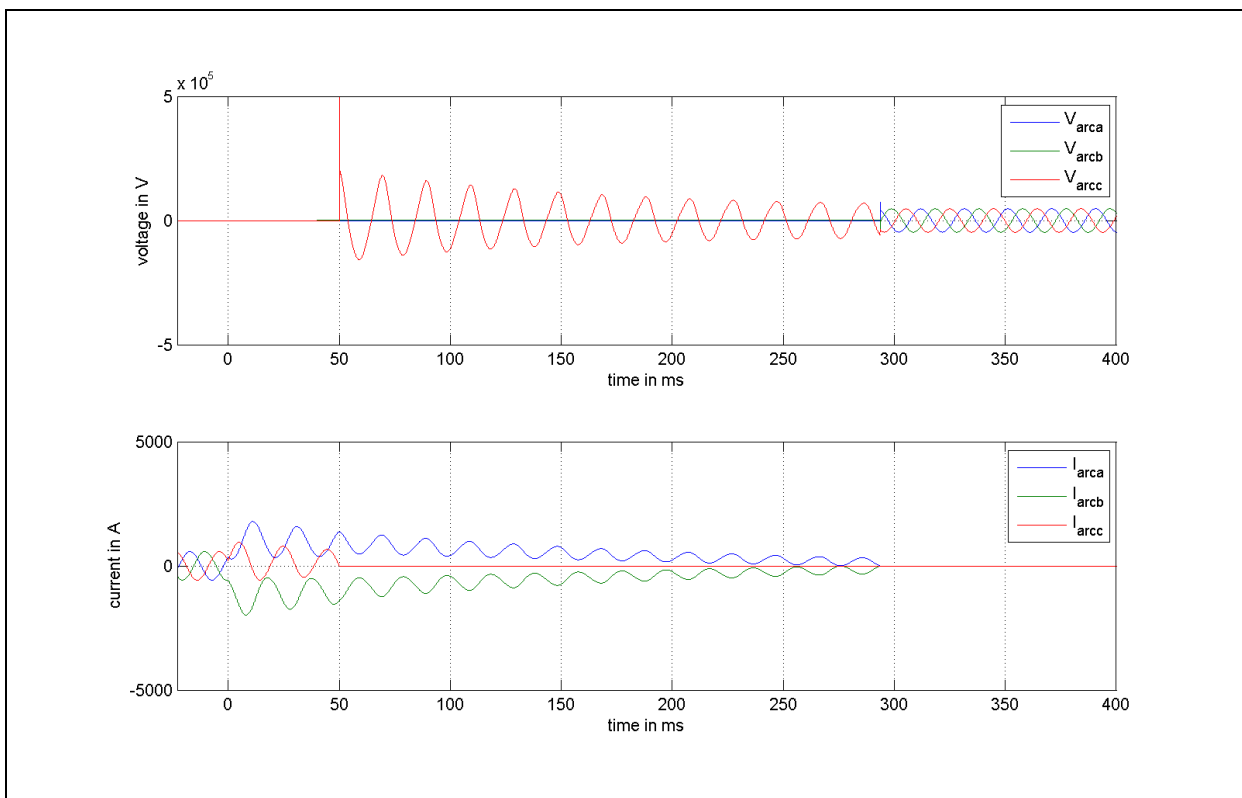


Figure 54: OP 4: signal sequences V_{arc} and I_{arc} – model with $V_{DC} = 1000 \text{ V}$, $t_{contactseparation} = 40 \text{ ms}$

In contrary to a circuit with an YNd5-transformer, by using an Yd5-transformer the characteristics of the two residual phases are symmetric after interrupting in one phase (cf. phase C in the figure above). This effect of symmetry doesn't appear in a circuit with an YNd5-transformer.

The influence of the transformer's wye connection on the point of time of current's first zero-crossing is not very high. The figure below shows an overall comparison of point of current's first zero-crossing in most disadvantaged phases using an YNd5-transformer (left marks) and

an Yd5-transformer (right marks). There can be seen that the difference between the left-hand and the right-hand marks are small-sized.

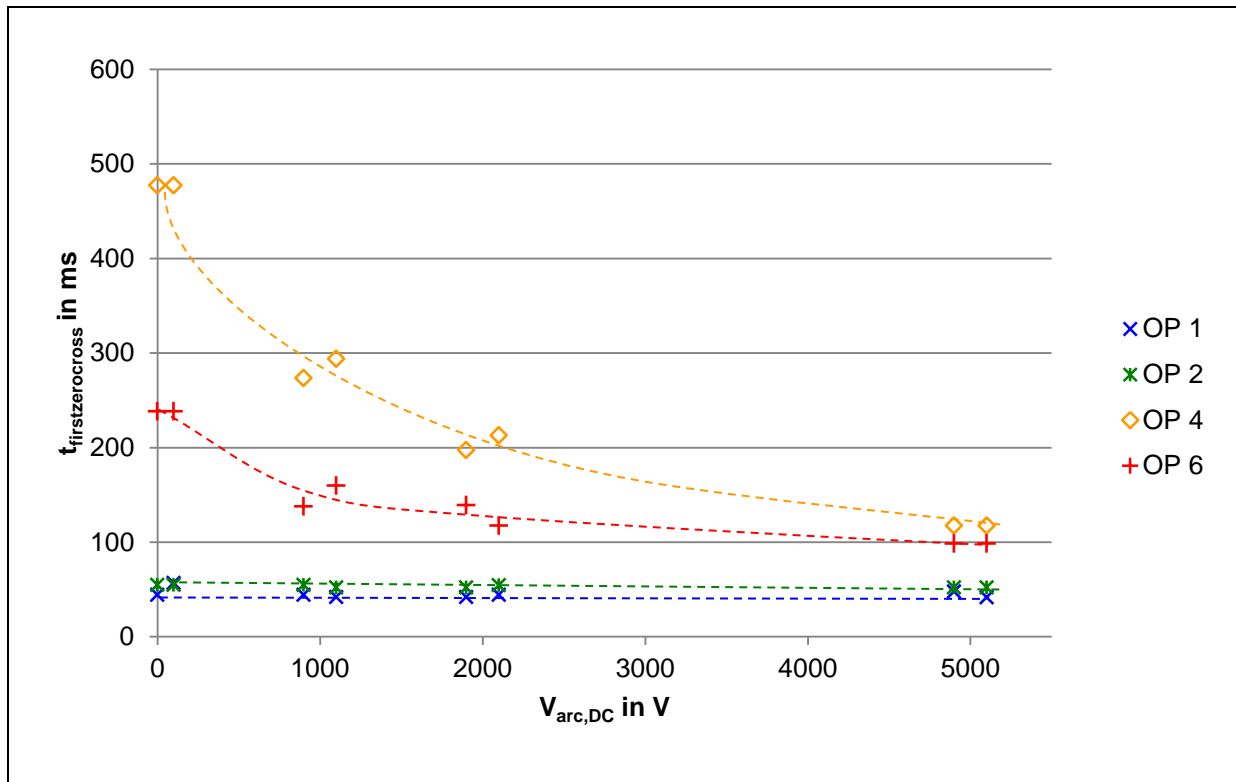


Figure 55: Overall comparison of point of current's first zero-crossing in most disadvantaged phases using an YNd5-transformer (left marks) and an Yd5-transformer (right marks)

The overall comparison in Figure 55 shows, that there is a relation between the value of the arc voltage and the point of time of current's first zero-crossing. The higher the arc voltage is, the earlier the first zero-crossing of current occurs. The wye connection of the transformer has no fundamental influence on this point of time, but on the characteristics of the residual currents after breaking the first phase.

4.7 Impact of arc voltage on zero-crossing of current considering the ground connection of the fault

For this analysis two different types of faults are needed:

- Three-phase short-circuit, without ground connection (3p fault)
- Three-phase short-circuit to ground (3pG fault)

The investigation of the influence of the arc voltage on the zero-crossing of current considering the ground connection of the fault are made by using operating point 4.

Figure 56 shows the schema of the two different used types of fault.

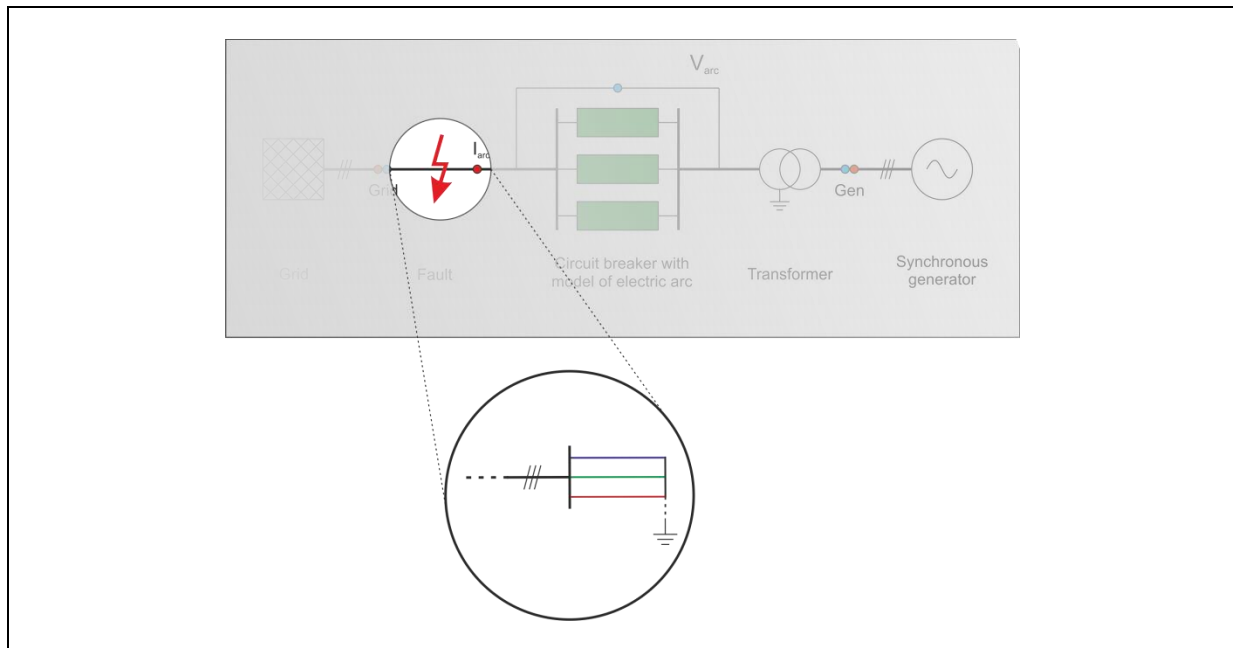


Figure 56: Schematic figure of a three-phase short-circuit with/without ground-connection

Figure 57 shows the signal sequences after a three-phase short-circuit to earth and by using the model with constant d.c. arc voltage.

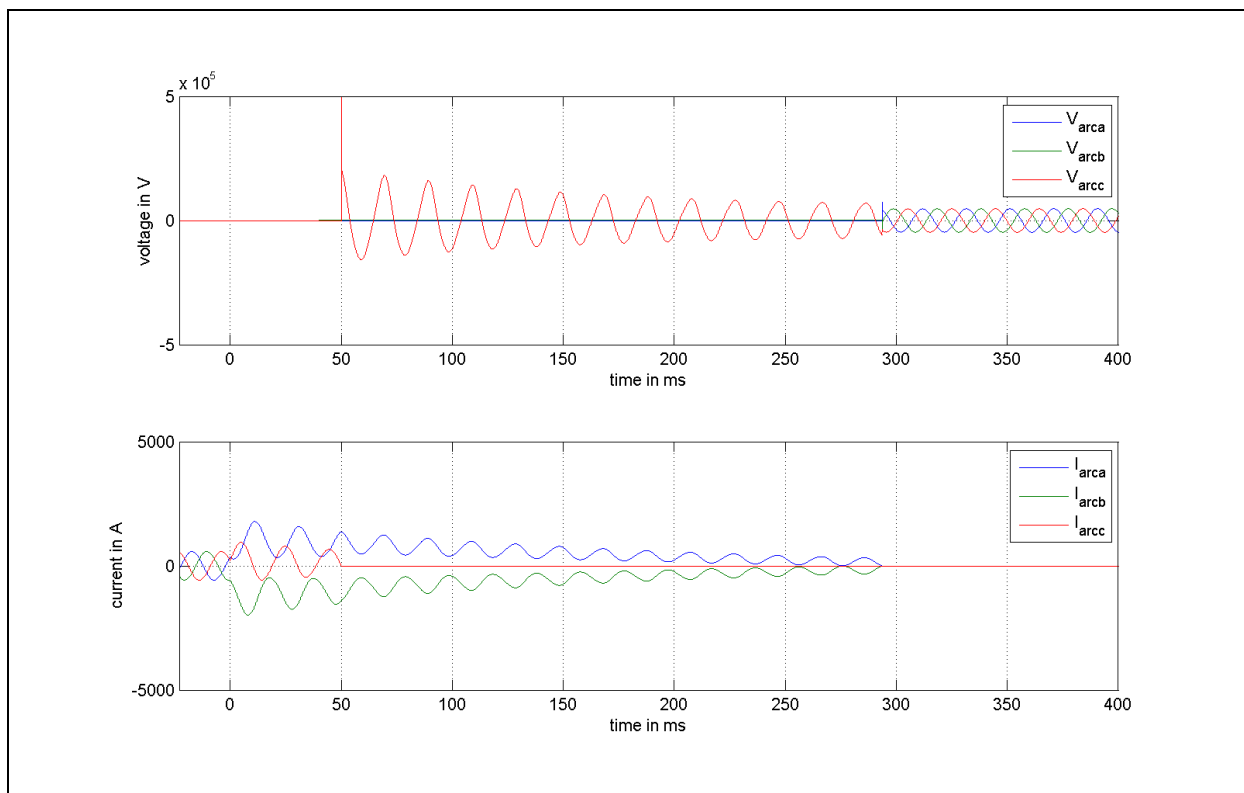


Figure 57: OP 4: signal sequences V_{arc} and I_{arc} – model with $V_{DC} = 1000$ V, $t_{contactseparation} = 40$ ms

In contrary to a circuit with a three-phase short-circuit without ground connection, in a circuit with a three-phase short-circuit to earth, the characteristics of the two residual phases are

symmetric after circuit breaking in one phase (cf. phase C in the figure above). This effect of symmetry doesn't appear in a circuit with a fault without ground connection.

The following figure shows the differences in the point of time of current's first zero-crossing in most disadvantaged phases by using a three-phase short-circuit with/without ground connection.

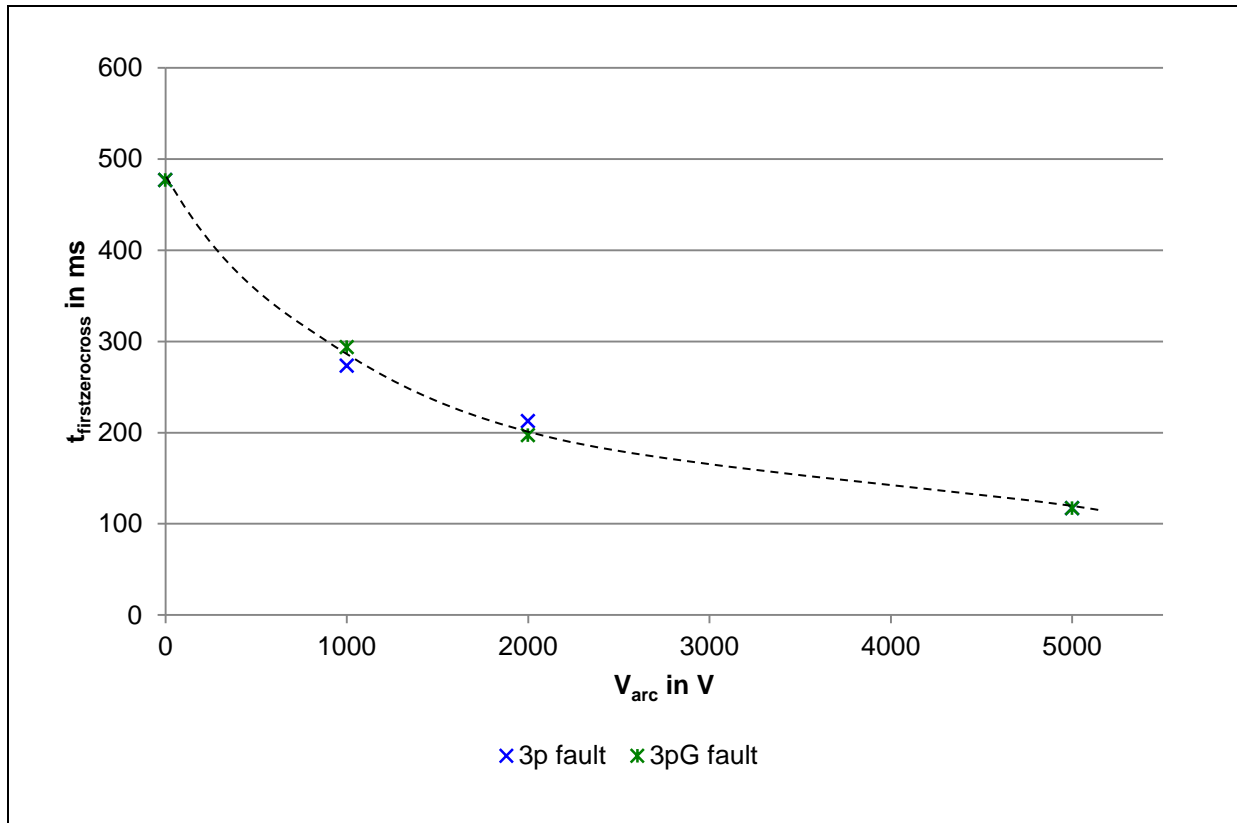


Figure 58: OP4: comparison of point of current's first zero-crossing in most disadvantaged phases at three-phase short-circuit (blue marks) and at three-phase short-circuit to ground (green marks)

The difference of point of time of current's first zero-crossing between the two cases of fault can be explained by the difference of current characteristics. While the currents in the two residual phases (after circuit breaking in one phase) are symmetric after a three phase short-circuit to ground, this effect of symmetry does not appear after a three phase short-circuit fault without any ground connection.

All in all, the influence of the fault's ground connection on the point of time of current's first zero-crossing is not very high after a three phase short-circuit fault and under the given parameters.

5 Conclusion

Summarized it can be noted, that the exact modeling of arc voltage is a complex task. It requires excellent knowledge in arc physics and fundamental knowledge in basic electrical engineering, with respect on circuit breakers and their operation task as well as on their function.

To analyze the influence of the breaking arc voltage on the decay characteristic of the current's DC-component, some groundwork has to be done before. The question concerning that influence only arises if current zero-crossings are missing. The missing current zero-crossings only occur under unlucky circumstances (initial conditions of salient-pole machine, fault location, temporal arising of the fault).

It is shown, that the state of the synchronous generator's initial condition is significant decisive for missing current zero-crossings. The missing of current zero-crossings is advantaged if the generator is in under-excited mode. Additionally the fault's point on wave is a key factor concerning the maximum value of the current's DC-component. The worst-case point on wave concerning the DC-component is if the fault occurs at the zero-crossing of the line-to-ground voltage in one phase. Furthermore the active reactances of the salient-pole machine must be regarded if analyzing the current characteristic, because they are mainly responsible for it in case of short-circuits.

Scientists concentrate on the electric arc for many years. Cassie and Mayr developed models of the electric arc based on the thermal capacity of the arc column in the 1930s and 1940s. While Cassie's equation of electric arc is useful to model the current through the arc in higher current regions, Mayr's equation models the arc in regions of zero-crossing. Out of that, the combination of Cassie's and Mayr's equations is commonly used. Many other arc models, based on the combined Cassie-Mayr equation have been found since then, and the level of complexity increased. The more comprehensive arc models are ongoing with a significant amount of investment concerning the identification of suitable model parameters, which causes more difficulties. In the literature there can be found a few parameters, but with the fact, that most of them are not universal. They are determined by experimental studies and mainly valid in those individual cases.

The on hand master's thesis is concerned with a non-complex arc model: a model with constant d.c. arc voltage, that means that the arc voltage is set as a constant value for the duration of the arc. The advantage of this model is, that only one parameter is needed and that one may be estimated well or is known because of several manufacturer information or data sheets of the circuit breakers. A disadvantage of this more or less easy model is the not exactly reproduced arc voltage. But the on hand results show, that this is not necessary for basic studies. The relevant parameter to determine the influence of the arc voltage on the decay characteristic of current's DC-component is the level of the arc voltage. The higher the arc voltage, the higher its impact on the decay characteristic of current's DC-component is. The exact modeling of the arc voltage's temporal sequence is not necessary for basic statements about that influence.

Regarding the impact of the arc voltage on the zero-crossing of the current considering the ground connection of the fault it can be noted that there are only small differences. But they could also appear, because of the characteristics of the two residual phases, which are symmetric after breaking one phase in case of a three-phase short-circuit with ground connection. That described effect of symmetry doesn't appear in a circuit with a fault without ground connection. The impact of the arc voltage on the decay characteristic of the current's DC-component is nearly the same in both three-phase short-circuits with and without ground connection.

The scientists studying the electric arc are asked for further universal investigations concerning the modeling of the electric arc and universal arc models. The last developments force a trend to experimental studies of the electric arc in individual cases. A focus on general statements with a sufficient physical relevance would be desirable instead of investigations in individual cases which are based on mathematical optimizations and model parameter fitting afterwards.

Bibliography

ABB AB (Ed.): Live Tank Circuit Breakers, Application Guide, Ludvika (Sweden) 2013

BALZER, G.; NELLES, D.; TUTTAS, C.: Kurzschlussstromberechnung nach IEC und DIN EN 60909-0, Grundlagen, Anwendung der Normen, Auswirkungen der Kurzschlussströme, 2nd revised edition, Berlin 2009

BERGER, S.: Modell zur Berechnung des dynamischen elektrischen Verhaltens rasch verlängerter Lichtbögen, Dissertation, Zürich 2007

BIZJAK, G.; ZUNKO, P.; POVH, D.: Combined Model of SF6 Circuit Breaker for Use in Digital Simulation Programs in: IEEE Transactions on Power Delivery, vol. 19, no. 1, 2004, p. 174-180

BRINKHOFF, R.; KULICKE, B.; SCHRAMM, H.-H.: Ausschalten nicht-simultaner Kurzschlüsse mit ausbleibenden Stromnulldurchgängen durch SF6-Blaskolbenschalter in: VEREINIGUNG DEUTSCHER ELEKTRIZITÄTSWERKE (Ed.): Elektrizitätswirtschaft, vol. 77, no. 11, 1978, p. 384-393

CANAY, D.: Beitrag zum Problem des Abschaltens von asymmetrischen Stosskurzschlußströmen ohne Nulldurchgänge, 1969, p. 484-493

CANAY, D., KLEIN, H.: Asymmetrische Kurzschlussströme von Generatoren unter Berücksichtigung des Lichtbogens beim Abschalten, 1974, p. 199-206

CASSIE, A.: A New Theory of Rupture and Circuit Severity, CIGRE Report 102, 1939

CRASTAN, V.: Elektrische Energieversorgung 1, Netzelemente, Modellierung, stationäres Verhalten, Bemessung, Schalt- und Schutztechnik, 3rd revised edition, Berlin, Heidelberg 1999, 2006, 2012

DARWISH, H.; ELKALASHY, N.: Comparison of Universal Circuit Breaker Arc Representation with EMTP Built-in Model, IPST – International Conference on Power Systems Transients, New Orleans 2003

DOMMERQUE, R.: Einfluss des Elektrodenabbrandes auf das Schaltverhalten eines SF6-Selbstblaskalters, Dissertation, Aachen 2006

EMTP-RV: EMTP-RV | The reference for power system transients, <http://www.emtp.com/>, accessed 19 October 2013

FENSKE, S.: Ermittlung des Schaltvermögens von Hochspannungs-Leistungsschaltern beim Auftreten generatornaher Kurzschlussströme mit ausbleibenden Nulldurchgängen, Dissertation, Cottbus 2011

FILIPOVIC-GRCIC, B.; UGLESIC, I.; FILIPOVIC-GRCIC, D.: Analysis of Transient Recovery Voltage in 400 kV SF6 Circuit Breaker Due to Transmission Line Faults in: I.R.E.E. International Review of Electrical Engineering, vol. 6, no. 5, 2011, p. 2652-2658

GREENWOOD, A.: Electrical Transients in Power Systems, 2nd edition, US 1991

- HABEDANK, U.; SIEMENS AG: Application of a New Arc Model for the Evaluation of Short-Circuit Breaking Tests in: IEEE Transactions on Power Delivery, vol. 8, no. 4, 1993, p. 1921-1925
- HUTTER, S.; UGLESIC, I.; Universal Arc Resistance Model "Zagreb" for EMTP, in: CIGRE – 19th International Conference on Electricity Distribution, CIGRE2007 Session1, Vienna 2007
- JUÁREZ-CALTZONTZIN, L.; TRINIDAD-HERNÁNDEZ, G., ASIAÍN-OLIVARES, T; et al: Theoretical and Experimental Analysis of the Short Circuit Current Components in Salient Pole Synchronous Generators
- KIZILCAY, M.; LA SETA, P.; Digital Simulation of Fault Arcs in Medium-Voltage Distribution Networks in: 15th PSCC, Session 36, Paper 3, Liege 2005, p. 1-7
- KLAMT, J.: Berechnung und Bemessung elektrischer Maschinen, Berlin, Göttingen, Heidelberg 1962
- KOMITEE 311 (Ed.): Drehende elektrische Maschinen, Erläuterungen zu DIN EN 60034 (VDE 0530), VDE-Schriftenreihe Normen verständlich, 7th revised edition, vol. 10, Berlin 2004
- KONDALA RAO, B.; GAJJAR, G.: Development and Application of Vacuum Circuit Breaker Model in Electromagnetic Transient Simulation in: IEEE, 2006
- KOSHIZUKA, T.; SHINKAI, T.; UDAGAWA, K; et al: Circuit Breaker Model using Serially Connected 3 Arc Models for EMTP Simulation in: IPST – International Conference on Power Systems Transients, Kyoto 2009
- LEUSENKAMP, M.: Vacuum Interrupter Model Based on Breaking Tests in: IEEE Transactions on Plasma Science, vol. 27, no. 4, 1999, p. 969-976
- LINDMAYR, M.: Lichtbogensimulation – ein Überblick in: 20. VDE-Tagung Kontaktverhalten und Schaltung, Karlsruhe 2009
- LOWKE, J.; LUDWIG, H.: A Simple Model for High-Current Arcs Stabilized by Forced Convection in: J. Applied Physics, vol. 46, 1975, p. 3352-3360
- LOWKE, J.; KOVITYA, P, AHMED, S.; et al: Upstream Boundary Conditions for Channel Model representation of Arcs in Gas Flow in: J. Applied Physics, vol. 55, 1984, p. 789-791
- MARTINEZ, J.; MAHSEREDJIAN, J.; KHODABAKHCHIAN, B.: Parameter Determination for Modeling System Transients- Part IV: Circuit Breakers in: IEEE Transaction on Power Delivery, vol. 20, no. 3, 2005, p. 2079-2085
- MAYR, O.: Beiträge zur Theorie des statischen und des dynamischen Lichtbogens in: Archiv für Elektrotechnik, vol. 37, 1943, p. 588-608
- NEUMANN, C.: Kapitel 5: Lichtbogenlöschung in: Skriptum zur Vorlesung Hochspannungsschaltgeräte und –anlagen, Technische Universität Darmstadt, Darmstadt, p. 63-76
- NGAMSANROAJ, K.; PREMRUDEEPRECHACHARN, S.: Transient Study for Single Phase Reclosing Using Arc Model on the Thailand 500 kV Transmission Lines from Mea Moh to Tha To Ko in: IPST – International Conference on Power Systems Transients, Kyoto 2009

- NITU, S.; NITU, C.; MIHALACHE, C.; et al: Comparison between model and experiment in studying the electric arc in Journal of optoelectronics and advanced materials, 2008, p. 1192-1196
- ORAMA-EXCLUSA, L.: Numerical Modeling of Vacuum Arc Dynamics at Current Zero Using ATP in: IPST – International Conference on Power Systems Transients, Montreal 2005
- ORAMA-EXCLUSA, L.; RODRÍGUEZ-MEDINA, B.: Numerical Arc Model Parameter Extraction for SF6 Circuit Breaker Simulations in: IPST – International Conference on Power Systems Transients, New Orleans 2003
- PHANIRAJ, V.; PHADKE, A.: Modelling of circuit breakers in the Electromagnetic Transients Program in: IEEE Transactions on Power Systems, vol. 3, no. 2, 1988, p. 799-805
- PRIKLER, L.; KIZILCAY, M.; BÁN, G.; et al: Improved Secondary Arc Models Based On Identification Of Arc Parameters From Staged Fault Test Records in 14th PSCC, Session 24, Paper 3, Sevilla 2002, p. 1-7
- RAGALLER, K.: Current interruption in high-voltage networks, New York 1978
- REECE, M.P.: Power circuit breaker theory and design in: FLURSCHEIN, C.H. (Ed.), London 1985
- RIEDER, W.: Plasma und Lichtbogen, Braunschweig 1967
- SCHAVEMAKER, P.; VAN DER SLUIS, L.: An Improved Mayr-Type Arc Model Based on Current-Zero Measurements in: IEEE Transaction in Power Delivery, vol. 15, no. 2, 2000, p. 580-584
- SCHAVEMAKER, P.; VAN DER SLUIS, L.: The Arc Model Blockset in: EuroPES – Proceedings of the Second IASTED International Conference POWER AND ENERGY SYSTEMS, Crete 2002, p. 644-648
- SCHWAB, A.: Elektroenergiesysteme, Berlin, Heidelberg 2012
- SINDER, D.; LIMA, A.; CARNEIRO JR., S.; et al: Analysis of Circuit Breaker Application Based on Transient Recovery Voltage Using Frequency Domain Techniques in: IPST – International Conference on Power Systems Transients, Kyoto 2009
- SPRING, E.: Elektrische Maschinen, Eine Einführung, 3rd edition, Dordrecht, Heidelberg, London, New York 1998, 2006, 2009
- WANG, X.; SUMNER, M.; THOMAS, D.: Application of TLM and Cassie-Mayr Arc model on Transformer Aging and Incipient Fault Simulation in: Engineering Letters, 16:1, EL_16_1_12, 2008

Figures

Figure 1: Overview of the described structure	1
Figure 2: Schematic figure of the procedure	2
Figure 3: Equivalent network	4
Figure 4: Capability diagram and operating points of the chosen synchronous generator.....	6
Figure 5: Schematic figure of current characteristic in case of short-circuit.....	8
Figure 6: Main components of a self-blast circuit breaker	13
Figure 7: Process of high current interruption by a self-blast SF ₆ interrupter with pre-compression.....	15
Figure 8: Characteristic of Mayr's arc voltage.....	18
Figure 9: Characteristic of Cassie's arc voltage	20
Figure 10: Equivalent network	24
Figure 11: Connection symbol of Yd5/YNd5-transformer.....	26
Figure 12: Schematic diagram of arc voltage if arc voltage is a constant d.c. voltage.....	29
Figure 13: Implementation of model with constant d.c. arc voltage	29
Figure 14: Implementation of Cassie's equation	30
Figure 15: Implementation of Mayr's equation	31
Figure 16: Implementation of the combined Cassie-Mayr equation.....	31
Figure 17: Chart of signal sequences including the naming	32
Figure 18: Relative DC-component of phase current in different phases	33
Figure 19: Relative DC-component of current in each phase in due consideration of different operating points.....	34
Figure 20: Point of time of current's first zero-crossing in each phase in due consideration of different operating points	35
Figure 21: Equivalent network	36
Figure 22: Reference current basic signal	36
Figure 23: Signal sequences at different arc voltages by using the model with constant d.c. arc voltage.....	37
Figure 24: Comparison of arc voltages and shape of currents of different arc models	37
Figure 25: Equivalent network	38
Figure 26: Signal sequences at different arc voltages, model with constant d.c. arc voltage.....	40
Figure 27: Signal sequences at different arc voltages by using Cassie's equation.....	40
Figure 28: Signal sequences at different arc voltages by using Mayr's equation.....	41

Figure 29: Signal sequences at different arc voltages by using the Cassie-Mayr model41

Figure 30: Schematic diagram of Helmholtz’ superposition theorem.....42

Figure 31: Characteristic of Mayr’s arc voltage42

Figure 32: Sharp decline of the current in circuits with different load (pure resistive load and inductive load) and combined Cassie-Mayr-equation43

Figure 33: Signal characteristics (sketch) of circuits with different load.....43

Figure 34: Representation of arc voltage as a virtual resistance.....44

Figure 35: Comparison of point of time of current’s first zero-crossing using different models46

Figure 36: Comparison of virtual arc resistances using different models46

Figure 37: Comparison of current’s first zero-crossing by using the model and the virtual arc resistance.....47

Figure 38: OP 4: uninfluenced signal sequences V_{arc} and I_{arc} 49

Figure 39: OP 4: signal sequences V_{arc} and I_{arc} – ideal circuit breaker, $t_{contactseparation} = 40$ ms, YNd5-Transformer.....49

Figure 40: OP 4: signal sequences V_{arc} and I_{arc} – model with $V_{DC} = 1000$ V, $t_{contactseparation} = 40$ ms.....50

Figure 41: OP 4: signal sequences V_{arc} and I_{arc} – model with $V_{DC} = 1000$ V, $t_{contactseparation} = 40$ ms – zoom in at arc voltage50

Figure 42: Overall comparison of point of current’s first zero-crossing in most disadvantaged phases by using the model with constant d.c. arc voltage52

Figure 43: OP 4: arc resistance R_{arc} in all phases – model with $V_{DC} = 1000$ V, $t_{contactseparation} = 40$ ms.....53

Figure 44: OP 4: actual virtual arc resistances by using different arc voltages (green) compared to the virtual arc resistances which are needed to get the same results as by using the model (blue)54

Figure 45: OP 4: point of time of current’s first zero-crossing by using different values of virtual arc resistances (depending on the arc voltages)54

Figure 46: OP 4: signal sequences V_{arc} and I_{arc} – Mayr’s equation with an average arc voltage of about 1000 V, $t_{contactseparation} = 40$ ms.....55

Figure 47: OP 4: signal sequences V_{arc} and I_{arc} – Mayr’s equation with an arc voltage of about 1000 V, $t_{contactseparation} = 40$ ms, zoom in at arc voltage.....56

Figure 48: Overall comparison of points of time of current first zero-crossings in most disadvantaged phases by using Mayr’s equation.....57

Figure 49: OP 4: arc resistance R_{arc} in all phases – Mayr’s equation with an arc voltage of about 1000 V, $t_{contactseparation} = 40$ ms.....58

Figure 50: OP 4: virtual arc resistances by using different arc voltages58

Figure 51: OP 4: Comparison of point of time of current’s first zero-crossing in most disadvantaged phases.....59

Figure 52: OP 4: comparison of virtual arc resistance by using different arc models60

Figure 53: Connection symbol of Yd5/YNd5-transformer.....61

Figure 54: OP 4: signal sequences V_{arc} and I_{arc} – model with $V_{DC} = 1000 V$, $t_{contactseparation} = 40 ms$61

Figure 55: Overall comparison of point of current’s first zero-crossing in most disadvantaged phases using an YNd5-transformer (left marks) and an Yd5-transformer (right marks).....62

Figure 56: Schematic figure of a three-phase short-circuit with/without ground-connection ..63

Figure 57: OP 4: signal sequences V_{arc} and I_{arc} – model with $V_{DC} = 1000 V$, $t_{contactseparation} = 40 ms$63

Figure 58: OP4: comparison of point of current’s first zero-crossing in most disadvantaged phases at three-phase short-circuit (blue marks) and at three-phase short-circuit to ground (green marks).....64

Tables

Table 1: Operating conditions of synchronous generators	5
Table 2: Operating points of synchronous generator (belonging to Figure 4)	6
Table 3: Parameters of element grid.....	25
Table 4: Parameters of element transformer	25
Table 5: Parameters of element synchronous generator	26
Table 6: DC-component of current and point of time of current's first zero-cross in each phase in due consideration of different operating points	34
Table 7: Comparison of different models concerning time of zero-crossing	38
Table 8: Comparison of different models concerning time of zero-crossing	39
Table 9: Comparison of points of time of current's first zero-crossing and virtual arc resistances in different models	45
Table 10: Relative current's DC-component and point of time of current's first zero-crossing – model with $V_{arc} = 1000 \text{ V}$	51
Table 11: Relative current's DC-component and point of time of current's first zero-crossing – model with $V_{arc} = 2000 \text{ V}$	51
Table 12: Relative current's DC-component and point of time of current's first zero-crossing – model with $V_{arc} = 5000 \text{ V}$	51
Table 13: Points of time of current first zero-crossings – model with $V_{arc} \approx 1000 \text{ V}$	56
Table 14: Points of time of current first zero-crossings – model with $V_{arc} \approx 2000 \text{ V}$	57
Table 15: Points of time of current first zero-crossings – model with $V_{arc} \approx 5000 \text{ V}$	57

Abbreviations

μs	Microsecond
3p	Three-phase short-circuit without ground connection
3pG	Three-phase short-circuit to ground
A	Ampere
AC	Alternating current
CB	Circuit breaker
cf.	Compare (from Latin: confer)
const.	Constant
$\cos \varphi$	Power factor
d-axis	Direct axis
DC	Direct current
E_C	Arc column's gradient
f	Frequency
f_{rT}	Rated transformer frequency
g	Conductivity
g_C	Cassie conductance
Gen	Synchronous generator
g_M	Mayr conductance
H	Inertia constant
Hz	Hertz
I	Current
$i(t)$	Time-variant current
i_{AC}	Alternating current component
I_{arc}	Current through the electric arc
I_C	Steady-state short-circuit current
\hat{I}_C	Peak value of steady-state short-circuit current
I_C''	Sub-transient short-circuit current
\hat{I}_C''	Peak value of sub-transient short-circuit current
I_{cG}	Short-circuit current of synchronous generator
i_{DC}	Direct current component
$i_{DC}(t)$	Time-variant decaying direct current component
$i_{DC,rel}$	Relative current's DC-component
I_f	Field current
I_{rG}	Rated current of synchronous generator

K	Kelvin
kA	Kilo ampere
kV	Kilo volt
kV_{peak}	Peak value in kilo volts
$kV_{\text{RMS,LL}}$	Line-to-line root mean square voltage in kilo volts
kW	Kilo watt
L	Inductance
max	Maximum
ms	Millisecond
MVA	Mega volt-ampere
MW	Mega watt
no.	Number
OP	Operating point
p	Active power in per-unit
p.	Page
p.u.	Per-unit value
P_0	Cooling power in Schwarz and Avdonin model
P_0, P_1	Cooling constants in Schavemaker and Van der Sluis model
P_{diss}	Dissipated power
P_M	Dissipated power in Mayr's model
P_{out}	Stationary thermic losses
q	Reactive power in per-unit
Q	Thermal capacity
Q_0	Heat quantity
q-axis	Quadrature axis
R	Resistance
R_0	Zero sequence resistance
R_2	Negative sequence resistance
R_a	Armature resistance
R_{arc}	Arc resistance
$R_{\text{arc,virt}}$	Virtual value of arc resistance
R_{calc}	Calculated mean value of arc resistance
r_K	relative transformer's short-circuit resistance
R_{mean}	Mean value of arc resistance
rms	Root-mean-square
rpm	Rated speed
rpm	Rotations per minute
s	Second

S	Rated power
SF ₆	Sulphure hexafluoride
SM	Synchronous machine (generator)
S _{rG}	Rated power of synchronous generator
S _{rT}	Rated transformer power
S _{SC,1pol}	One-phase short-circuit power
S _{SC,3pol}	Three-phase short-circuit power
T	Time constant
t	time
T ₀	Thermal time constant in Schwarz and Avdonin model
t ₀	Starting point
T _a	Armature short-circuit time constant
T _C	Time constant in Cassie's equation
t _{contactseparation}	Point of time of circuit breaker contact separation
T _d '	Transient short-circuit time constant on direct axis
T _d ''	Sub-transient short-circuit time constant on direct axis
T _{d0} '	Transient open circuit time constant on direct axis
T _{d0} ''	Sub-transient open circuit time constant on direct axis
t _{fault}	Point of time of fault
t _{firstzerocross}	Point of time of current first zero-crossing
T _M	Time constant in Mayr's equation
T _q '	Transient short-circuit time constant on quadrature axis
T _q ''	Sub-transient short-circuit time constant on quadrature axis
T _{q0} '	Transient open circuit time constant on quadrature axis
T _{q0} ''	Sub-transient open circuit time constant on quadrature axis
u _K	relative transformer's short-circuit impedance
V	Rated voltage
V	Volt
v(t)	Time-variant voltage
V _{arc}	Arc voltage
V _{arc} (t)	Time-invariant arc voltage
V _C	Voltage in Cassie's equation
V _{DC}	Direct voltage
V _M	Voltage in Mayr's equation
V _{rG}	Rated voltage of synchronous generator
V _{source}	Source voltage
W	Watt
w ₁	Number of transformer windings on primary side

w_2	Number of transformer windings on secondary side
X	Impedance
X_0	Zero sequence reactance
X_2	Negative sequence reactance
X_d	Synchronous reactance on direct axis
$X_d(t)$	Time-variant synchronous reactance on direct axis
X_d'	Transient synchronous reactance on direct axis
X_d''	Sub-transient synchronous reactance on direct axis
X_{potier}	Potier-reactance
X_q	Synchronous reactance on quadrature axis
X_q'	Transient synchronous reactance on quadrature axis
X_q''	Sub-transient synchronous reactance on quadrature axis
Yd5	Winding connection of transformer
YNd5	Winding connection of transformer
Z'_{cG}	Short-circuit impedance of synchronous generator converted on high tension
Z_0	Zero sequence impedance
Z_2	Negative sequence impedance
Z_{cG}	Short-circuit impedance of synchronous generator
Z_{cT}	Transformer's short-circuit impedance
Z_{sum}	Sum of impedances
α	Parameter that influences the conductance dependency of T0
β	Parameter that influences the conductance dependency of P0
ϑ	Load angle
σ	Specific conductivity
φ	Phase angle
Ω	Ohm

Appendix

Appendix 1: Tables79
Appendix 2: Figures80

Appendix 1: Tables

Worst-case point on wave with respect to the current's DC-component

Point on wave		phase A	phase B	phase C
t_1 in ms	α in °	$i_{DC,rel}$ in %	$i_{DC,rel}$ in %	$i_{DC,rel}$ in %
0	0	66,53	41,99	24,87
0.5	9	67,26	33,21	34,36
1.0	18	66,36	23,59	42,98
1.5	27	63,83	13,38	50,53
2.0	36	59,74	2,84	56,83
2.5	45	54,18	7,77	61,74
3.0	54	47,26	18,18	65,14
3.5	63	39,17	28,12	66,95
4.0	72	30,08	37,34	67,14
4.5	81	20,24	45,63	65,69
5.0	90	9,89	52,78	62,64
5.5	99	0,71	58,63	58,05
6.0	108	11,28	63,04	52,01
6.5	117	21,56	65,92	44,69
7.0	126	31,28	67,20	36,24
7.5	135	40,25	66,84	26,88
8.0	144	48,15	64,85	16,84
8.5	153	54,88	61,28	6,37
9.0	162	60,27	56,19	4,25
9.5	171	64,18	49,71	14,75
10.0	180	66,53	41,99	24,87

Table 16: Relative DC-component of phase current in different phases

Appendix 2: Figures

Model with constant d.c. arc voltage (DC-model), three-phase short-circuit without ground connection

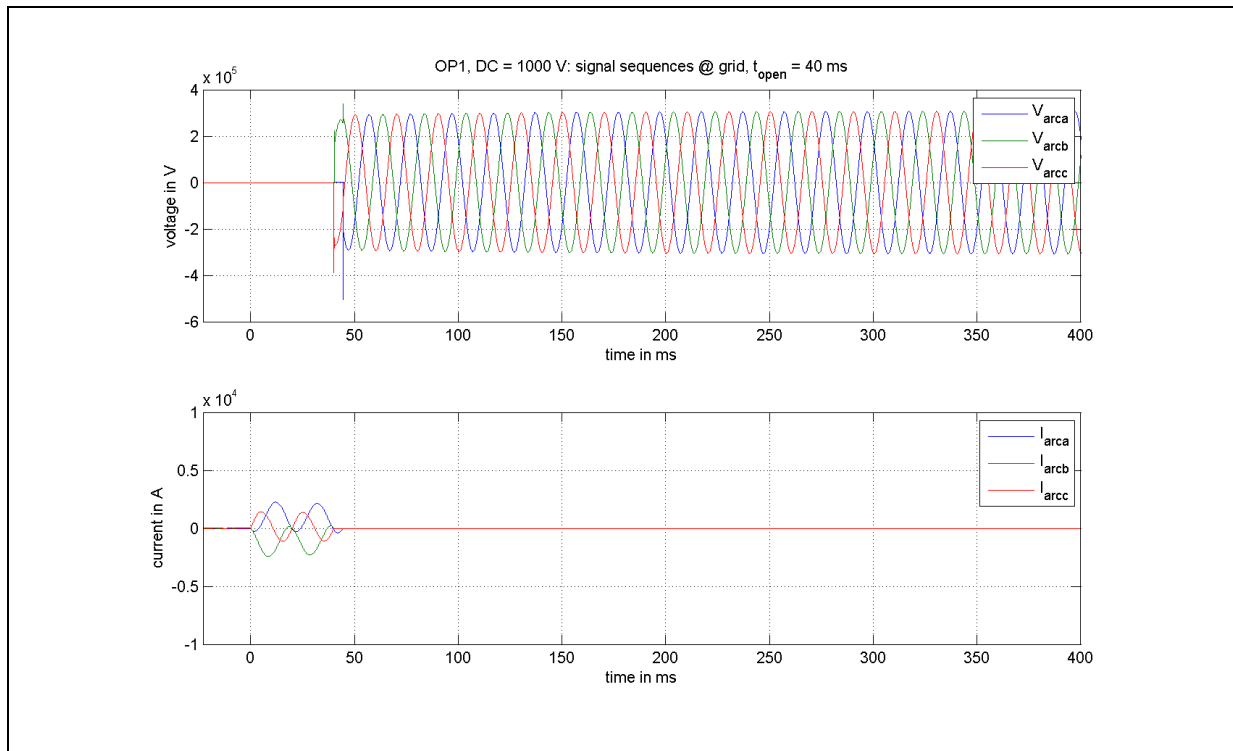


Figure 59: OP 1 (DC model): signal sequences V_{arc} and I_{arc} – $V_{arc} = 1000$ V, $t_{contactseparation} = 40$ ms

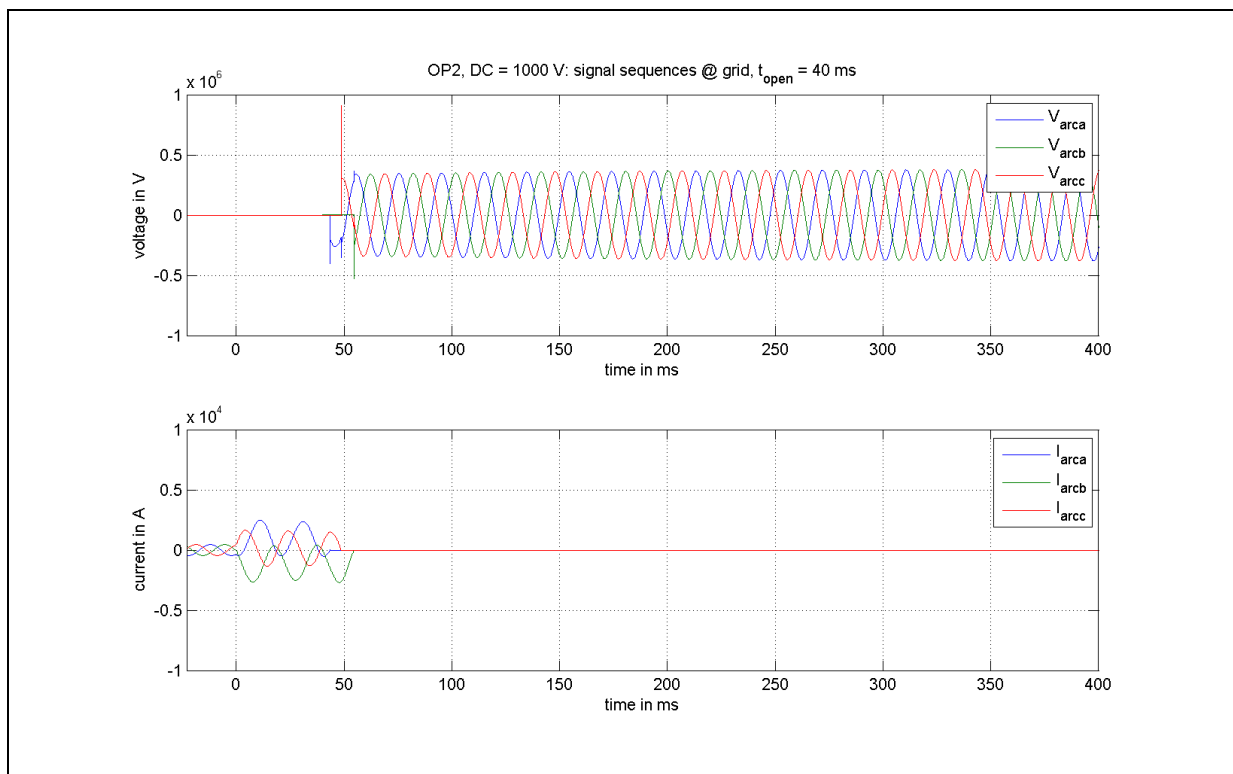


Figure 60: OP 2 (DC model): signal sequences V_{arc} and I_{arc} – $V_{arc} = 1000$ V, $t_{contactseparation} = 40$ ms

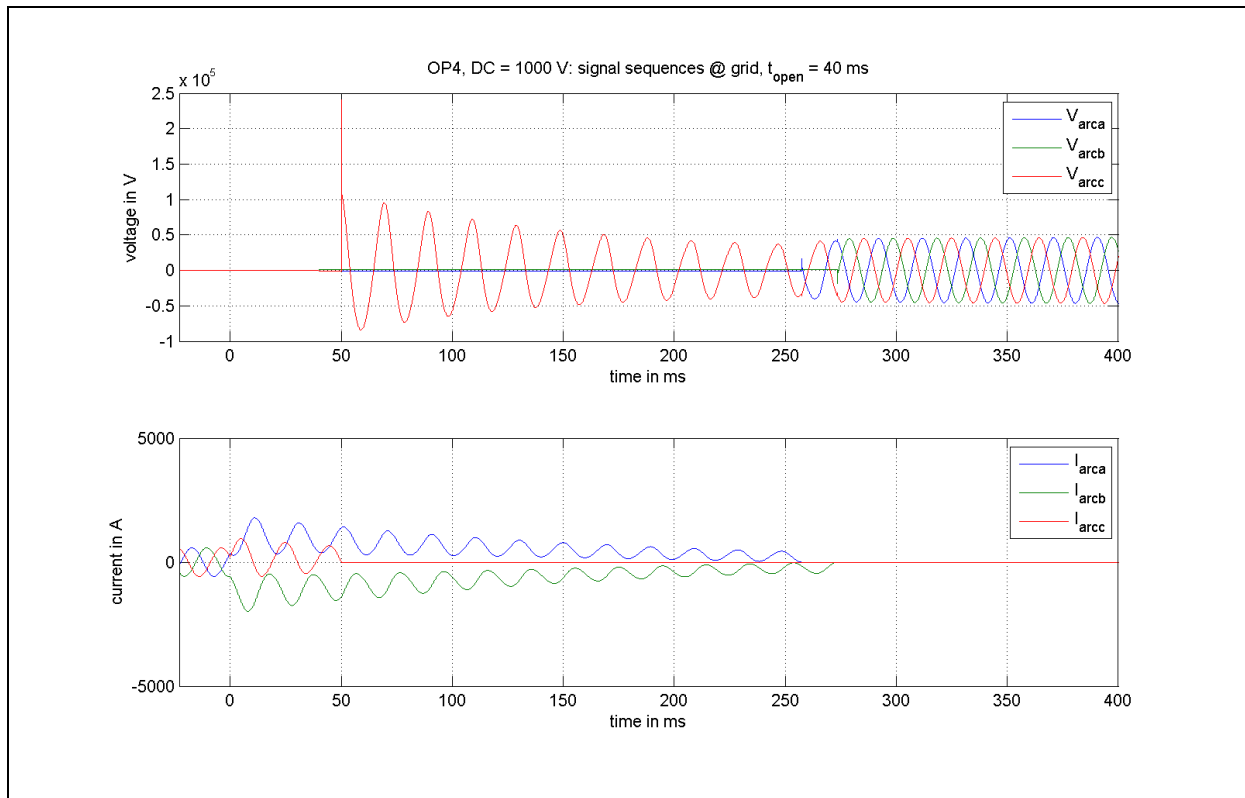


Figure 61: OP 4 (DC model): signal sequences V_{arc} and I_{arc} – $V_{arc} = 1000$ V, $t_{contactseparation} = 40$ ms

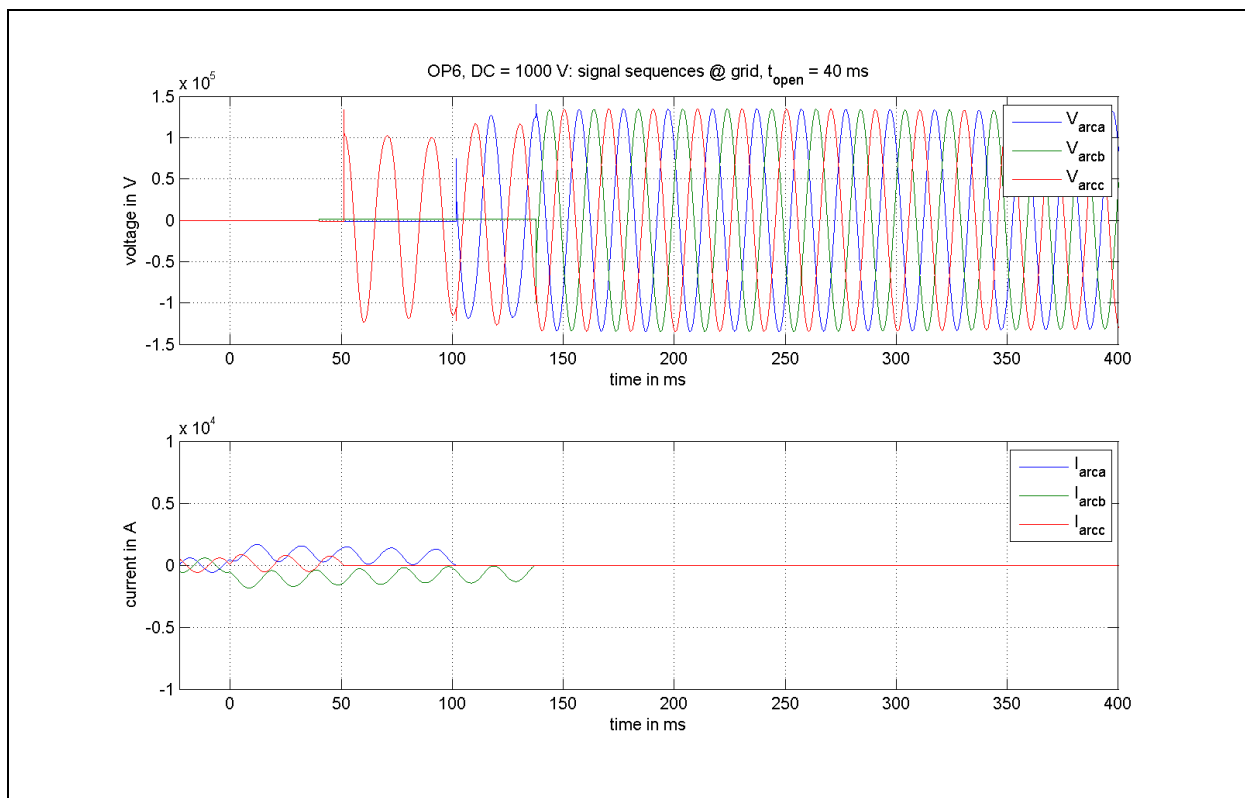


Figure 62: OP 6 (DC model): signal sequences V_{arc} and I_{arc} – $V_{arc} = 1000$ V, $t_{contactseparation} = 40$ ms

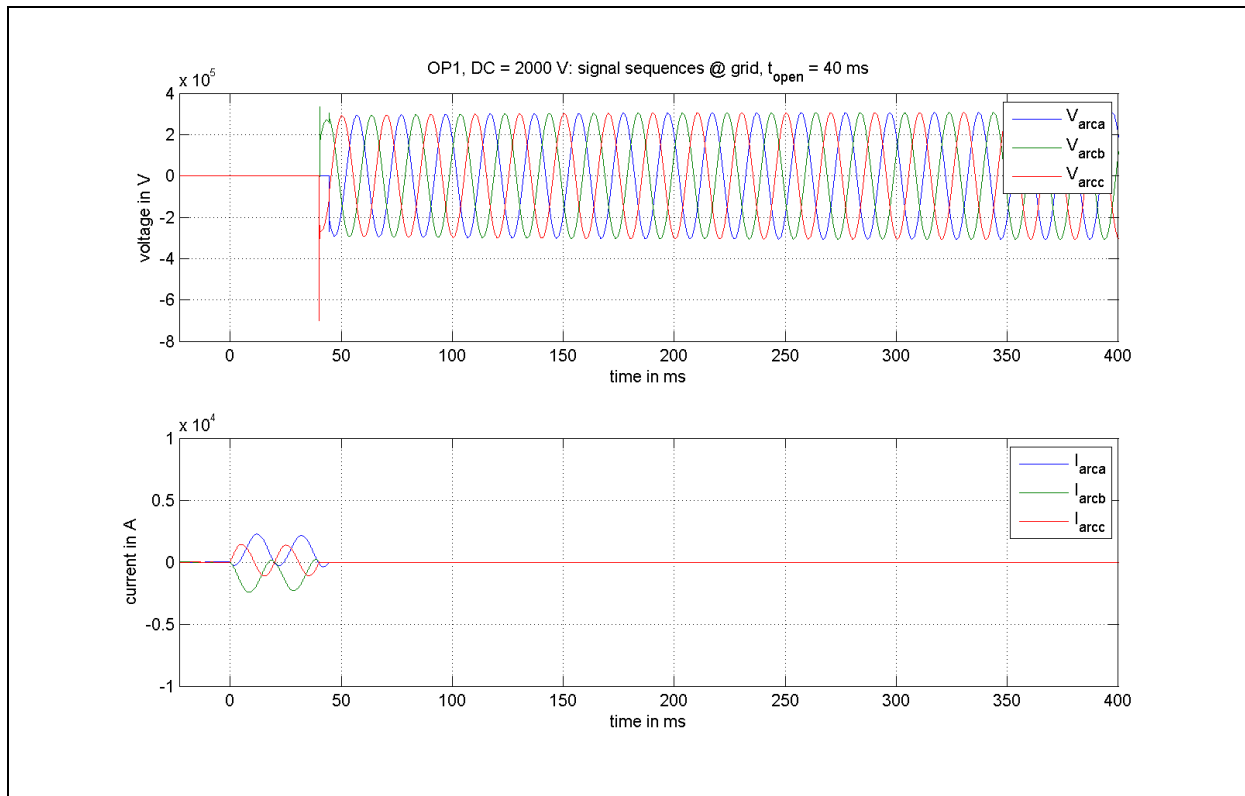


Figure 63: OP 1 (DC model): signal sequences V_{arc} and I_{arc} – $V_{arc} = 2000$ V, $t_{contactseparation} = 40$ ms

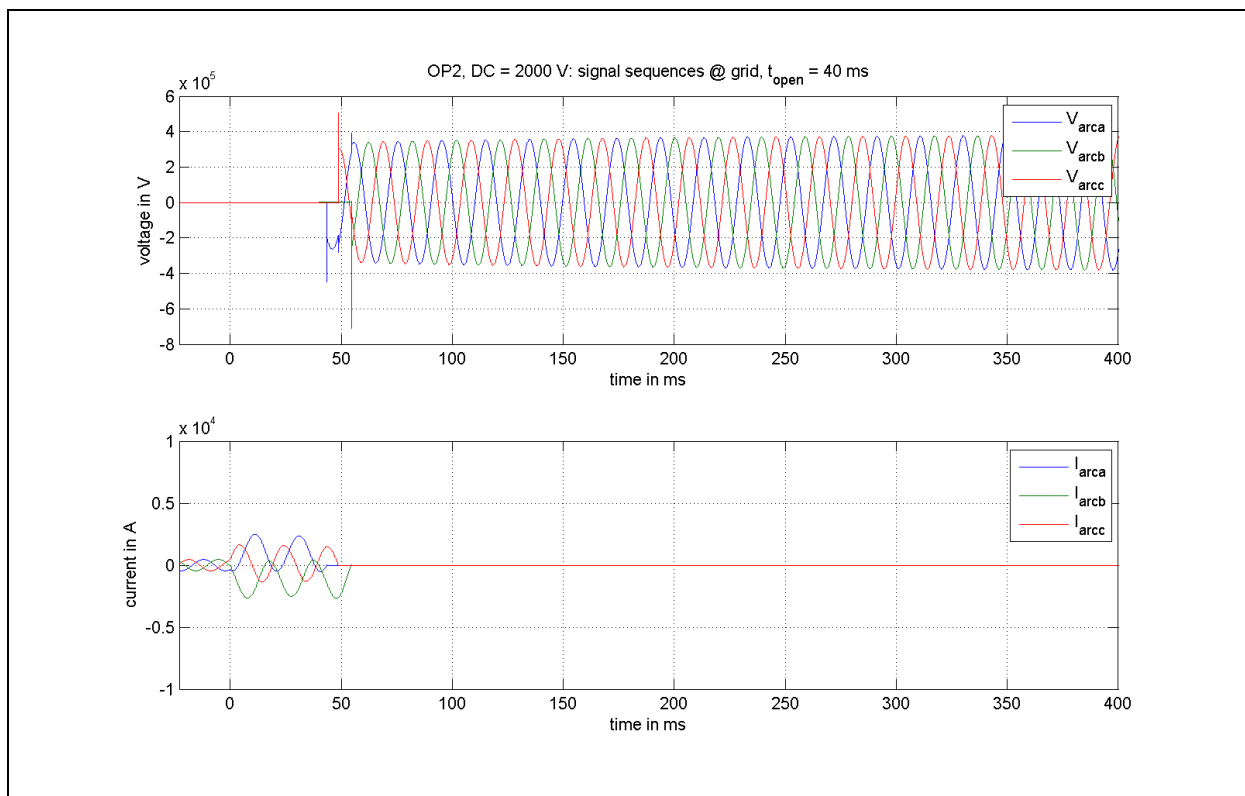


Figure 64: OP 2 (DC model): signal sequences V_{arc} and I_{arc} – $V_{arc} = 2000$ V, $t_{contactseparation} = 40$ ms

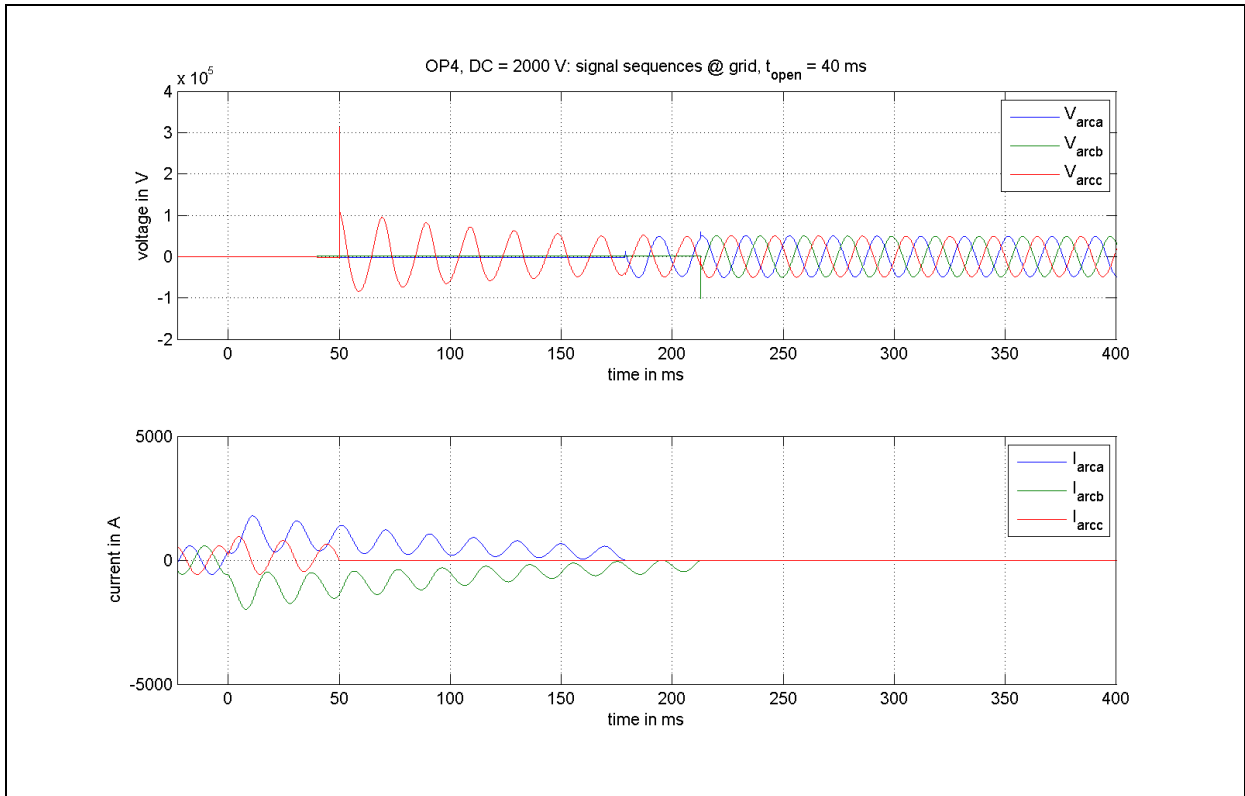


Figure 65: OP 4 (DC model): signal sequences V_{arc} and I_{arc} – $V_{arc} = 2000$ V, $t_{contactseparation} = 40$ ms

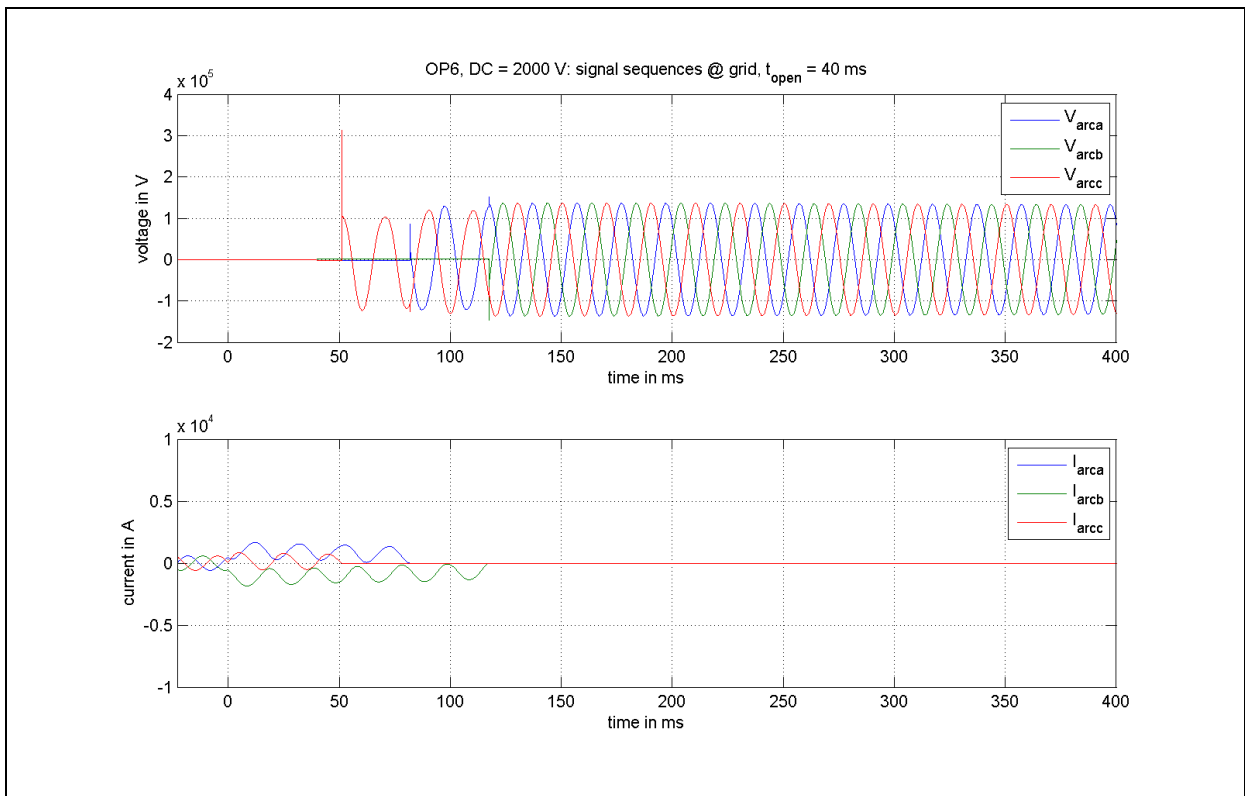


Figure 66: OP 6 (DC model): signal sequences V_{arc} and I_{arc} – $V_{arc} = 2000$ V, $t_{contactseparation} = 40$ ms

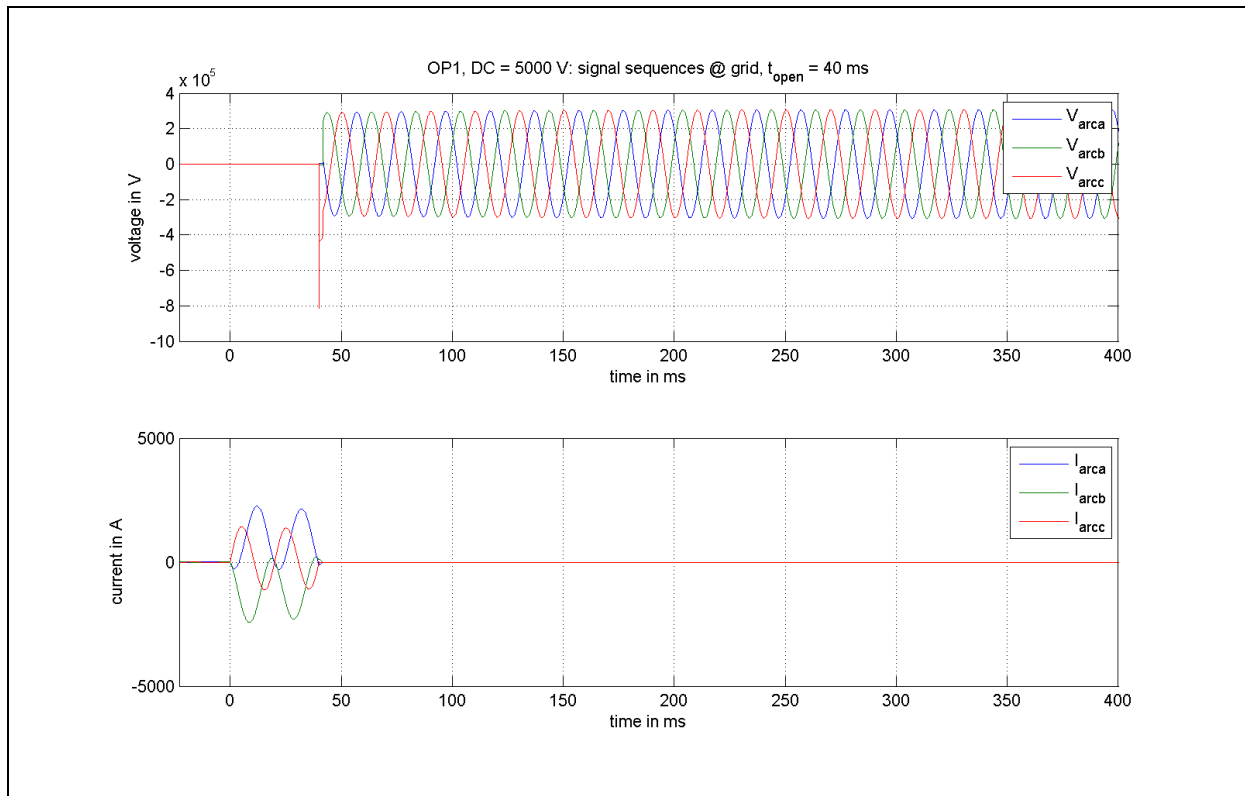


Figure 67: OP 1 (DC model): signal sequences V_{arc} and I_{arc} – $V_{arc} = 5000$ V, $t_{contactseparation} = 40$ ms

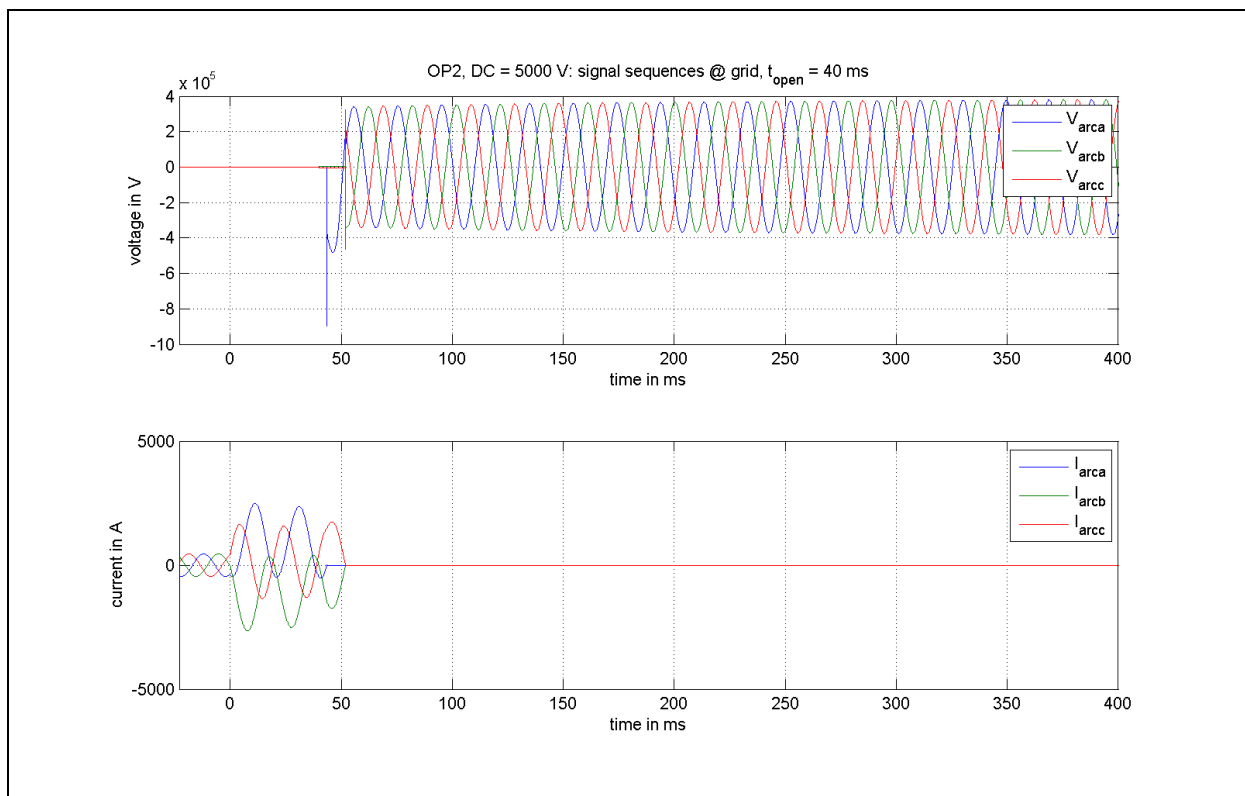


Figure 68: OP 2 (DC model): signal sequences V_{arc} and I_{arc} – $V_{arc} = 5000$ V, $t_{contactseparation} = 40$ ms

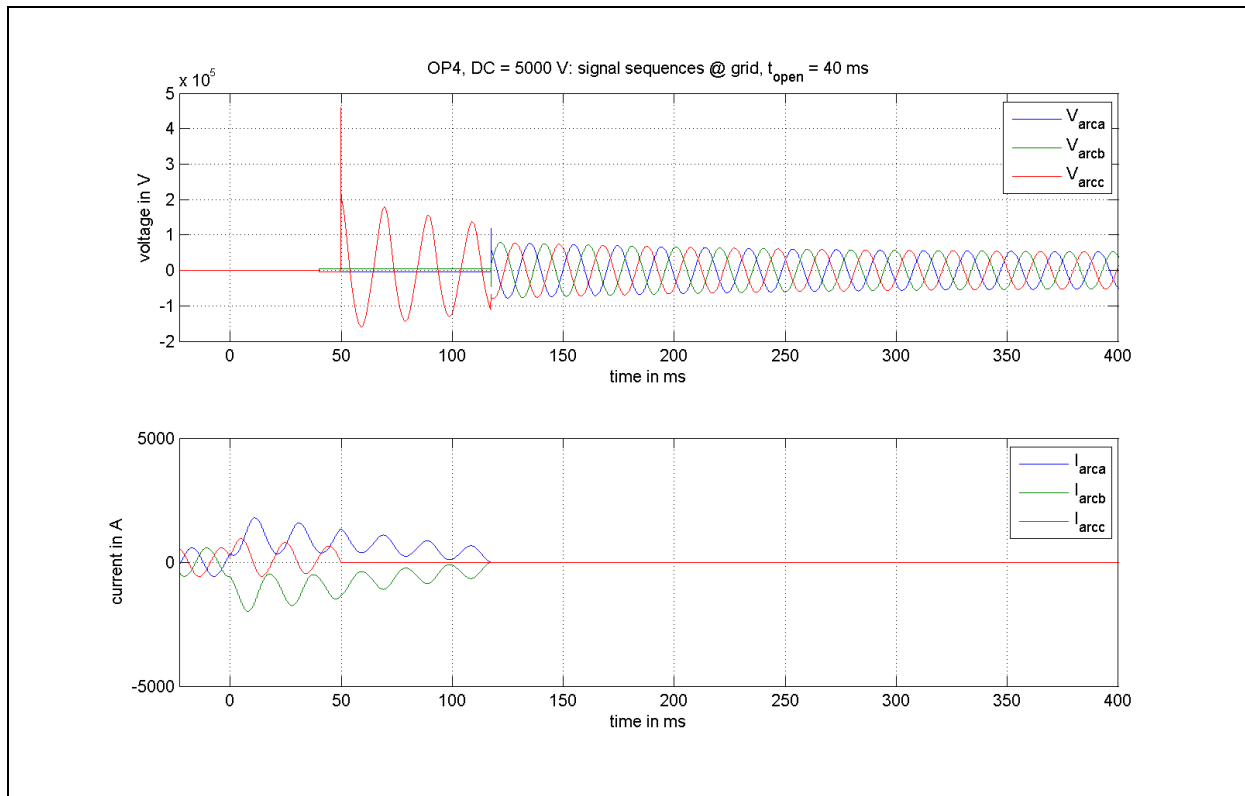


Figure 69: OP 4 (DC model): signal sequences V_{arc} and I_{arc} – $V_{arc} = 5000$ V, $t_{contactseparation} = 40$ ms

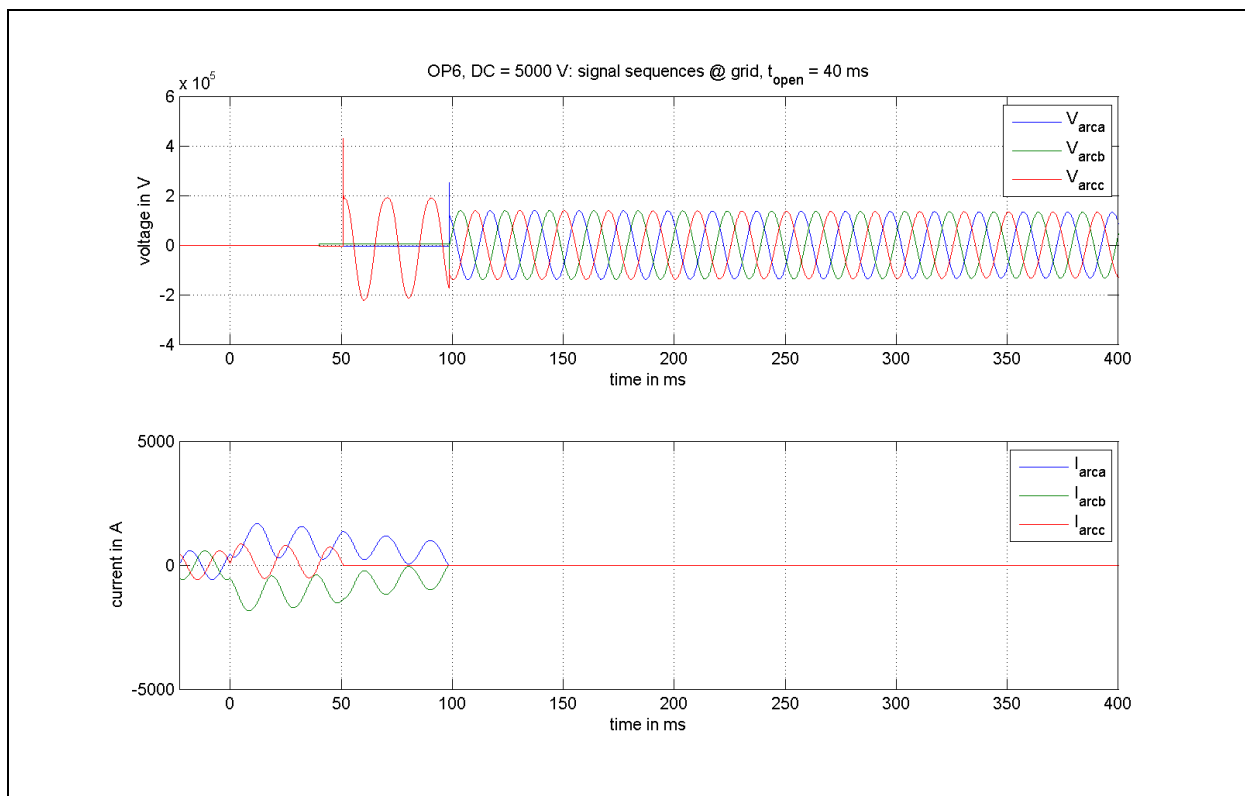


Figure 70: OP 6 (DC model): signal sequences V_{arc} and I_{arc} – $V_{arc} = 5000$ V, $t_{contactseparation} = 40$ ms

Mayr's model of electric arc (Mayr model), three-phase short-circuit without ground connection

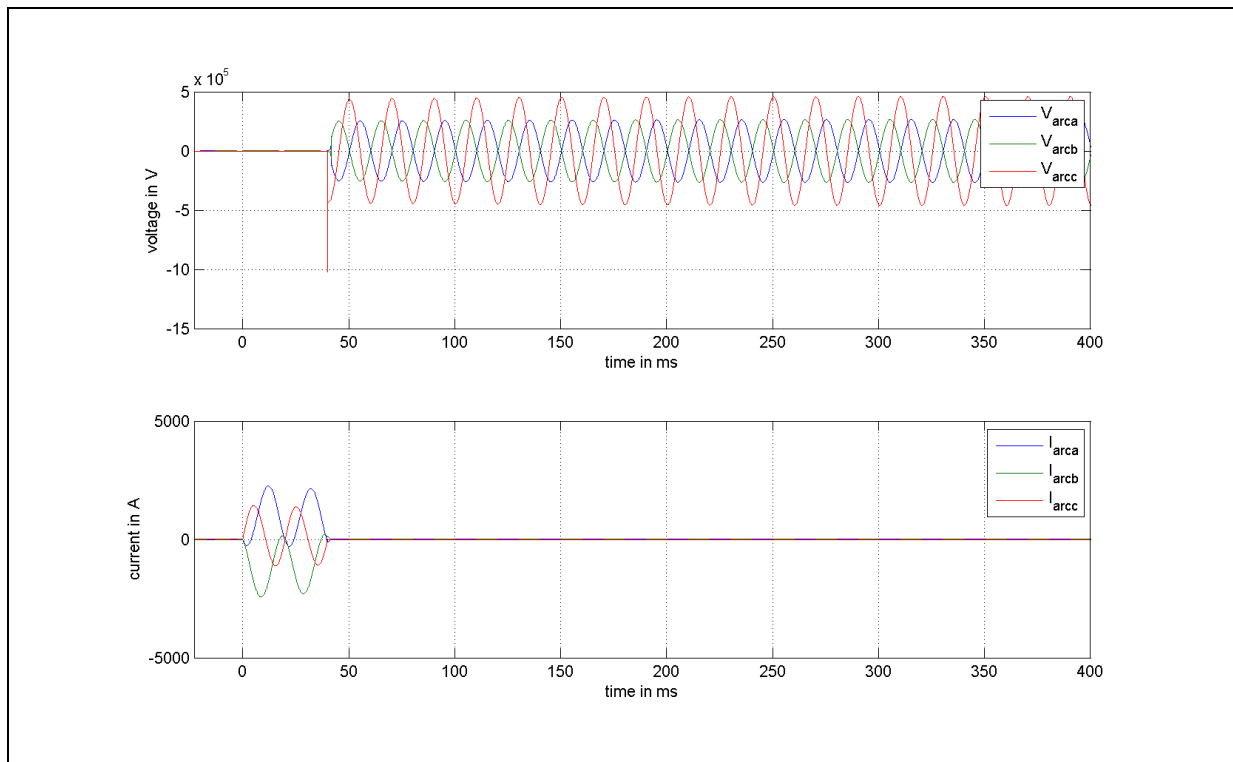


Figure 71: OP 1 (Mayr model): signal sequences V_{arc} and I_{arc} – $V_{arc} \approx 1000$ V, $t_{contactseparation} = 40$ ms

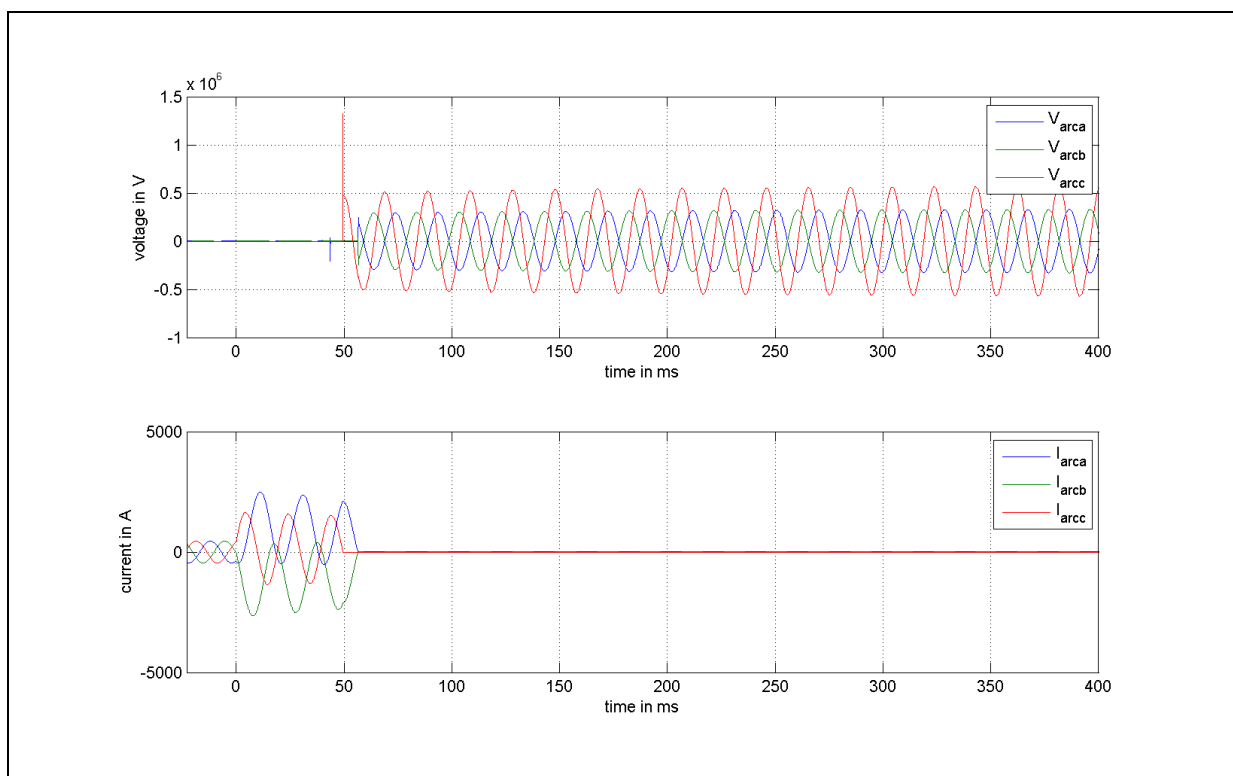


Figure 72: OP 2 (Mayr model): signal sequences V_{arc} and I_{arc} – $V_{arc} \approx 1000$ V, $t_{contactseparation} = 40$ ms

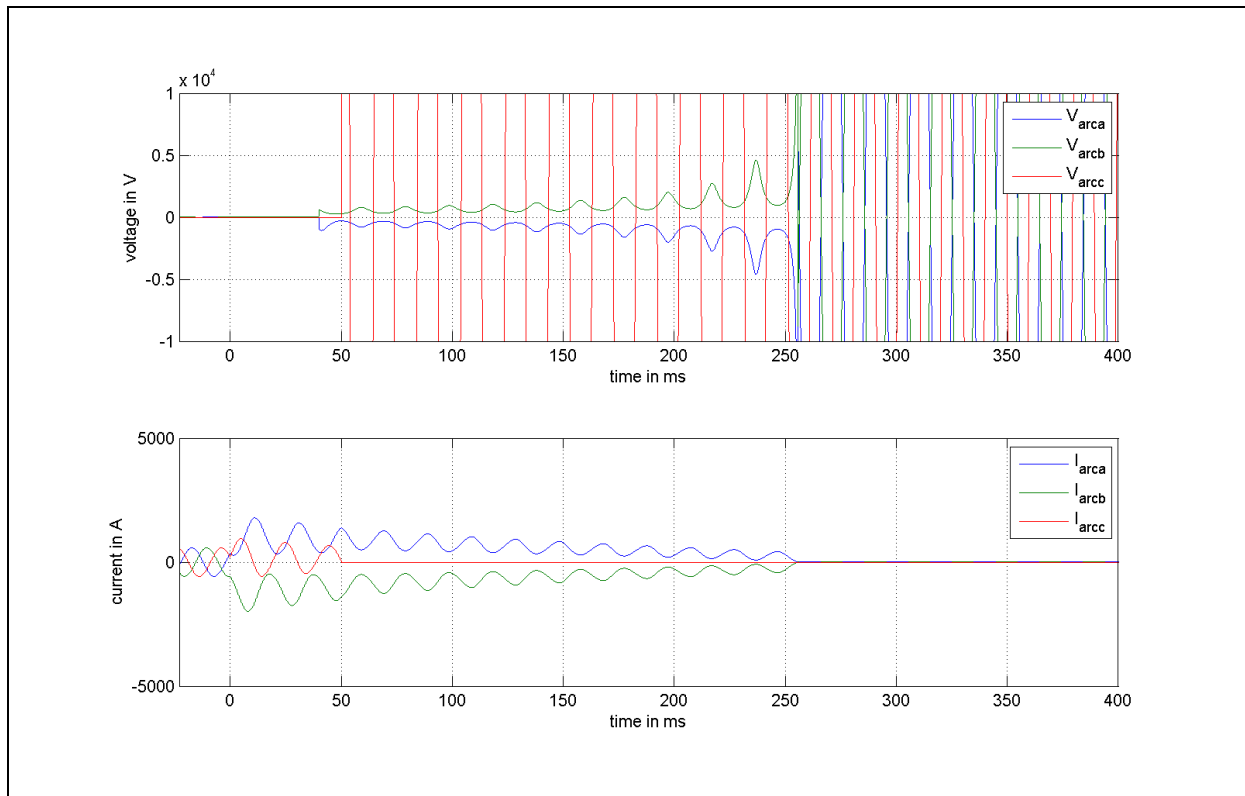


Figure 73: OP 4 (Mayr model): signal sequences V_{arc} and I_{arc} – $V_{arc} \approx 1000$ V, $t_{contactseparation} = 40$ ms

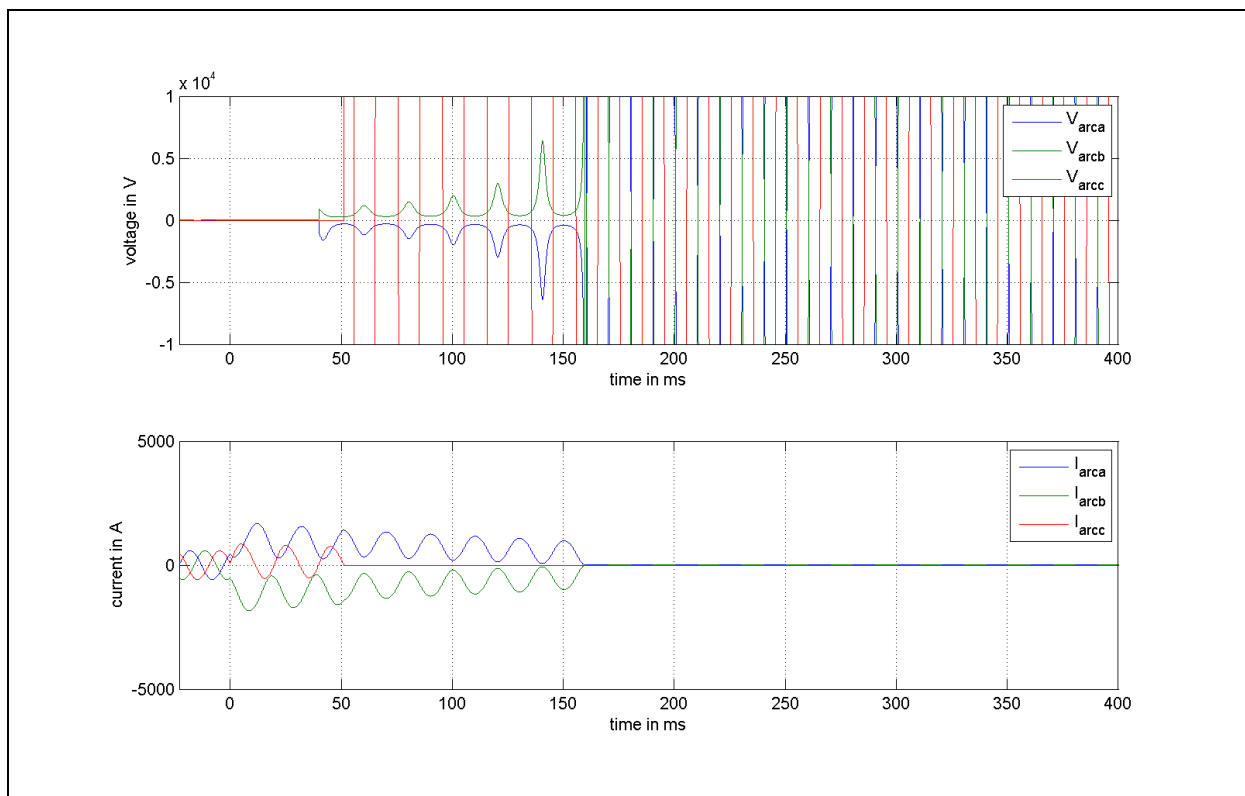


Figure 74: OP 6 (Mayr model): signal sequences V_{arc} and I_{arc} – $V_{arc} \approx 1000$ V, $t_{contactseparation} = 40$ ms

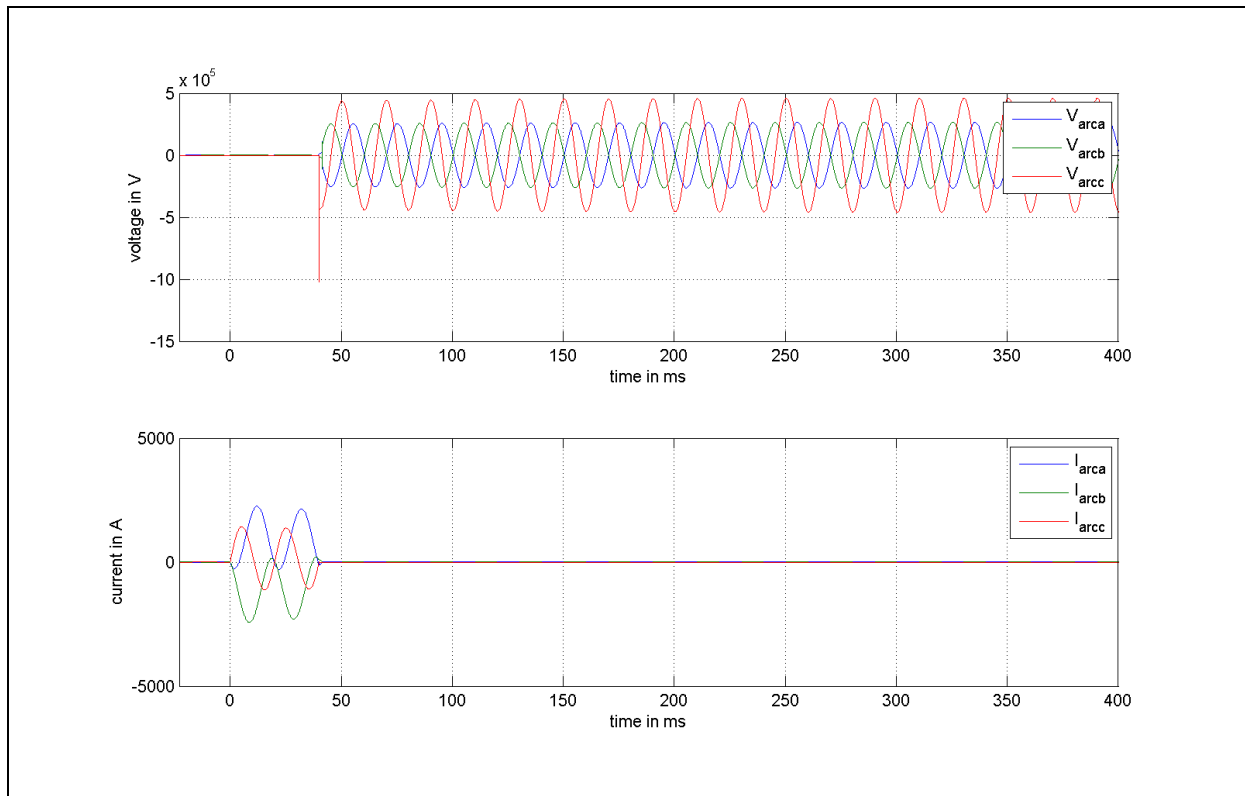


Figure 75: OP 1 (Mayr model): signal sequences V_{arc} and I_{arc} – $V_{arc} \approx 2000$ V, $t_{contactseparation} = 40$ ms

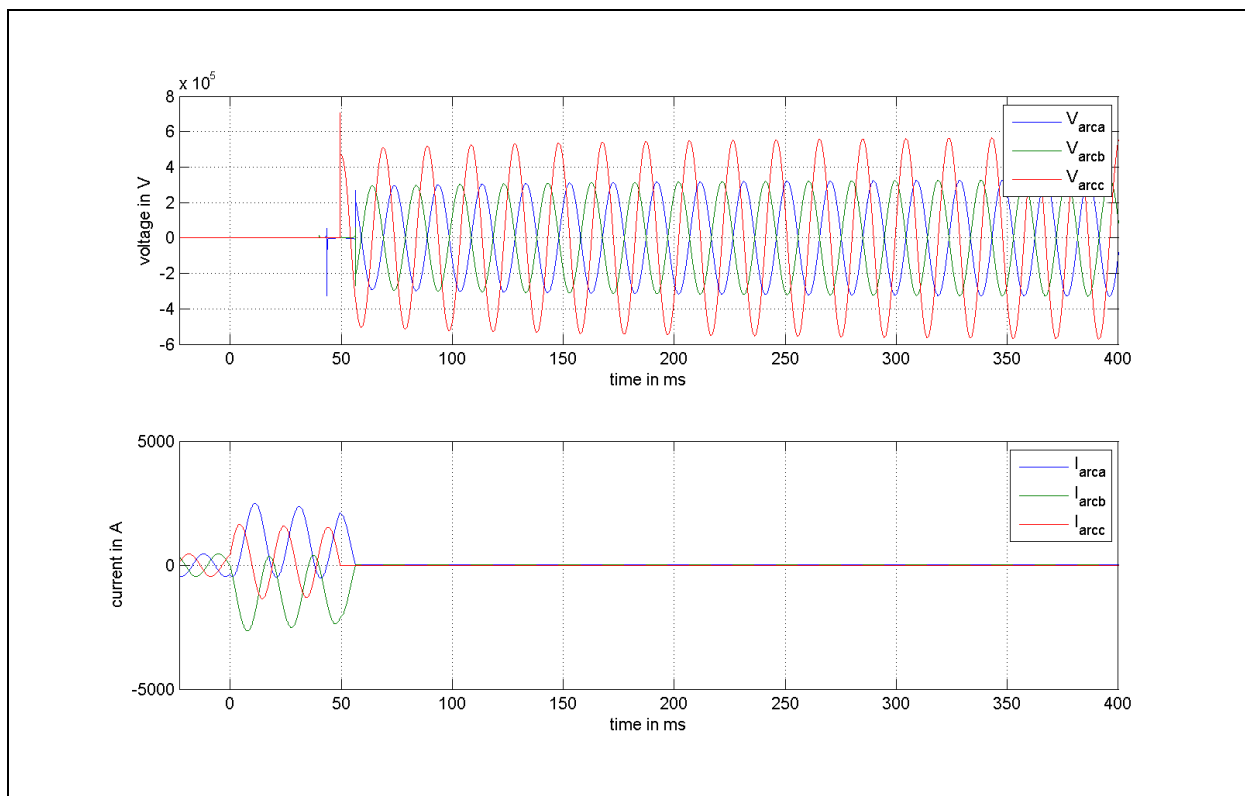


Figure 76: OP 2 (Mayr model): signal sequences V_{arc} and I_{arc} – $V_{arc} \approx 2000$ V, $t_{contactseparation} = 40$ ms

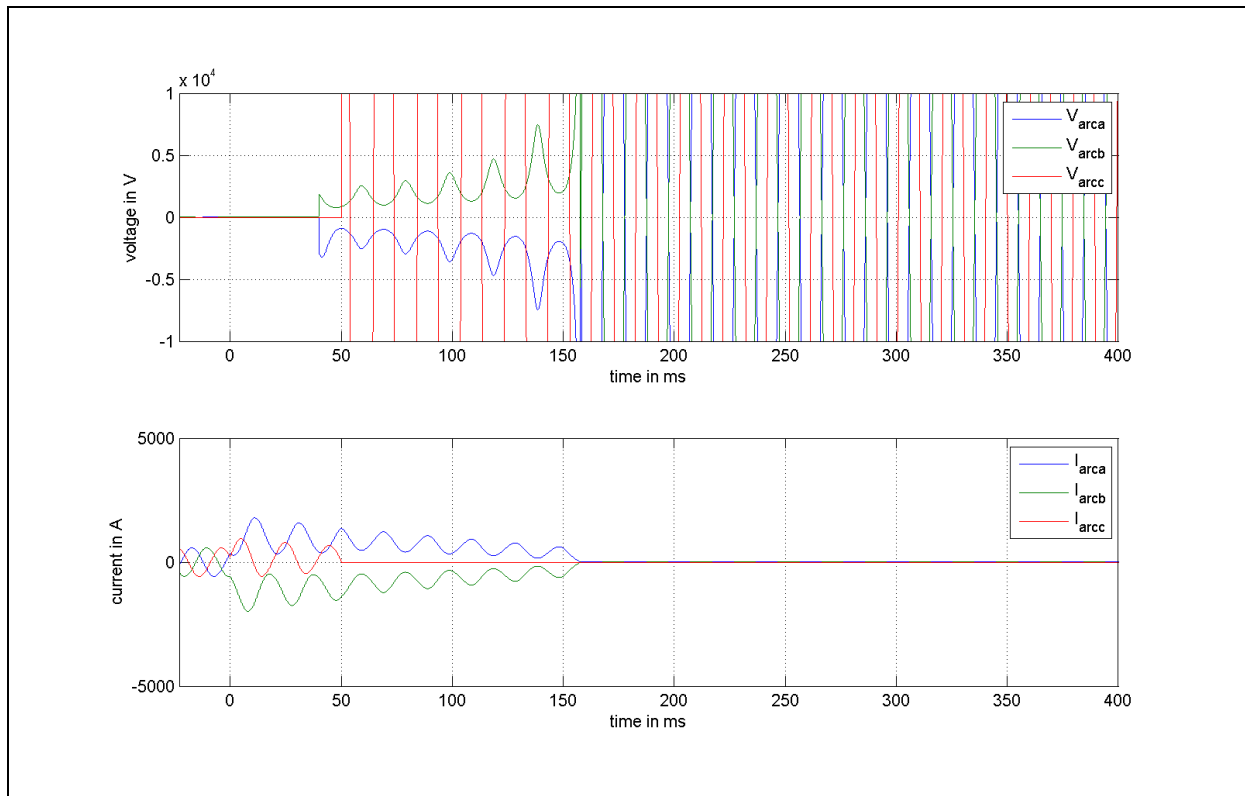


Figure 77: OP 4 (Mayr model): signal sequences V_{arc} and I_{arc} – $V_{arc} \approx 2000$ V, $t_{contactseparation} = 40$ ms

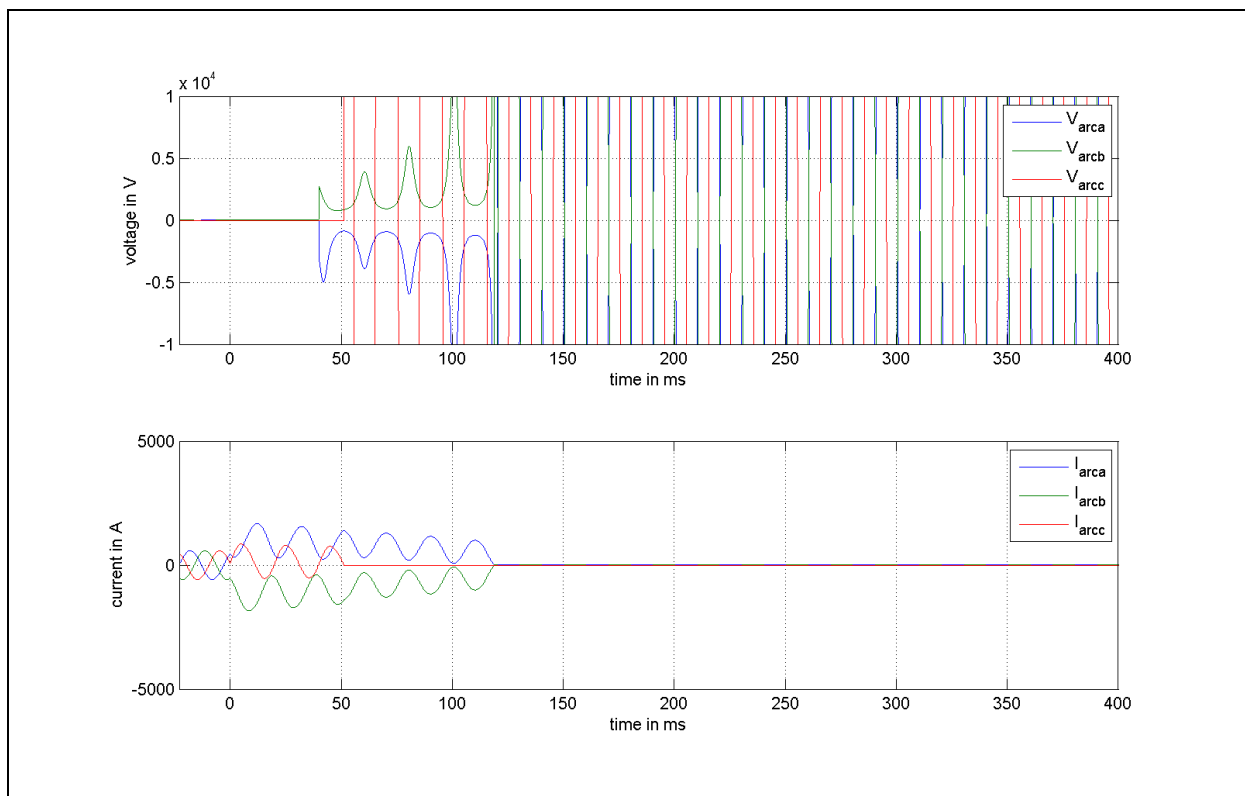


Figure 78: OP 6 (Mayr model): signal sequences V_{arc} and I_{arc} – $V_{arc} \approx 2000$ V, $t_{contactseparation} = 40$ ms

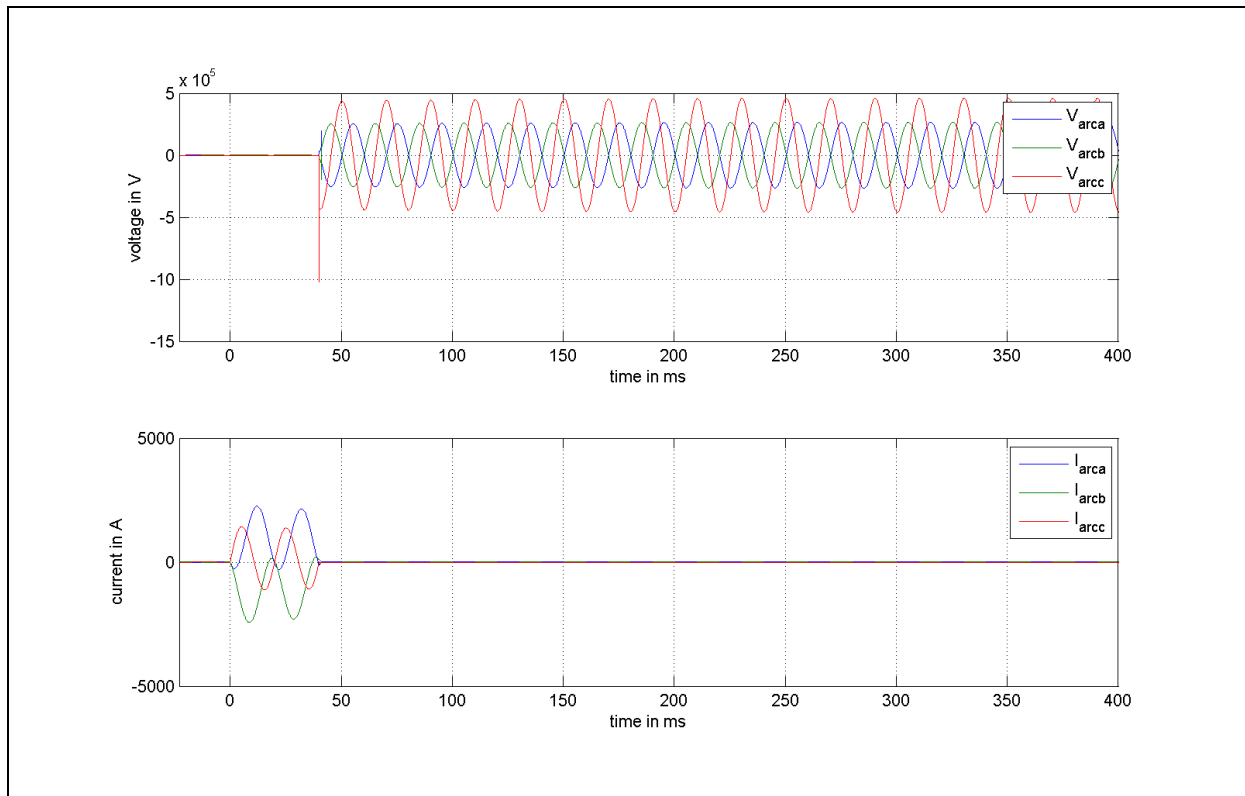


Figure 79: OP 1 (Mayr model): signal sequences V_{arc} and I_{arc} – $V_{arc} \approx 5000$ V, $t_{contactseparation} = 40$ ms

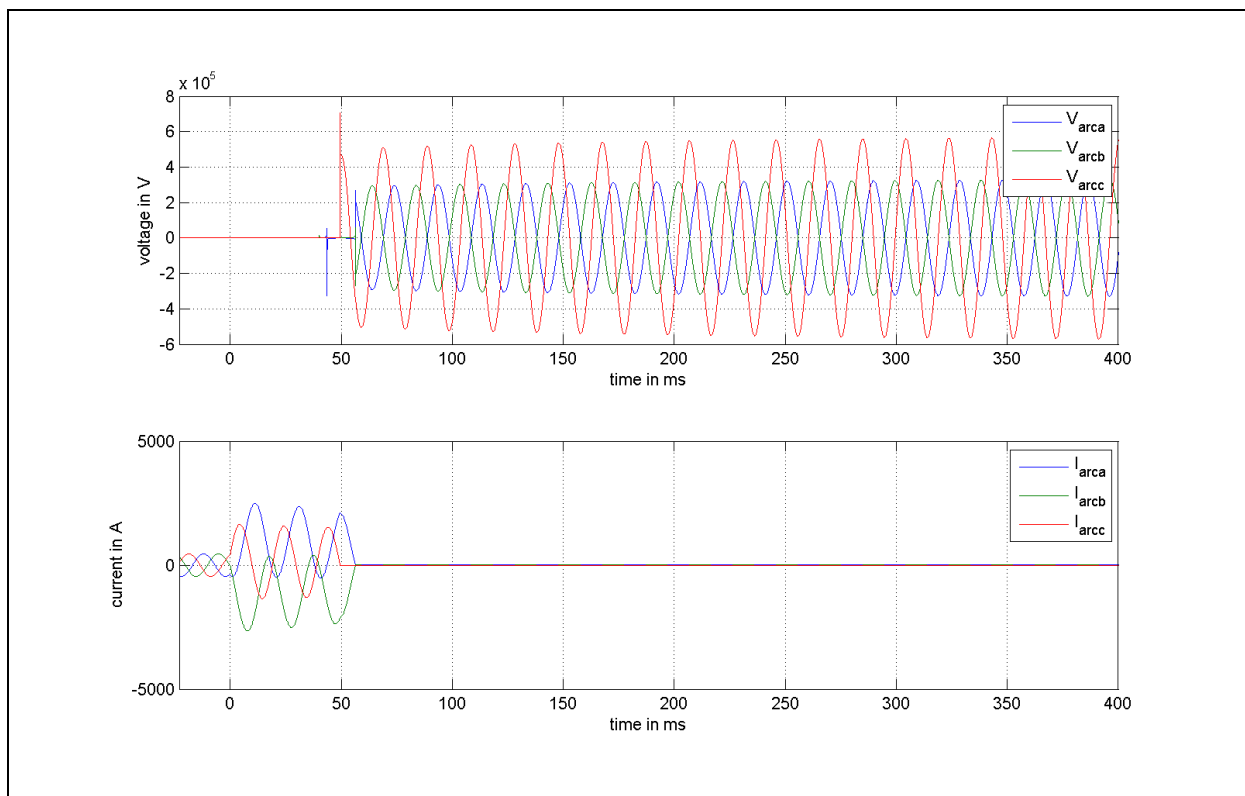


Figure 80: OP 2 (Mayr model): signal sequences V_{arc} and I_{arc} – $V_{arc} \approx 5000$ V, $t_{contactseparation} = 40$ ms

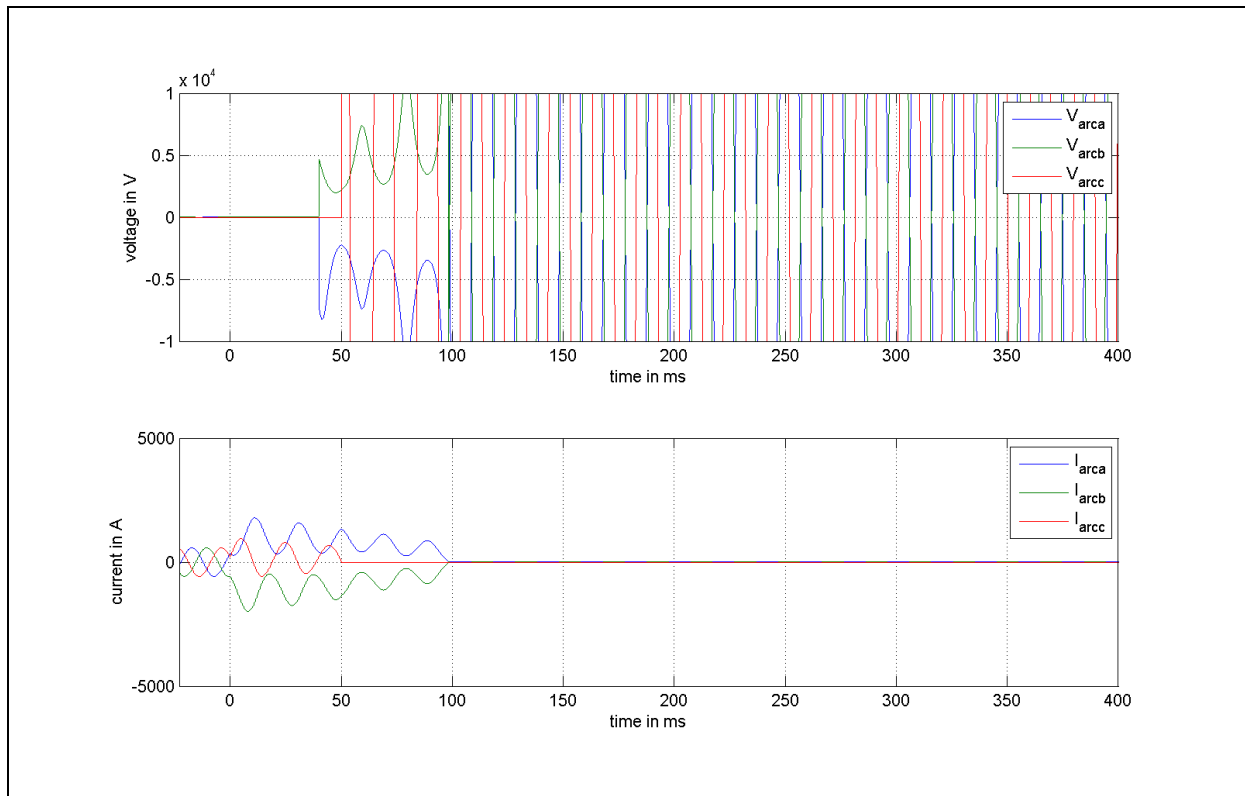


Figure 81: OP 4 (Mayr model): signal sequences V_{arc} and I_{arc} – $V_{arc} \approx 5000$ V, $t_{contactseparation} = 40$ ms

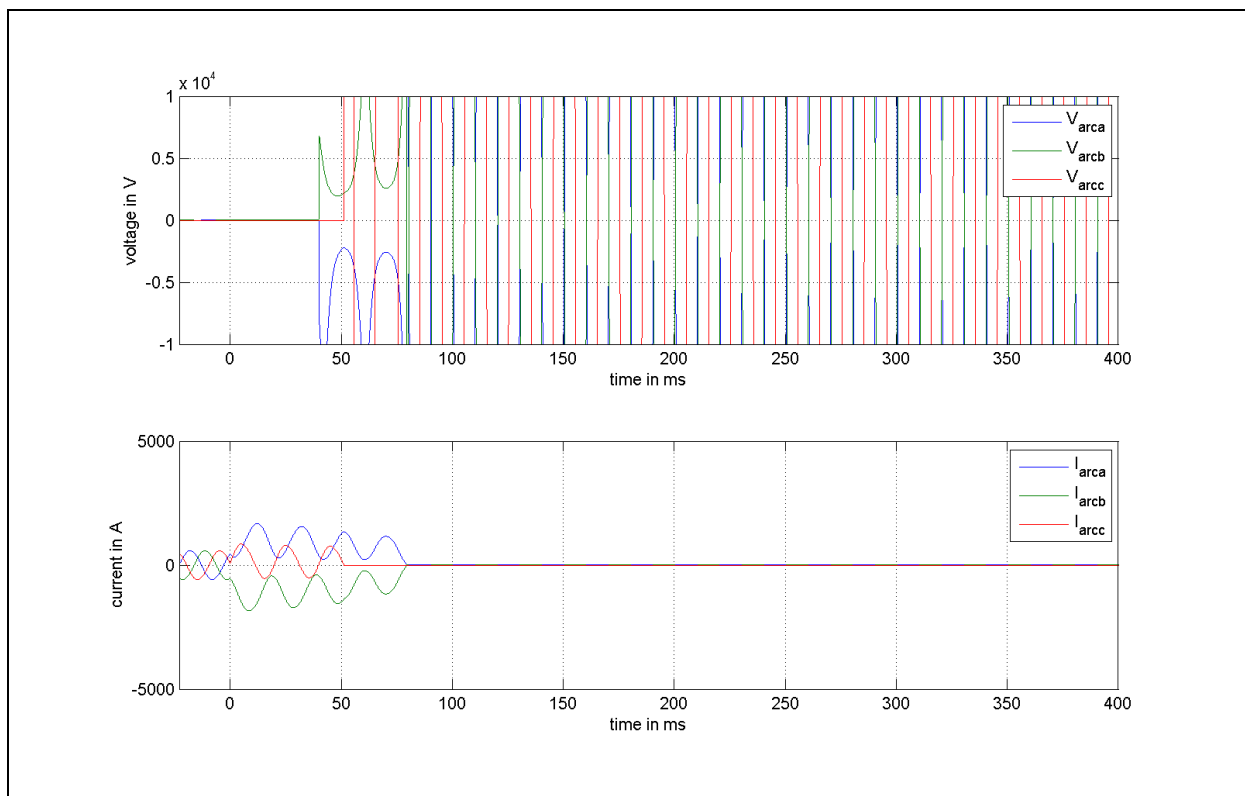


Figure 82: OP 6 (Mayr model): signal sequences V_{arc} and I_{arc} – $V_{arc} \approx 5000$ V, $t_{contactseparation} = 40$ ms

Model with constant d.c. arc voltage (DC-model), three-phase short-circuit to ground (3pG fault)

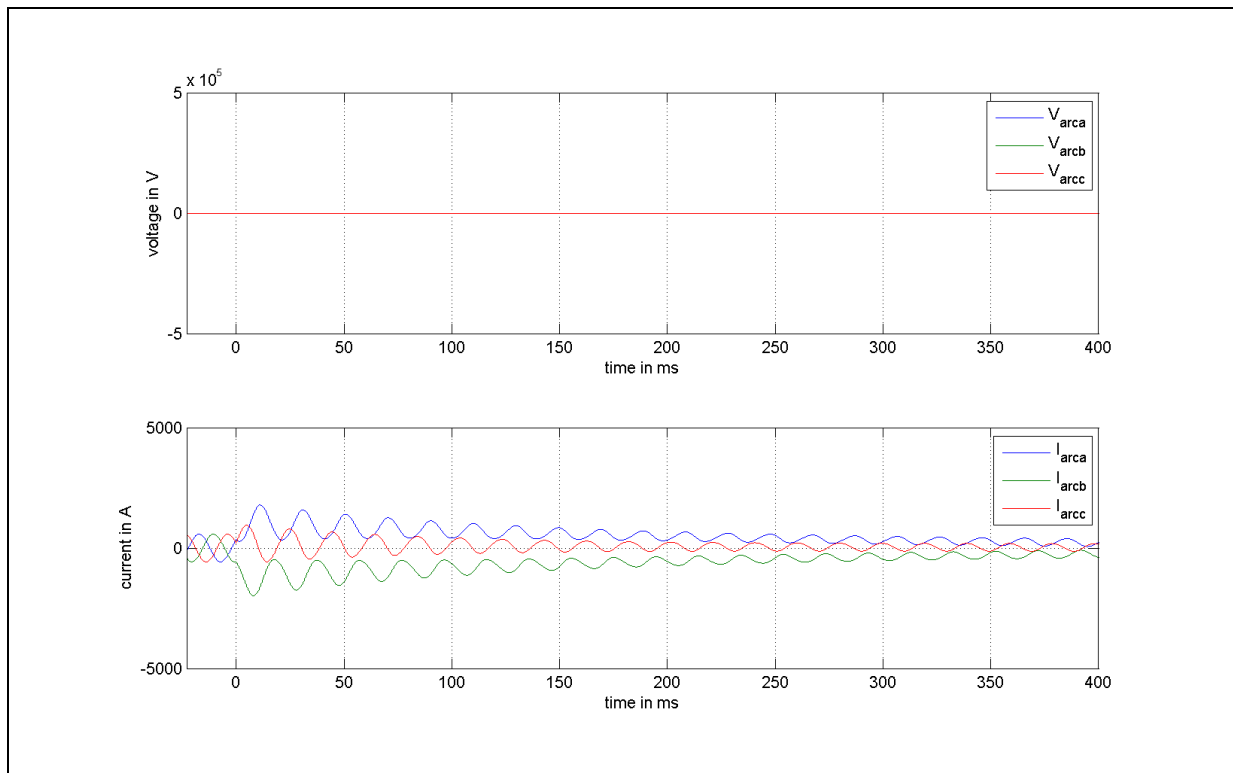


Figure 83: OP 4: uninfluenced signal sequences V_{arc} and I_{arc} after three phase short-circuit to ground – no contact separation

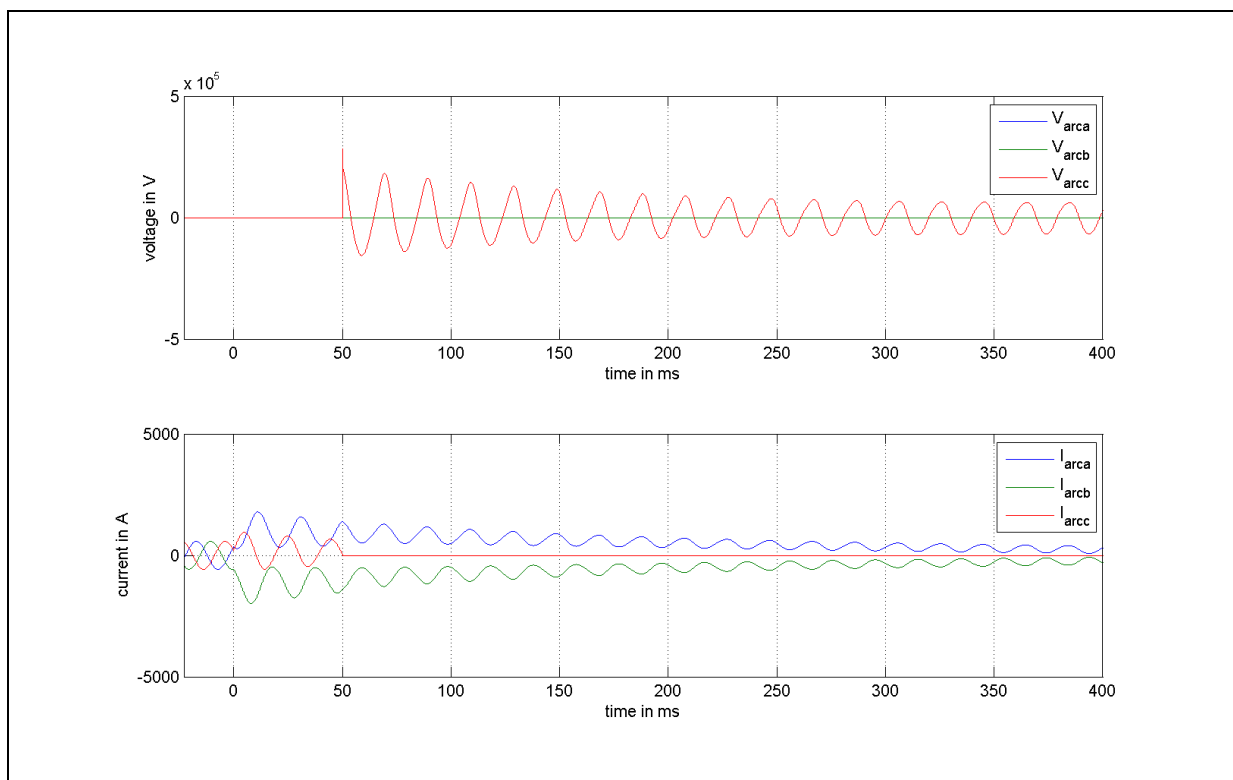


Figure 84: OP 4 (IDEAL circuit breaker): signal sequences V_{arc} and I_{arc} , $t_{contactseparation} = 40$ ms, 3pG fault

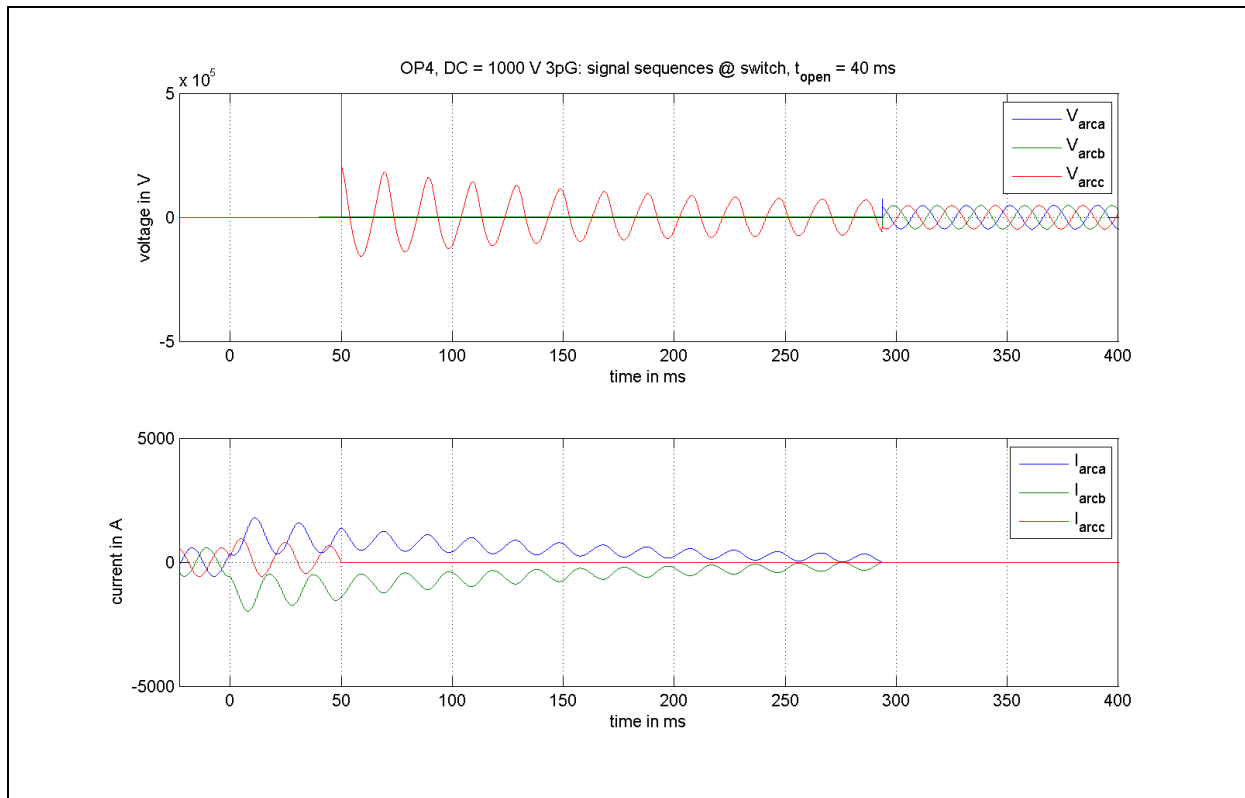


Figure 85: OP 4 (DC-model): signal sequences V_{arc} and I_{arc} – $V_{arc} = 1000$ V, $t_{contactseparation} = 40$ ms, 3pG fault

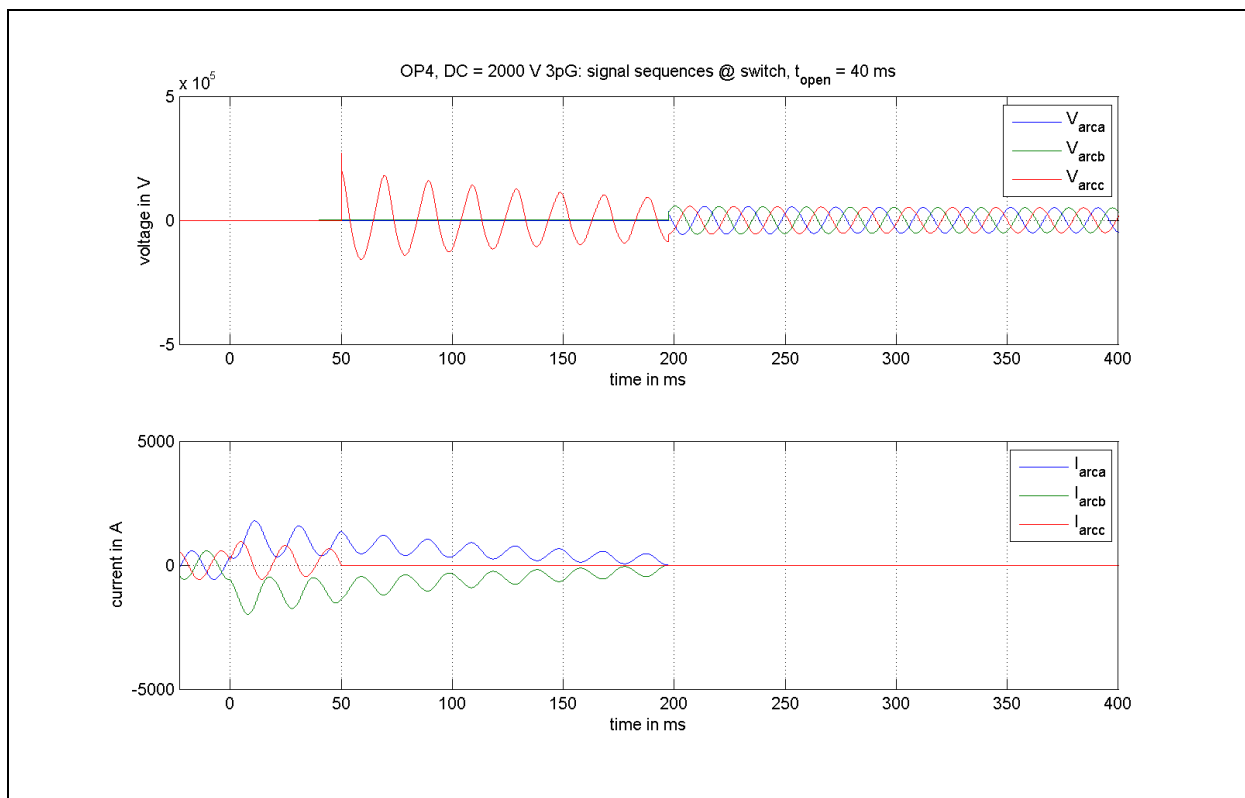


Figure 86: OP 4 (DC-model): signal sequences V_{arc} and I_{arc} – $V_{arc} = 2000$ V, $t_{contactseparation} = 40$ ms, 3pG fault

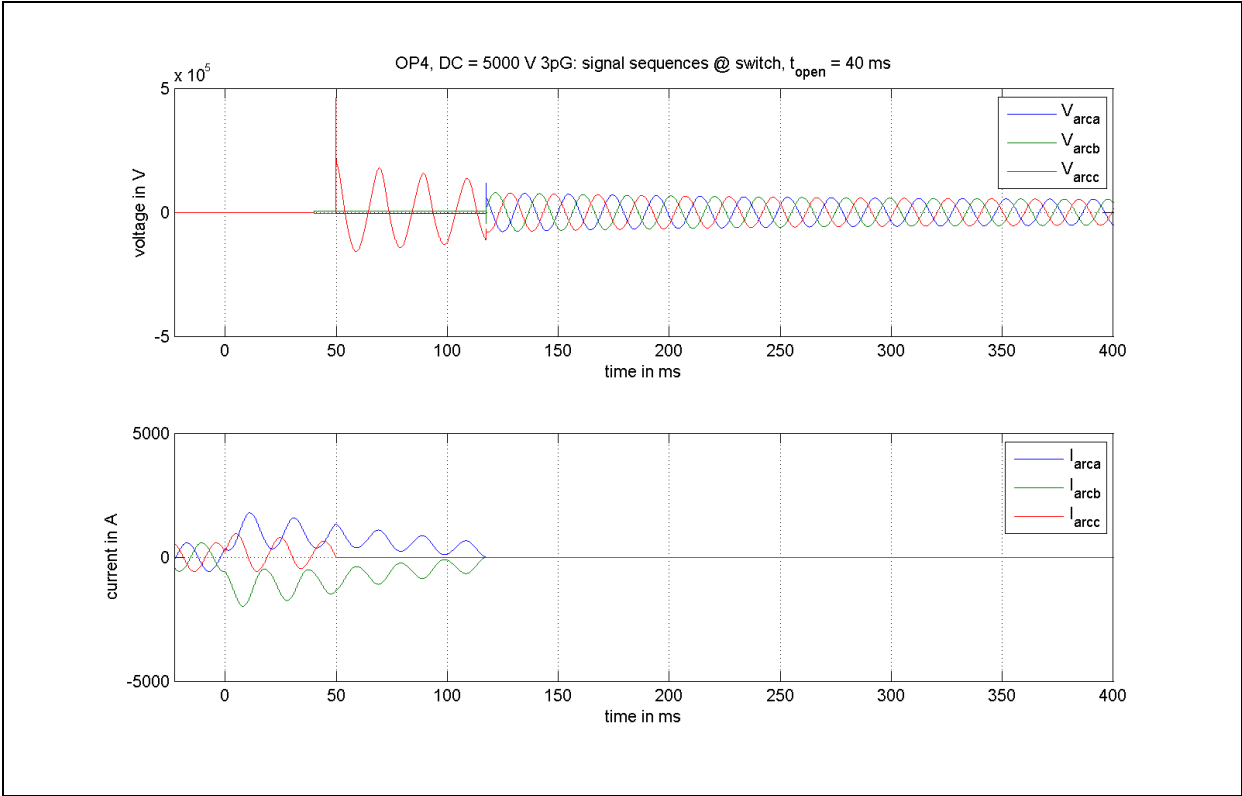


Figure 87: OP 4 (DC-model): signal sequences V_{arc} and I_{arc} – $V_{arc} = 5000$ V, $t_{contactseparation} = 40$ ms, 3pG fault

Appendix: Figures

Figure 59: OP 1 (DC model): signal sequences V_{arc} and I_{arc} – $V_{arc} = 1000 V$, $t_{contactseparation} = 40 ms$	80
Figure 60: OP 2 (DC model): signal sequences V_{arc} and I_{arc} – $V_{arc} = 1000 V$, $t_{contactseparation} = 40 ms$	80
Figure 61: OP 4 (DC model): signal sequences V_{arc} and I_{arc} – $V_{arc} = 1000 V$, $t_{contactseparation} = 40 ms$	81
Figure 62: OP 6 (DC model): signal sequences V_{arc} and I_{arc} – $V_{arc} = 1000 V$, $t_{contactseparation} = 40 ms$	81
Figure 63: OP 1 (DC model): signal sequences V_{arc} and I_{arc} – $V_{arc} = 2000 V$, $t_{contactseparation} = 40 ms$	82
Figure 64: OP 2 (DC model): signal sequences V_{arc} and I_{arc} – $V_{arc} = 2000 V$, $t_{contactseparation} = 40 ms$	82
Figure 65: OP 4 (DC model): signal sequences V_{arc} and I_{arc} – $V_{arc} = 2000 V$, $t_{contactseparation} = 40 ms$	83
Figure 66: OP 6 (DC model): signal sequences V_{arc} and I_{arc} – $V_{arc} = 2000 V$, $t_{contactseparation} = 40 ms$	83
Figure 67: OP 1 (DC model): signal sequences V_{arc} and I_{arc} – $V_{arc} = 5000 V$, $t_{contactseparation} = 40 ms$	84
Figure 68: OP 2 (DC model): signal sequences V_{arc} and I_{arc} – $V_{arc} = 5000 V$, $t_{contactseparation} = 40 ms$	84
Figure 69: OP 4 (DC model): signal sequences V_{arc} and I_{arc} – $V_{arc} = 5000 V$, $t_{contactseparation} = 40 ms$	85
Figure 70: OP 6 (DC model): signal sequences V_{arc} and I_{arc} – $V_{arc} = 5000 V$, $t_{contactseparation} = 40 ms$	85
Figure 71: OP 1 (Mayr model): signal sequences V_{arc} and I_{arc} – $V_{arc} \approx 1000 V$, $t_{contactseparation} = 40 ms$	86
Figure 72: OP 2 (Mayr model): signal sequences V_{arc} and I_{arc} – $V_{arc} \approx 1000 V$, $t_{contactseparation} = 40 ms$	86
Figure 73: OP 4 (Mayr model): signal sequences V_{arc} and I_{arc} – $V_{arc} \approx 1000 V$, $t_{contactseparation} = 40 ms$	87
Figure 74: OP 6 (Mayr model): signal sequences V_{arc} and I_{arc} – $V_{arc} \approx 1000 V$, $t_{contactseparation} = 40 ms$	87
Figure 75: OP 1 (Mayr model): signal sequences V_{arc} and I_{arc} – $V_{arc} \approx 2000 V$, $t_{contactseparation} = 40 ms$	88
Figure 76: OP 2 (Mayr model): signal sequences V_{arc} and I_{arc} – $V_{arc} \approx 2000 V$, $t_{contactseparation} = 40 ms$	88

Figure 77: OP 4 (Mayr model): signal sequences V_{arc} and I_{arc} – $V_{arc} \approx 2000$ V, $t_{contactseparation} = 40$ ms.....	89
Figure 78: OP 6 (Mayr model): signal sequences V_{arc} and I_{arc} – $V_{arc} \approx 2000$ V, $t_{contactseparation} = 40$ ms.....	89
Figure 79: OP 1 (Mayr model): signal sequences V_{arc} and I_{arc} – $V_{arc} \approx 5000$ V, $t_{contactseparation} = 40$ ms.....	90
Figure 80: OP 2 (Mayr model): signal sequences V_{arc} and I_{arc} – $V_{arc} \approx 5000$ V, $t_{contactseparation} = 40$ ms.....	90
Figure 81: OP 4 (Mayr model): signal sequences V_{arc} and I_{arc} – $V_{arc} \approx 5000$ V, $t_{contactseparation} = 40$ ms.....	91
Figure 82: OP 6 (Mayr model): signal sequences V_{arc} and I_{arc} – $V_{arc} \approx 5000$ V, $t_{contactseparation} = 40$ ms.....	91
Figure 83: OP 4: uninfluenced signal sequences V_{arc} and I_{arc} after three phase short-circuit to ground – no contact separation	92
Figure 84: OP 4 (IDEAL circuit breaker): signal sequences V_{arc} and I_{arc} , $t_{contactseparation} = 40$ ms, 3pG fault.....	92
Figure 85: OP 4 (DC-model): signal sequences V_{arc} and I_{arc} – $V_{arc} = 1000$ V, $t_{contactseparation} = 40$ ms, 3pG fault	93
Figure 86: OP 4 (DC-model): signal sequences V_{arc} and I_{arc} – $V_{arc} = 2000$ V, $t_{contactseparation} = 40$ ms, 3pG fault	93
Figure 87: OP 4 (DC-model): signal sequences V_{arc} and I_{arc} – $V_{arc} = 5000$ V, $t_{contactseparation} = 40$ ms, 3pG fault	94

Appendix: Tables

Table 16: Relative DC-component of phase current in different phases79